A critical assessment of the methods for intercalating anionic surfactants in layered double hydroxides

BY

LUMBIDZANI MOYO

Submitted in partial fulfilment of the requirements for the degree

Master of Science

in the Faculty of Natural and Agricultural Sciences, University of Pretoria

MAY 2009

DECLARATION

I, Lumbidzani Moyo , the undersigned, declare that the dissertation that I hereby submit for the degree MSc at the University of Pretoria is my own work, and has not previously been submitted by me for degree purposes or examination at this or any other university.

Pretoria, May 2009

……
Lumbidzani Moyo (Miss)

UNIVERSITEIT VAN PRETORIA
UNIVERSITY OF PRETORIA
YUNIBESITHI YA PRETORIA

A CRITICAL ASSESSMENT OF THE METHODS FOR INTERCALATING ANIONIC SURFACTANTS IN LAYERED DOUBLE HYDROXIDES

By

Lumbidzani Moyo

Supervisor: Prof. Walter W Focke

Department of Chemistry

DEGREE: MAGISTER SCIENTIAE

SYNOPSIS

The intercalation of surfactant anions, namely sodium dodecyl sulphate, sodium benzene sulphonate and lauric acid, into commercial layered double hydroxides (LDH-CO_3) with approximate composition $[Mg_{0.654}Al_{0.346}(OH)_2](CO_3)_{0.173} \cdot 0.5H_2O]$ was explored. LDH-CO_3 is commercially available in bulk form owing to its large-scale applications as a PVC stabiliser and acid scavenger in polyolefins. It is therefore of interest to investigate intercalation methods using LDH-CO_3 as starting material. The intercalation method used was compared with the pre-existing procedures, for instance the co-precipitation, ion exchange and regeneration methods. Due to the tenacity with which the carbonate ion is held in LDH-CO_3, direct ion exchange is an intricate matter. Hence, in the regeneration method the carbonate ion is removed by thermal treatment and the LDH-surfactant is obtained by reaction of the LDH and surfactant in an aqueous medium. Nevertheless, the resulting products are impure and poorly crystallised, and only partial intercalation is achieved. The underlying principle of the current method is protonation of the carbonate anion to a monovalent anion that is easily exchanged with surfactant anions.

Improved results were obtained when water-soluble organic acids were used, the most suitable being lower aliphatic carboxylic acids, e.g. acetic, butyric and hexanoic acid. In contrast, higher linear aliphatic carboxylic acids are preferentially intercalated to the anionic surfactants. In both cases the carboxylic acids are assumed to assist intercalation by facilitating the elimination of the carbonate ions present in the anionic clay galleries. X-ray diffraction analysis, thermal analysis and infrared spectroscopy confirmed the monolayer intercalation of LDH-dodecyl sulphate and LDH-dodecylbenzene sulphonate. In contrast, LDH-laurate featured a bilayer structure.

Keywords: Layered double hydroxide; intercalation; anionic surfactant; calcination; reconstruction; infrared spectroscopy; thermogravimetry; X-ray diffraction analysis

ACKNOWLEDGEMENTS

No author is an island, entire of itself. Every author has had many hands guiding his/her pen and many minds adding richness and depth to his/her thoughts…J. E. Ormrod

I wish to extend my sincere gratitude to:

- Prof. W. W. Focke for his guidance and supervision
- Ollie del Fabbro for his technical support and advice. Mr Alan Hall (SEM), Mila Maksa and Nontete (TG), Sabine Verryn (XRD), Maggi Loubser and Kgabo (XRF), for their help in the characterisation of the products
- The editor, Beverlie Davies, for her patience in reading through my work
- My colleagues at the Institute of Applied Materials – Hermino, Darren, Thabo and Pedro – for their input and thorough scrutiny of my work
- Nontete and Tumaini for encouraging me during the downs of the research and holding my hand through it all
- My brothers, Bue, Zwe and Andy – thanks, your support has been invaluable
- My parents, Anderson and Sylvia – thank you for loving and believing in me. You have been truly the wind behind my back and my number one fans
- God Almighty for giving me this opportunity, blessing me abundantly and meeting my every area of need to this day.

TABLE OF CONTENTS

LIST OF FIGURES

LIST OF TABLES

LIST OF SCHEMES

LIST OF CHARTS

Nomenclature and Abbreviations

AEC	Anion exchange capacity
CLDH	Calcined layered double hydroxide
CMC	Critical micelle concentration
DBS	Dodecylbenzene sulphonate
DS	Dodecyl sulphate
DSC	Differential scanning calorimetry
DTG	Derivative of the thermogravimetric curve
FT-IR	Fourier transform infrared spectroscopy
GC/MS	Gas chromatography/mass spectrometry
HT	Hydrotalcite, layered double hydroxide of composition $Mg_6Al_2(OH)_{16}CO_3.4H_2O$
LDH	Layered double hydroxide
LDH-DS	Layered double hydroxide intercalated with dodecyl sulphate
LDO	Layered double oxide, calcined LDH
Organo-LDH	LDH intercalated with organic material
SDBS	Sodium dodecylbenzene sulphonate
SDS	Sodium dodecyl sulphate, $CH_3(CH_2)_{11}SO_4Na$
SEM	Scanning electron microscopy
TGA/TG	Thermogravimetric analysis/thermogravimetry
TG-MS	Thermogravimetry-Mass spectroscopy
TG-FT-IR	Thermogravimetry-Fourier transform infrared spectroscopy
XRD	X-ray diffraction
XRF	X-ray fluorescence spectroscopy

CHAPTER 1: INTRODUCTION

Clay minerals and clays constitute the world's largest and most widely used material, dating back many years. Clays are both versatile and have many beneficial features, such as low cost, selectivity, catalytic properties, and a wide range of preparation and modification methods (Vaccari, 1998). They hold promise for providing sought-after, environmentally friendly technologies for the 21st century.

Clay is defined as a material with a particle size of less than 2 μm and that possesses a layered structure. Clay minerals are classified into two groups, namely cationic and anionic clays. The former normally refers to negatively charged alumino-silicate layers, while the latter consists of positively charged mixed metal hydroxide layers. Cationic clays are further divided into four groups, i.e. kaolinite, montmorillonite/smectite, illite and chlorite.

Layered double hydroxides (LDHs) are anionic clays also known as 'hydrotalcite-like' compounds. They can also be described as mixed metal hydroxides as they consist of positively charged metal hydroxide sheets with metals of different oxidation states (Reichle, 1986). The crystallography of these clays is similar to that of hydrotalcite, with the formula $Mg_6Al_2(OH)_{16}(CO_3).4H_2O$. Hydrotalcite is a mineral that was discovered in Sweden in 1848. The name is derived from the strong resemblance of the mineral to talc and its high water content. It is formed naturally by the weathering of basalt rocks and co-precipitation of the cations in saline water sources. However, unlike cationic clays, hydrotalcites are rarely found in nature.

LDHs are 2-D nanostructured clays, which demonstrate expandable galleries that can accommodate various anionic species. This leads to the formation of inorganic-organic host-guest hybrids. LDHs are of interest due to their ease of preparation, inexpensiveness and versatility. Moreover, they are potentially recyclable in their fields of application (Li & Duan, 2005). These clays possess high anion exchange capacity (200–500 cmol/kg) as compared with anion exchange resins. In addition, they are resistant to moderate to high-temperature

treatment (Li & Duan, 2005). Interlayer anions confined between layers exhibit restricted geometry, giving the potential for improved control of their stereochemistry, rate of reaction and product distribution.

A considerable amount of research has been done in this field in the past century. Table 1.1 summarises the achievements in the field.

Table 1.1: Milestones in research into layered double hydroxides (LDHs)

1910-1914	Hydrotalcite and pyroaurite family described (Flink ***et al***.,1910 & 1914)
1920	Hydrotalcite identified as mixed hydroxides (Foshag, 1920).
1930	pH precipitation of Mg^{2+} in the presence of $Al(OH)_3$. The pH used was lower than the one deemed essential for brucite precipitation (Treadwell & Bernasconi, 1930). Discovery of the two polymorphs having rhombohedral and hexagonal symmetry respectively (Aminoff & Broome, 1930).
1936-1942	Precipitation of hydrotalcite by addition of alkali to a solution of M (II) and M (III). Freitknecht ***et al***.,(1936-1942) mistakenly described it as alternating magnesium-rich and aluminium-rich layers. He named the structures ***doppelschichtenstruktur***, meaning layered double structures, from which the expression layered double hydroxide is derived.
1944	Thermal degradation of hydrotalcite and conversion into spinel (Caillere, 1944).
1960	Clinical antacid use of Mg-Al LDH (Beekman, 1960).
1968-1969	Correct identification of layered double hydroxide, consisting of both metal ions localised in one sheet, (Allmann, 1968 & Taylor, 1969).
1970	Patent on hydrotalcite-like structures, being the optimal precursors for the preparation of hydrogenation catalysts, (Brocker & Kaempfer, 1975).
1973	Miyata's ground-breaking work on a range of formation and anion exchange techniques for the mineral (Miyata & Kumura, 1973).

1975 Patent on the use of hydrotalcite as a flame retardant (Soma ***et al***., 1975)

Interest in this mineral therefore dates back to at least 1910 and has continued to grow rapidly to date. LDHs appear to have limitless applications in various fields of industry, for example catalysis, environmental remediation, pharmaceuticals and polymer technology.

1.1 Problem Statement

Hydrotalcite is a hydroxycarbonate of magnesium and aluminium. The high layer charge density leads to very strong electrostatic attraction existing between the sheets. Hydrotalcites have a higher affinity for multivalent anions than their monovalent counterparts. The electrostatic interaction between these multivalent anions, e.g. carbonates, and the charged layer is strong, and this makes exchange difficult.

Numerous trials have been attempted to obtain a pure organo-LDH using methods such as co-precipitation (Kopka ***et al.***, 1988; Meyn ***et al.***, 1990), regeneration (Costa ***et al***., 2005; You ***et al.***, 2002b) and elimination (decarbonation) (Iyi ***et al***., 2005).

Co-precipitation methods are characterised by long reaction hours or even days, and a product with low crystallinity and homogeneity. Precipitation by urea hydrolysis results in the incorporation of the carbonate anion, which is not easily exchangeable. In some cases, the LDHs are found to have impurities of $M(OH)_2$ and $M(OH)_3$ or mixed phases of the metal hydroxides, resulting in undesired charge density (He ***et al***., 2005).

The ***regeneration*** method deals with the removal of the carbonate anion by thermal treatment. The resulting intercalates have a perforated surface morphology and the crystallinity of the product is low. The calcination of LDHs makes them prone to damage in the crystal structure and the original shape is not conserved (Hibino & Tsunashima, 1998; Stanimirova ***et al.***, 2001). Decarbonation

using mineral acids has been found to be a challenge (Iyi ***et al.***, 2005) due to the strong acidity of HCl and the low acid tolerance of Mg-Al LDH.

1.2 Aims of this Research

The aim of this study was to introduce a new preparation method for LDH-surfactants and also to investigate the known surfactant intercalation procedures. Previous research work appeared to prove that direct intercalation of various surfactant anions was impossible due to the tenacity with which the carbonate anion is held between the LDH layers. Rigorous intercalation methods have since been explored but still yield unsatisfactory results, as mentioned in the previous section. The method proposed here provides an innovative means of simultaneous elimination of carbonate and insertion of surfactant ions into the interlayer. The method presents an alternative, easy and convenient route for the intercalation of surfactant anions, such as dodecyl sulphate and dodecylbenzene sulphonate.

The proposed reaction will proceed at ambient temperature, pressure and in normal laboratory conditions without requiring the exclusion of carbon dioxide (inert atmosphere). The method seeks to use readily available raw material of LDH-CO_3 which is easily produced on a large scale at a relatively low price. Other aspects of the method that are of interest entail safe reaction conditions, water as the medium of exchange rather than the use of organic solvents, favourable economics, and the maintenance of crystallinity after intercalation. The purity of the modified clay is also to be investigated for contamination by residual ions from the intercalation process, e.g. sodium and carbonate ions.

1.3 Outline of the Dissertation

The dissertation comprises five chapters. Chapter 1 is an introduction to layered double hydroxides, briefly defining their nature and history. The problems encountered when working with these materials are discussed in Section 1.1, ***Problem Statement***. The aims of this research are also outlined. Chapter 2 provides a brief description of the preparation methods for LDHs, their structure and formulae. The classification of surfactants, their properties and their interaction with clay minerals, namely anionic clays, are then discussed.

Intercalation and various methods of surfactant intercalation, as well as the orientation of intercalated anions, are also examined. The characterisation techniques employed in the structural elucidation of LDHs are introduced. The chapter concludes with a discussion about the applications in which these modified clays may be used.

Chapter 3 gives a description of the raw materials and experimental procedure used in the study. Chapter 4 sets out the results obtained from this study. These results are then discussed and classified according to the characterisation techniques used. Chapter 5 presents the conclusions and recommendations.

CHAPTER 2: LITERATURE REVIEW

2.1 Structure of Hydrotalcite

The basic structure of the clay is closely related to that of brucite, $Mg(OH)_2$. In a typical brucite layer, each Mg^{2+} is octahedrally surrounded by six OH^- ions, resulting in an octahedron that shares its edges with neighbouring $Mg(OH)_6$ octehedra (Bhattacharyya ***et al.***, 1995; Allmann, 1979). Layered double hydroxides/hydrotalcites are structurally characterised as brucite-like layers in which some of the divalent cations are replaced by trivalent ones, resulting in an overall positive charge. This charge is neutralised by the incorporation of exchangeable anions and the water molecules between the layers. The neutrality in hydrotalcite is maintained by carbonate ions. It also contains interlayer water which forms hydrogen bonds with layer OH or with the interlayer anions. Hence the 3-D structure of the clay is maintained by the electrostatic interaction and hydrogen bonding between the layer and interlayer anions or molecules (Cavani ***et al.***, 1991; Trifiro & Vaccari, 1996)***.*** The height of each layer is 4.77 Å of the Mg (OH) sheet (Smyth & Bish, 1988). These sheets are stacked one on top of the other and held together by hydrogen bonding (Cavani ***et al.***, 1991).

Two known polymorphs of the mineral exist: the rhombohedral (R) hydrotalcite a = 3.1 Å and c = 23.1 Å and the hexagonal (H) manasseite a = 3.1 Å and c = 15.3 Å (Miyata, 1980; Kooli ***et al.***, 1995). The structures of these compounds have been explored by means of X-ray diffraction (XRD) analysis. The polymorphs give the stacking sequence of the brucite-like sheets as 3R and 2H for pyroaurite/hydrotalcite and syögrenite respectively.

As mentioned earlier, the substitution of Mg ions with Al ions leaves a net positive charge in the interlayer. The carbonate anion counterbalances the positive charge in natural hydrotalcite. However, in the case of their synthetic counterparts, the net positive charge is counterbalanced by various anions. The predominant bonding that exists is electrostatic; however, with long-chain alkyl groups hydrophobic interactions among surfactant anions play an essential role.

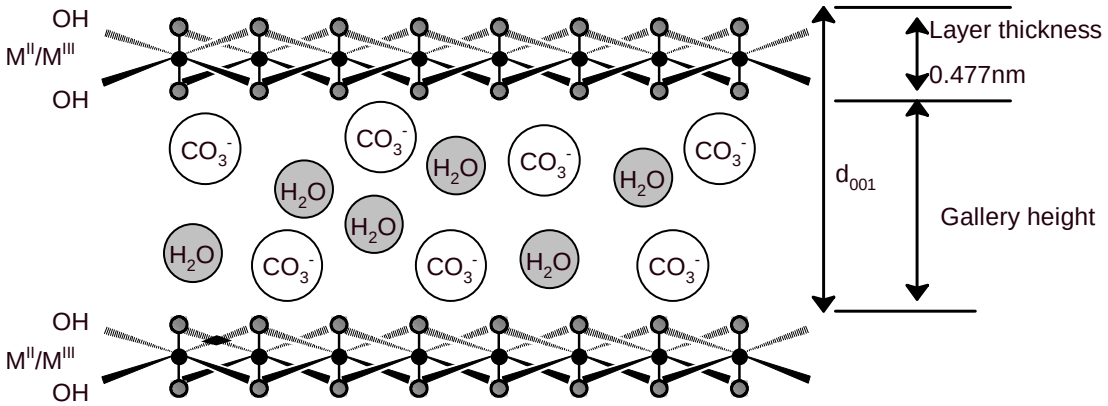

Figure 2.1: Layered structure of LDH

In Figure 2.1 M^{II} and M^{III} represent the divalent and trivalent metal ions respectively. The interlayer region is composed of hexagonal close-packed sites parallel to the close-packed layers of the hydroxyl groups and metal cations.

LDHs may include variations, such as containing more than two species of the second cation (Kooli ***et al.***, 1995). Xiang ***et al***. (2009) also prepared Co/Fe/Al LDHs to be used in the preparation of carbon nanotubes. Apart from the conventional layer, which consists of M^{II} and M^{III} metal cations, a mono- and trivalent cation matrix layer may be prepared as well (Williams ***et al.***, 2004; Nayak ***et al.***, 1997).

2.2 Formula

$$[M^{2+}_{(1-x)}M^{3+}_{x}(OH)_2]^{x+}(A^{n-}_{(x/n)}).mH_2O \qquad (1)$$

where
M^{2+} is Mg, Zn, Ni, Co
M^{3+} is Al, Cr, Fe, Mn, etc.

The formula implies that there are several different compounds with differing stoichiometries that can be synthesised. The M (II) and M (III) that make up the hydrotalcite-like compounds usually have ionic radii that are close to that Mg^{2+}. In

the natural form of these layered double hydroxides ***x*** = 0.25. The ratio of the M (II) to M (III) ions is 3: 1 which, with further calculation, gives the value ***x.*** This value is calculated in the following manner:

$$X = \frac{M(III)}{M(II) + M(III)} \qquad (2)$$

Hydrotalcite-like compounds exist for x-values in the range of 0.1 to 0.5 with the pure compounds being 0.2≤ ***x*** ≤0.33 (Cavani ***et al.***, 1991; Miyata, 1980; Mascolo & Marino, 1980; Brindley & Kikkawa, 1979). Al^{3+} ions within the hydrotalcite layer are far apart so as to minimise the repulsion between the ions. For ***x*** values that are high, the Al^{3+} ions tend to be neighbouring, hence leading to the formation of $Al(OH)_3$. In the case of low ***x*** values, this leads to a high density of Mg octahedra, resulting in the formation of $Mg(OH)_2$ sheets (Cavani ***et al.***, 1991; Brindley & Kikkawa, 1979). LDHs can be delineated by chemical composition, basal spacing and stacking sequence (Vaccari, 1998) (see Table 2.1).

Table 2.1: Composition; cell parameters and symmetry of LDHs

Mineral	Chemical composition	Unit cell parameter		Symmetry
		***a*(nm)**	***c*(nm)**	
Hydrotalcite	$Mg_6Al_2(OH)_{16}CO_3{\cdot}4H_2O$	0.3054	2.281	3R
Manasseite	$Mg_6Al_2(OH)_{16}CO_3{\cdot}4H_2O$	0.31	1.56	2H
Pyroaurite	$Mg_6Fe_2(OH)_{16}CO_3{\cdot}4H_2O$	0.3109	2.341	3R
Sjögrenite	$Mg_6Fe_2(OH)_{16}CO_3{\cdot}4H_2O$	0.3113	1.561	2H
Stichitite	$Mg_6Cr_2(OH)_{16}CO_3{\cdot}4H_2O$	0.310	2.34	3R
Barbertonite	$Mg_6Cr_2(OH)_{16}CO_3{\cdot}4H_2O$	0.310	1.56	2H
Takovite	$Ni_6Al_2(OH)_{16}CO_3{\cdot}4H_2O$	0.3025	2.259	3R
Reevesite	$Ni_6Fe_2(OH)_{16}CO_3{\cdot}4H_2O$	0.3081	2.305	3R
Meixnerite	$Mg_6Al_2(OH)_{16}(OH)_2{\cdot}4H_2O$	0.3046	2.292	3R
Coalingite	$Mg_{10}Fe_2(OH)_{24}CO_3{\cdot}4H_2O$	0.312	3.75	3R

2.3 Preparative Methods

There are numerous methods by which LDHs may be synthesised. These include electrochemical methods, co-precipitation (Miyata, 1980; Kopka ***et al.***, 1988;

Reichle, 1986; Yang & Zhou, 2008), sol-gel (Lopez ***et al.***, 1997; Aramendia ***et al.***, 2002; Ramos ***et al.***, 1997; Prinetto ***et al.***, 2000), hydrothermal crystallisation (Mascolo, 1995), chimie douce (Delmas & Borthomieu, 1993) and the urea hydrolysis reaction (Adachi-Pagano ***et al.,*** 2003). These preparative methods give a wide variety of compositions, M^{II}:M^{III} ratios and metal combinations.

Mascolo ***et al.,*** (1995) describe the preparation of LDHs from amorphous acidic precursors of M_2O_3, which are then reacted with an appropriate basic crystallising agent, MO. These are subjected to hydrothermal crystallisation where the MO and M_2O_3 are in suspension at temperatures ranging between 7 and 160 °C. It is vital for the successful synthesis of LDHs that a weakly acid M_2O_3 precursor and a strongly basic MO be used. Alternative means by which hydrothermal crystallisation can be carried entail heating a sample in an autoclave under high pressure ranging between 10 and 150 MPa (Morioka ***et al.,*** 1995).

The sol-gel method involves the formation of a mobile colloidal suspension that gels due to internal cross-linking. Prinetto ***et al.*** (2000) prepared Al/Mg and Al/Ni LDHs from the hydrolysis of alkoxides or acetylacetonate precursors with HNO_3 and HCl. The underlying principle is hydrolysis and condensation of a solution of metal alkoxides. The alkoxides are first dissolved in an organic solvent and thereafter refluxed. Water is added to the refluxed solution, which results in cross-linking, hence forming LDHs (Braterman ***et al.,*** 2004). Ramos ***et al.*** (1997) prepared LDHs from magnesium ethoxide and various aluminium salts such as acetylacetonate, nitrate, sulphate and chloride of aluminium. Their studies revealed that the crystallinity of sol-gel products is dependent on the aluminium salt used, in the order: aluminum acetylcetonate > aluminum chloride > aluminum nitrate > aluminium sulphate. The method was also found to influence the textural properties of LDHs (Aramendia ***et al.,*** 2002). In addition, the specific area of the sol-gel product was three times greater than that obtained by the co-precipitation method. LDHs from the sol-gel method have the following traits: good homogeneity, good control of M(II):M(III) ratio, high surface area and porosity features (Braterman ***et al.,*** 2004).

The co-precipitation method is a classical, easy and convenient way to prepare LDHs in large amounts. Co-precipitation implies the simultaneous precipitation of cations in the predetermined ratios of their starting solution. The method is believed to proceed by means of condensation of hexa-aquo complexes in solution, hence building brucite-like layers, with a homogeneous distribution of both metal cations and interlayer anions (He ***et al.***, 2005). The first product was obtained by precipitation of the aqueous metal salts in a basic solution. The precipitate was washed and filtered off. Due to the nature of the precipitate, washing of the gels was difficult and hence the yields obtained were small. In an effort to increase the yields, fellow researchers increased the concentration of individual metal salts, and reacted with sodium hydroxides and carbonate (Miyata, 1980). Reichle (1985) further concentrated the magnesium and aluminium salt solution and precipitated the hydrotalcite in a very concentrated sodium hydroxide and carbonate solution. The synthesis was followed up by crystallisation from 65 to 350 °C for 18 h. The product obtained was well ordered, with a predictable morphology and surface area (Reichle, 1986). However, the disadvantage of using such concentrated solutions is the repeated washings that have to be carried out to free the alkali metal ions, especially when the LDH is used in catalytic applications (Rao ***et al.***, 2005).

The co-precipitation method is divided into two: low and high supersaturation (He ***et al***., 2005). Supersaturation conditions are reached by physical or chemical means, for example evaporation and pH variation respectively. Low supersaturation entails the slow addition of a mixed metal oxide solution to a second solution containing the anion to be intercalated, with concurrent pH regulation by the addition of the alkali solution (Aramendia ***et al.***, 2002; Prinetto ***et al.***, 2000; Corma ***et al.***, 1992; Meyn ***et al.***, 1990). In high supersaturation the mixed metal oxide solution is added to an alkaline solution of the required anion (Reichle, 1986; Constantino & Pinnavaia, 1995). Low supersaturation co-precipitation normally results in precipitates with a high crystallinity because the rate of crystal growth is higher than the rate of nucleation. The method allows precise control of the charge density [M^{II}:M^{III} ratio] of the LDH by means of pH control of the solution. On the other hand, high supersaturation results in a less crystalline product due to the high number of crystallisation nuclei. Constantino and Pinnavaia (1995)

prepared a series of Mg/Al compounds by the latter method. However, several drawbacks emanate from this method such as impurities $M(OH)_2$ and/or $M(OH)_3$ phases, and therefore ultimately the LDH product will have an undesired charge density (He ***et al.***, 2005).

Generally, co-precipitation products are amorphous with poorly ordered phase crystallites, which are gel-like and require a long drying time of 12 to 24 h in a temperature range of 60 to 120 °C (Reichle, 1986; Yang & Zhou, 2008). The formation of crystallites occurs in two stages: nucleation and aging. Hence, post-preparative treatments should be carried out on them, for instance aging, hydrothermal crystallisation, microwave and/or ultrasound-assisted crystallisation or a spray technique (Yang & Zhou, 2008). Ageing of the LDH suspension usually entails heating of the sample to between 25 and 100 °C or to a gentle reflux for several hours/days. Hypothetically, the process occurs through Ostwald ripening in which larger crystals grow at the expense of smaller ones. This is a thermodynamically driven process in which larger particles are more energetically favoured than smaller particles, and as the process proceeds the overall energy of the system is lowered.

In the hydrothermal treatment method, the LDH suspension is heated in a stainless steel autoclave under high pressure, i.e. 10 to 150 MPa, and/or at temperatures exceeding 120 °C (Braterman ***et al.***, 2004; He ***et al.***, 2005). The treatment facilitates the dissolution and recrystallisation of LDH through heating during LDH formation (Braterman ***et al.***, 2004). Hydrothermal treatment is usually carried out to achieve one of three objectives, i.e. preparation of LDHs, transformation of small cystallites into large ones, and transformation of amorphous precipitates into crystalline LDHs. Crystallinity of LDHs is essential for characterisation purposes (Cavani ***et al.***, 1991).

Microwave-assisted crystallisation was explored by Hussein ***et al.*** (2000) for the intercalation of Zn-Al LDHs with sodium dodecyl sulphate (SDS). The method was found to be favourable as it offered a shorter reaction time, as well as a product with a high surface area. However, the researchers (Hussein ***et al.***, 2000) noted that the results obtained from this work showed no significant differences in the

physico-chemical properties of the resulting intercalate, either prepared by conventional means or by microwave-assisted intercalation.

Modification of the co-precipitation method also includes hydrothermal synthesis of Mg–Al LDHs by urea hydrolysis (Rao ***et al.,*** 2005). This method offers the synthesis of LDHs with homogeneous size. The urea hydrolysis reaction was explored by Adachi-Pagano ***et al.*** (2003) in the preparation of mono-dispersed sub-micron-sized Mg/Al LDH. It was concluded from the work that a better product was obtained as compared with the co-precipitation method. Advantages of the method include control of particle size distribution and particle growth. Urea combines the following attributes to achieve its role as precipitating agent: it forms a homogeneous solution, it is a weak Bronsted base $pK_b = 13.8$, highly soluble in water and the hydrolysis rate is controlled by the temperature of the reaction (He ***et al.,*** 2005). Therefore, hydrolysis may be conducted slowly, leading to low supersaturation during precipitation as compared with NaOH precipitation. The mechanism (see equations 3 & 4) follows the hydrolysis of ammonium cyanate to ammonia, and carbonate to hydrogen carbonate giving a pH of approximately 9, which is suitable for the precipitation of hydroxides.

$$CO(NH_2)_2 \longrightarrow NH_4CNO \quad (3)$$

$$NH_4CNO + 2H_2O \longrightarrow (NH_4)_2CO_3 \quad (4)$$

The disadvantage of the above method is the incorporation of the carbonate anion, which is subsequently very difficult to eliminate.

Chimie douce reactions are topotactic, meaning the structural integrity of the reactants is preserved in the product; however, the composition changes. Delmas and Borthomieu (1993) prepared LDHs by this method from $NaNi_{1-y}Co_yO_2$ cobalt-substituted sodium nickelate ($0 \leq y \leq 0.5$). The sequence of events included oxidising hydrolysis of the cobalt-substituted sodium nickelate slab using NaClO and KOH; the γ-oxyhydroxide was reduced in the presence of the sodium salt of the desired anion and hydrogen peroxide to give LDH. A well-crystallised product was obtained from the method as compared with that obtained from precipitation methods.

The factors that affect preparative methods of LDHs are compared in Table 2.2.

Table 2.2: Factors influencing the synthesis of hydrotalcites (Cavani ***et al.,*** 1991; Trifiro ***et al.,*** 1996; Vaccari, 1998; Reichle, 1986)

Structural variables	**Preparation variables**
Cationic size	pH
Value of ***x*** i.e. M^{II}:M^{III} ratio	Precipitation method
Cation stereochemistry	Precipitation temperature
Cation mixture (nature and ratio)	Reagent concentration
Nature of interlayer anions	Aging
Amount of interlayer water	Washing and drying
Crystal morphology and size	Presence of impurities
	Nature and concentration of ionic species of the precipitating solution

2.4 Surfactant Nature and Aggregation

Surface-active agents (surfactants) are molecules with both a polar and non-polar segment (amphiphilic), e.g. alcohols, amides, alkylsulphates, alkylsulphonates, carboxylic acids and so on. They consist of different polarities, i.e. a hydrophilic head group and a hydrophobic tail (see Figure 2.2). The hydrophobic tail usually consists of an alkyl chain. The hydrophilic head is water-loving; the polar group and water molecules associate with each other by dipole or ion dipole interactions (Tadros, 2005). However, the same hydrophilic head shows very little compatibility with non-polar solvents. In contrast, the hydrophobic tail has a high affinity for non-polar solvents and a low affinity for polar solvents. To reduce contact of alkyl chains with the polar solvent, surfactant molecules aggregate, to form micelles. Hence, Texter (1999) defines surfactants as “surface active amphiphiles that aggregate in water and other polar solvents to form numerous microstructures such as micelles and bilayers”. The self-assembly of surfactant molecules into micellar aggregates occurs above the critical micelle concentration or CMC. The formation of such microstructures leads to the reduction of the free energy of the system (Tadros, 2005; Texter, 1999). Surfactants reduce the surface and interfacial tensions by adsorbing on available surfaces and interfaces

respectively. The surfaces on which surfactants adsorb are either between two liquids, liquid and gas or solid and liquid.

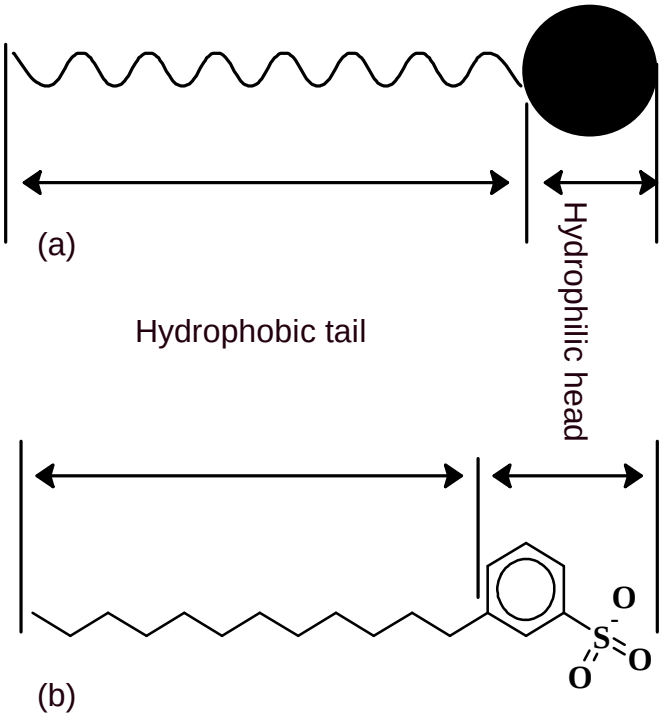

Figure 2.2: Illustration of different segments of (a) surfactant molecule (b) alkylbenzene sulphonate

Figure 2.3 shows various forms micellar aggregation; just above the CMC the micelles have a spherical shape with surfactant molecules arranged such that the hydrophilic part is on the outside and the hydrophobic part in the centre. As the concentration is increased, the micelles coalesce first to form elongated 'worm-like' tubes and later to convert into lamellar sheets of organised molecules.

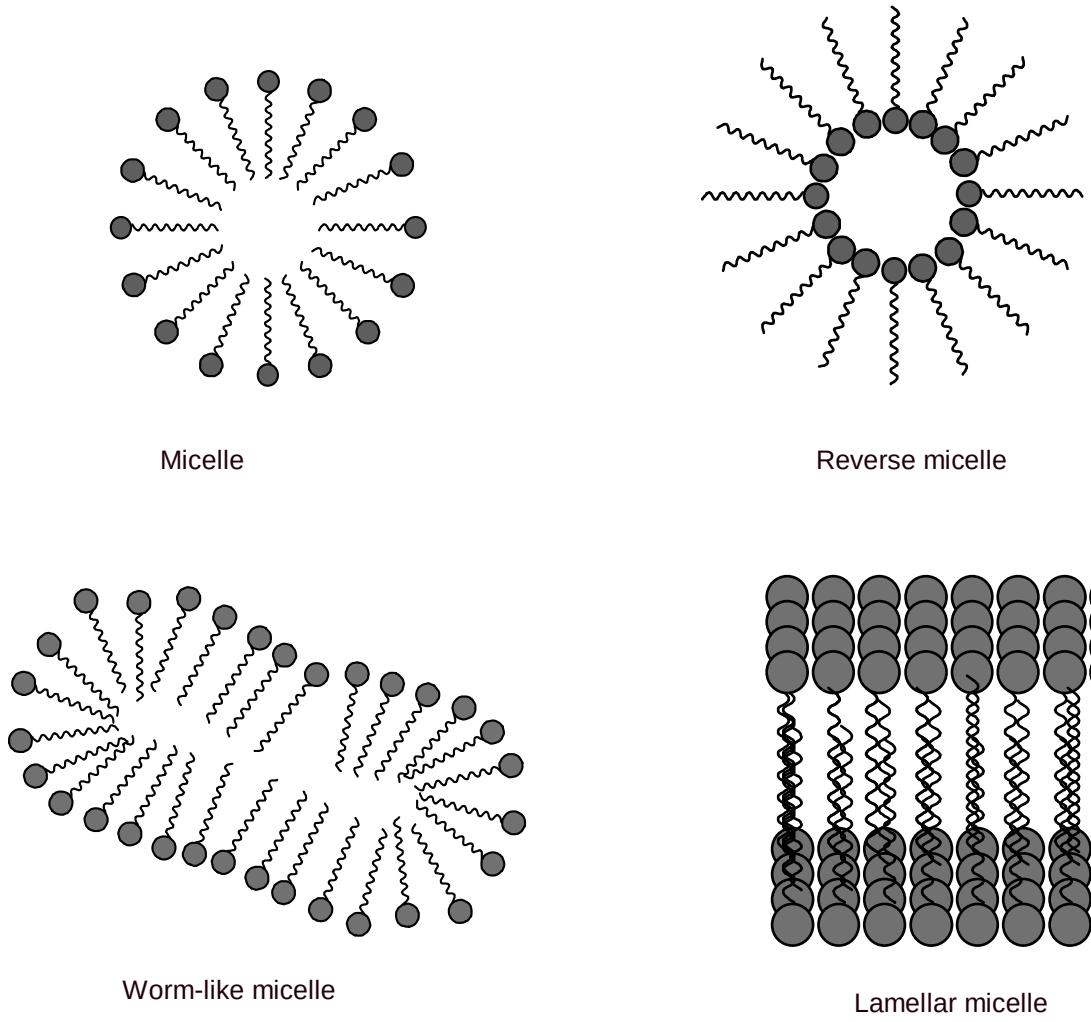

Figure 2.3: Micellar aggregation

Surfactants are classified according to their physical properties. These include overall size, ionicity and crystallinity. When functionality is the criterion of classification, the technological application of the surfactant is considered, e.g. emulsifiers, dispersants, anti-foaming and flocculating agents, and flotation agents (Texter, 1999). The most common classification is the ionicity or the charge carried by the head group of the amphiphile molecule. There are four classifications: anionic, cationic, amphoteric and non-ionic surfactants.

2.4.1 Anionic surfactants

Anionic surfactants have a linear alkyl chain with a polar head group that carries a negative charge. These include carboxylic acids, alkylsulphates, alkylsulphonates and phosphonates, to mention a few. They are manufactured on a large scale, are

widely used, and are relatively inexpensive compared with other surfactants. The most important members of this group are carboxylic acids, sulphates and sulphonates and these have been ranked according to hydrophilicity (Texter, 1999):

$$-CO_2^- << -SO_3^- < -OSO_2^-$$

Scheme 2.1 shows examples of sulphate and sulphonate anionic surfactants, which are normally salts of sodium.

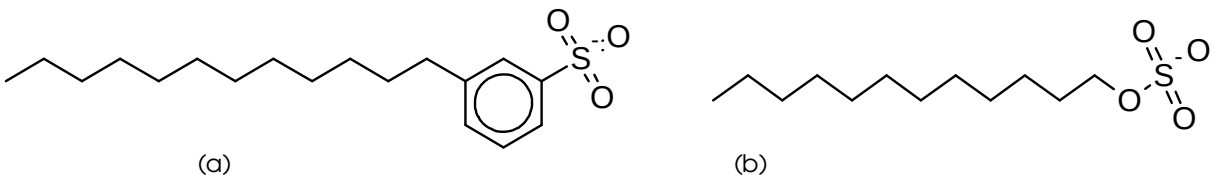

Scheme 2.1: (a) Dodecylbenzene sulphonate and (b) dodecyl sulphate

SDS is produced by sulphating lauryl alcohol with sulphuric acids. However, the most commonly used means of production is reaction of the alcohol with chlorosulphonic acid or a sulphur dioxide/air mixture (Tadros, 2005). Sodium dodecylbenzene sulphonate (SDBS) is prepared from several steps involving Friedel-Crafts alkylation of the benzene with linear alkane and sulphonation by a sulphur trioxide/air mixture, followed by neutralisation with sodium hydroxides or ammonia. Generally, the sulphonates are chemically stable compared with the sulphates as the latter are susceptible to hydrolysing to an alcohol in acidic conditions.

2.4.2 Cationic surfactants

Cationic surfactants carry a positive charge on the head group and hence they adsorb onto negative adsorbents. The most common members of the group are alkyl quaternary amines, e.g. alkyl ammonium halides such as dodecyl ammonia bromide (DAB) (see Scheme 2.2).

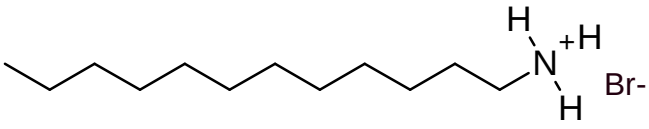

Scheme 2.2: Dodecyl ammonia bromide (DAB)

2.4.3 Amphoteric surfactants

Amphoteric surfactants are also referred to as zwitterions, and consist of both anionic and cationic groups in an individual amphiphilic molecule. This characteristic is dependent on the pH of the medium into which they are dissolved. In acidic conditions the surfactant molecule is positively charged, whereas in alkaline conditions the molecule bears a negative charge, rendering cationic and anionic properties respectively (Tadros, 2005). At the isoelectric point, the surfactant molecule carries both charges. This phenomenon is a result of intramolecular protonation (Texter, 1999) (see Scheme 3.3). Of importance in the group are the betaines.

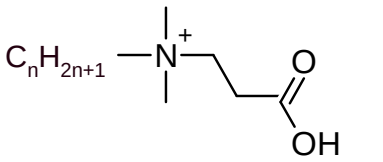

(a)

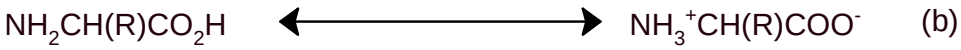

(b)

Scheme 2.3: (a) Betaine molecule and (b) intramolecular protonation of α-amino acids (Texter, 1999)

2.4.4 Non-ionic surfactants

Non-ionic surfactants have no charge on the head group of the surfactant molecule and are ethoxylated surfactants. These include alcohol ethoxylates, alkyl phenol ethoxylates, sorbitan ester ethoxylates, glycol esters and so on (see Scheme 2.4).

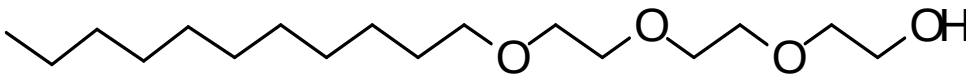

Scheme 2.4: Non-ionic surfactant with ethylene oxide (EO) and hydroxyl (OH) groups

2.5 Clay-surfactant interactions

Clay minerals offer two forms of solid surface for interaction with a surfactant molecule, i.e. intercalation and adsorption. Adsorption refers to the association or interaction of surfactant molecules on the outside of the clay particles, whereas intercalation refers to a scenario where the surfactant molecules aggregate in the interlayer, i.e. between pairs of adjacent clay sheets (Crepaldi ***et al.***, 2002).

2.5.1 Adsorption

The adsorption of surfactants is a type of aggregate formation on the mineral or solid surface. Harwell ***et al***. (1985) refer to these as 'admicelles' to emphasise the micelle-like aspects of their structure and behaviour. The degree of adsorption of dodecyl sulphate salts on oxide minerals is a function of pH, counterion type and counterion concentration (Bitting & Harwell, 1987). The formation of ionic surfactant aggregates is favoured at higher counterion concentrations. Monovalent counterions tend to adsorb between the surfactant aggregate and the mineral surface. The extent of adsorption is dependent on the pH, as well as on the nature of the counterion. It is determined by both steric and surface complexation effects. The planar geometry of the admicelles present is expected to provide more favourable steric interactions compared with the spherical micelles in the bulk solution (Harwell ***et al.***, 1985; Bitting & Harwell, 1987). Pavan ***et al.*** (1999) also discuss the various factors that affect surfactant adsorption on mineral oxides. Amongst these are the nature of the structural groups, the molecular structure of the surfactant and the environment of the aqueous phase.

To provide clarity on the manner in which the adsorption of surfactants takes place on the mineral oxide surface, a model in which the adsorption isotherm is divided into four regions is used (Bitting & Harwell, 1987; Pavan ***et al.***, 1999). Figure 2.4

illustrates a typical adsorption isotherm, showing the adsorption regions and the orientation of the surfactant monomers on the mineral oxide surface. Region I is characterised by low surface coverage of the surfactant. Region II represents the onset of aggregate formation, shown by the rapid increase in adsorption with concentration, giving rise to microstructures referred to as 'admicelles' or 'hemimicelles'. The decrease in the slope observed in Regions III and IV is thought to be attributable to the electrostatic repulsion of ions or monomers. This occurs at the CMC or upon completion of the bilayer coverage of the surfactant (Bitting & Harwell, 1987).

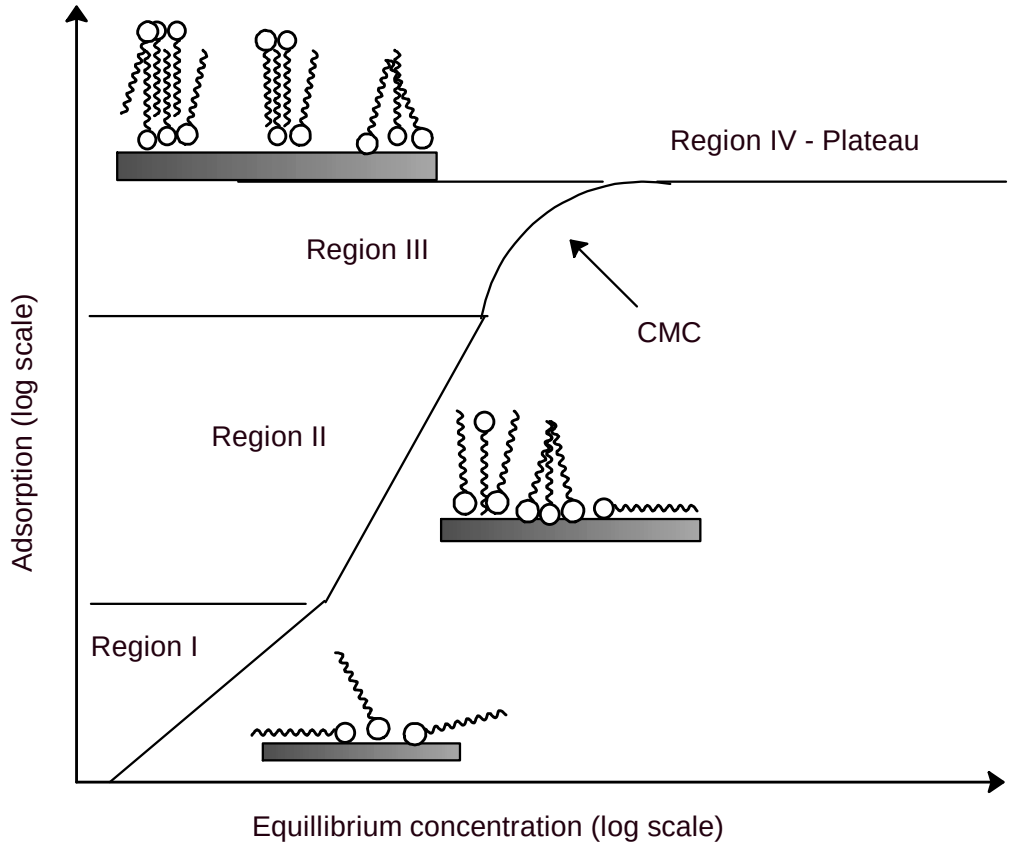

Figure 2.4: Adsorption regions and orientation of surfactant monomers on mineral oxide surface (Bitting & Harwell, 1987; Pavan ***et al.,*** 1999)

Pavan ***et al.*** (2000) concluded that the adsorption on LDH emulates the surfactant adsorption behaviour on mineral oxides with respect to the effects of pH, counterion type and ionic strength (Bitting & Harwell, 1987). The adsorption of surfactants such as sodium dodecyl sulphate (SDS) and sodium dodecylbenzene sulphonate (SDBS) on LDH-CO_3 results in hydrophobisation of the surfaces

(Pavan ***et al.***, 1998, 1999 & 2000; Dèkány and Haraszti, 1996; Dèkány ***et al.***, 1997). Pavan ***et al***. (2000) clearly state that these surfactants do not intercalate when the LDH contains the difficult-to-exchange carbonate anion. The diffraction patterns of the LDH remained unchanged after adsorption and hence the LDH-CO_3 maintains its original basal spacing, leading to the conclusion that the interlamellar carbonate anions were not substituted by the SDS anions. This was substantiated by Ulibarri ***et al.*** (2001) with respect to the interaction between SDBS and Mg_3Al-LDH-CO_3 under ambient conditions. In addition to the factors that affect adsorption, temperature is found to play a pivotal role. SDS was found to adsorb at 25 °C (Pavan ***et al.***, 2000), while some intercalation was observed when the reaction mixture was heated to 70 °C (Anbarasan ***et al.***, 2005). SDBS, however, did not intercalate at the latter temperature (Anbarasan ***et al.***, 2005; Dos Reis ***et al.***, 2004), but partial replacement of carbonate did occur under reflux conditions and at very long reaction times (Xu & Braterman, 2003). The high affinity of LDH for the carbonate ion prevents the latter's displacement by the sulphonate ions, even at high contact temperatures. Xu and Braterman (2003) argue that the replacement of carbonate with RSO_3^- is kinetically, rather than thermodynamically, controlled as the carbonate is very tightly bonded (Colvin ***et al***., 1992; Fendler & Meldrum, 1995) and its removal requires the scaling of a high activation energy.

2.5.2 Intercalation

Intercalation is defined as the reversible insertion of mobile guest species into a crystalline host lattice, during which the structural integrity of the latter is formally conserved (O'Hare, 1991) (see Figure 2.5). It has also been described as a form of reversible topochemical process (Whittingham, 1979; Schollhorn, 1980). The 2-D framework of LDHs provides great flexibility as to the size of the guest species that can be intercalated. The overall positive charge results in there being a wide selection of suitable modifiers, for example carboxylic acids, sulphates, sulphonates, phosphonates and various organic anions. Intercalation generally proceeds at intermediate temperature, as high temperatures lead to an unstable matrix which may result in irreversible structural alteration. In the case of low temperatures, the reaction is inhibited, as the activation energy barrier for diffusion will be high (Schollhorn, 1980).

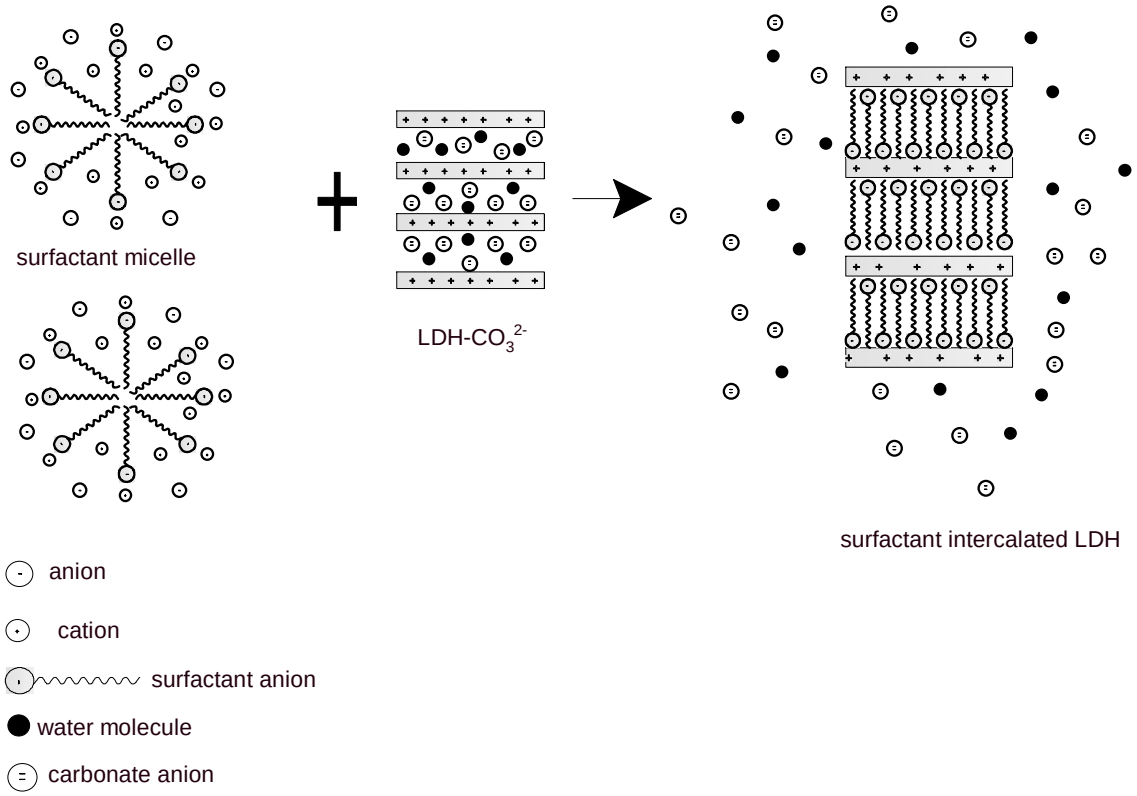

Figure 2.5: Schematic presentation of the intercalation process

The aim of intercalation is to increase the interlayer spacing; this is achieved by the insertion of exchangeable anions within the interlayer. The insertion of these anions results in the reduction of the solid-solid interaction within the clay layers. This is essential as the Van der Waals interaction between solid surfaces decreases with the square of the separating distance (Utraki, 2004). It also improves the interaction of the clay with the polymer matrices; moreover, this helps in the making the polymer–nanocomposites (Utraki, 2004). The insertion of anions such as surfactants functionalises the clay by converting the hydrophilic nature of the interlayer into a hydrophobic one. Consequently, non-polar and low-water-soluble organic molecules may be absorbed into the interlayer.

With regard to the anions that can be intercalated, there is no limitation, provided that the anion does not cause any distortion of the LDH lattice, e.g. by extracting metals ions from the lattice. An additional factor is that there must be sufficient

charge density within the lattice. Table 2.3 shows some of the anions that have been successfully intercalated.

Table 2.3: Summary of anions intercalated from the literature

Group	Example of anion	Reference
Inorganic anions	halides (X^-), CO_3^{2-}, NO_3^-, OH^-, SO_4^{2-}, $Al(OH)_4^-$	(Xu & Zeng, 2001)
Organic anions	carboxylates benzenecarboxylates alkysulphates and alkanesulphonates glycolate	(Meyn ***et al.***, 1990; Carlino, 1997; Newman & Jones, 1998, Chibwe & Jones, 1989; Boehm ***et al.***, 1977)
Polymeric anions	poly(vinylsulphonate), poly(styrene sulphonate), poly(acrylate)	(Oriaki ***et al.***, 1996)
Complex anions	$CoCl_2^-$, $NiCl_2^-$ $Fe(CN)_6^{4-}$	(Lopez-Salinas & Ono, 1993; Crespo ***et al.***, 1997)
Macrocyclic ligands and their metal derivatives	Porphyrin and phthalocyanine with their Cu^{2+} and Zn^{2+} complexes	(Robins & Dutta, 1996)
Iso- and heteropolyoxometalates (POM)	$Mo_7O_{24}^{6-}$ $W_7O_{24}^{6-}$	(Gardner ***et al.*** 1998; Drezdon, 1998)
Biochemical anions	Amino acids DNA with 500–1 000 base pairs ATP, ADP and related species	(Choy ***et al.***, 1999; Choy, 2004; Fudala ***et al.***, 1999; Whilton ***et al.***, 1997)

2.6 Surfactant Intercalation

The direct intercalation method, or 'spontaneous self-assembly' (Messersmith & Stupp, 1995), employs synthesis by a co-precipitation technique in which the anion

is included in the reaction solution, followed by aging. Self-assembly is facilitated by electrostatic attraction, chemisorption, hydrophobicity and hydrophilicity (Whitesides ***et al.*** 1991). In the co-precipitation methods, the metal hydroxide layer is grown from an aqueous solution of the metal salts, in the presence of the anion to be exchanged, under basic conditions facilitated by sodium hydroxide. The desired anion must have a high affinity for the hydroxide layer. Generally, metal nitrates and chlorides are easily exchangeable. pH plays a pivotal role in the nucleation and growth of the hydroxide layer and hence the pH is kept constant.

Intercalated LDHs can be prepared by direct synthesis methods, e.g. hydrothermal crystallisation of gels formed by the co-precipitation of the M^{2+} and M^{3+} hydroxides in the presence of the required organic anion (Crepaldi ***et al.***, 2002; Xu & Braterman, 2003; Drezdon, 1988; Clearfield ***et al.***, 1991; Zhao & Nagy, 2004; Trujillano ***et al.***, 2005). Hussein ***et al.*** (2000) used microwave heating to accelerate the co-precipitation-driven intercalation of SDS into Zn_4Al-LDH.

Indirect intercalation involves the modification and treatment of the host and finally the insertion of the guest molecules within the layer. Crepaldi ***et al.*** (1999) identified three main indirect techniques: (i) direct anion exchange; (ii) LDH reconstruction from a layered double oxide form obtained by calcinations of a suitable precursor; and (iii) anion replacement by elimination of the precursor interlamellar species.

2.6.1 Direct ion exchange

Miyata & Kumura (1973) pioneered direct ion exchange. The pristine LDH (LDH-CO_3) is first modified by incorporating an easily exchangeable anion, A^-. The anions that are normally used in this intermediate step are monovalent, such as chlorides (You ***et al.***, 2002a and 2002b) and nitrates (Kopka ***et al.***, 1998; Meyn ***et al.***, 1990; Boehm ***et al.***, 1977; Drezdon, 1988). This class of anions is easily exchangeable as they exhibit weak electrostatic force interactions with the layer. The carbonate anion is divalent and is held tightly to the hydroxyl layers; hence, it is very difficult to exchange. The ease of anion exchange with the interlayer is as follows according to Miyata (1977) and Carlino (1997):

$$CO_3^{2-} >> SO_4^{2-}$$

$OH^- > F^- > Cl^- > Br^- > NO_3^- > I^-$

Consequently, the carbonate anion becomes a major contaminant in intercalation chemistry of hydrotalcites.

Intercalation entails the incorporation of the anion into the LDH-A by direct contact with the desired surfactant solution of the appropriate concentration (Kopka ***et al.***, 1988; Meyn ***et al.***, 1990; Xu & Braterman, 2003; Boehm ***et al.***, 1977; Clearfield ***et al.***, 1991; Zhao & Nagy, 2004; You ***et al.***, 2000b; Venugopal ***et al.***, 2006; Crepaldi ***et al.***, 2000). Kopka ***et al.*** (1988) dealt with the anion exchange of Zn_2Cr-LDH-NO_3 with alkyl sulphate ions [$C_nH_{2n+1}SO_4^-$ with ***n*** = 6, 8 -18], including dodecyl glycol ether sulphate ions [$C_{12}H_{25}(OCH_2CH_2)_nSO_4^-$ with ***n*** = 0, 1, 2, 4]. The exchange reaction of the anionic species investigated was claimed to proceed to 90–95% in theory. The authors describe co-intercalation of the alkyl sulphate ion and alkanols (alcohols), hence forming a bimolecular layer orientation of the guest molecules in the interlayer. The d-spacings of the dodecyl ethoxysulphate and the dodecyl diethoxysulphate with dodecyl alcohol were 43.6 and 46.7Å respectively. Water and small organic molecules, e.g. diols, N-methylformamide (NMF), dimethyl sulphoxide (DMSO), etc., were also co-intercalated.

Meyn ***et al***. (1990) studied the intercalation of anionic surfactants by such anion exchange into a wide range of LDH compounds. They observed that dodecylbenzene sulphonate (DBS) intercalated as monolayers, while secondary alkyl sulphonates intercalated as bimolecular layers. They proposed that the smaller equivalent area causes the anionic surfactant chains to point away from the interlamellar surfaces, hence intercalated anions lie perpendicular to the layers. The theoretical calculated d-spacing is 26.9 Å for DBS-intercalated LDH based on the perpendicular orientation of the anion within the layers. The observed d-spacing ranged from 26.8 to 30 Å (Meyn ***et al***., 1990).

Crepaldi ***et al.*** (2002) prepared both sulphated and sulphonated substituted Zn (II)-Cr (III) – LDH by an ion exchange method, based on the formation and organic phase extraction of a salt between dodecyl sulphate and a cationic surfactant. They reported an intercalation efficiency that exceeded 98.5%. This was achieved

within 30 minutes of contact time. The results obtained from this work were in good agreement to the work carried out by Boehm (1977) and Drezdon (1988) for the product maintained at a constant pH of 7±0.2.

Clearfield ***et al***. (1991) worked with nickel aluminium hydroxychlorides, using magnesium aluminium hydroxychlorides and zinc chromium hydroxychlorides for the intercalation of SDS. In this investigation it was found that the basal spacings obtained were 26, 36 and 47 Å for the LDH-SDS. As the pH of the exchange solution increased, so did the basal spacing, but the amount of SDS in the interlayer decreased with the increase in the pH. The different basal spacings are therefore attributed to the arrangement of the dodecyl sulphate within the layer, i.e. 26 Å results from the dodecyl sulphate anions perpendicular to the LDH layer in a monolayer array; 36 Å contain a bilayer of the dodecyl sulphate in which the layers partially overlap; and in 47 Å the dodecyl sulphate chains are perpendicular to the layers in a bilayer end-to-end arrangement. This work concluded that there are several possible arrangements of dodecyl sulphate chains in LDHs depending on the exchange pH. By contrast, Zhao & Nagy (2004) concluded that it was not only the pH of the exchange solution that had an effect on the basal spacing, but also the Mg:Al molar ratio of the LDH.

The intercalation reaction for a surfactant such as SDS into LDH-Cl may be expressed as follows (Takagi ***et al.***, 1993):

$$R\text{-}OSO_3^-Na^+_{(aq)} + clay^+Cl^- \xrightarrow{K_f} R\text{-}OSO_3^-clay^+ + Na^+_{(aq)} + Cl^-_{(aq)}$$

where

K_f defines the equilibrium constant for the intercalation reaction.

You ***et al***. (2000b) investigated the intercalation of sodium octyl sulphate (SOS), sodium dodecyl sulphate (SDS), 4-octylbenzene sulphonate (SOBS) and sodium dodecylbenzene sulphonate (SDBS) into Mg_3Al-LDH-Cl via ion exchange in an aqueous medium. They found that the equilibrium amount of surfactant intercalated decreased in the order SDS > SOBS > SDBS > SOS. SOS formed

bilayers, but the other surfactants exhibited monolayer arrangements. Moyo ***et al***. (2008) suggest that this behaviour is due to the hydrolysis of the dodecyl sulphate to an alcohol form.

Xu & Braterman (2003) suggest a high affinity of DBS for LDH in which the sulphonate is taken up in preference to chloride and partly replaces the carbonate on refluxing. Thus kinetics and thermodynamics are both important in the intercalation of surfactants into the LDH. The sulphonate anion exhibits superior selectivity to the sulphated surfactant, and equally comparable to the carbonate anion. This is attributed to the hydrophobic interactions which reinforce the stability of the intercalate. The intercalated DBS product had a d-spacing of 3.05 nm, consistent with anti-parallel monolayer packing of interpenetrating chains.

Anbarasan ***et al***. (2005) attempted the direct ion exchange reaction using Mg_2Al-LDH-CO_3 at 70 °C. They found no evidence for the intercalation of SDBS. The XRD spectrum of the product obtained using SDS features new peaks at lower angles, consistent with a basal spacing of 2.09 nm, which the researchers interpret as evidence of a monolayer intercalation of SDS.

True ion exchange is a topotactic reaction, implying that any layer-stacking defects in the precursor will also appear in the pillared LDH product (Williams ***et al.***, 2004; Dimotakis & Pinnavaia, 1990). Another proposed mechanism by which ion exchange occurs is a two-step process involving dissolution of the LDH and recrystallisation of the new LDH with the exchanged anions (Palmer ***et al.***, 2009). Xu & Braterman (2003) observed changes in crystal habit on intercalating SDS in LDH at elevated temperatures. This implies that at least some recrystallisation must have accompanied the intercalation process. Other suggestions regarding the direct ion exchange mechanism include first-order kinetics and a two-step process involving the adsorption of the desired anion and the desorption of the initial anion (Palmer ***et al.***, 2009; Kooli ***et al.***, 1997).

2.6.2 Rehydration/reconstruction/regeneration

This is a procedure which entails the intercalation of the anion with calcined LDH (CLDH) to obtain the desired LDH by rehydration/regeneration. The resulting

layered double oxide (LDO/CLDH) has the following advantageous attributes: basic properties, higher anion exchange capacity, larger surface area and reconstruction of the LDO under mild conditions by memory effect. The memory effect is an attribute that is limited to specific LDHs, e.g. Mg-Al-LDHs and Zn-Al-LDHs. The LDOs formed are homogeneously mixed, thermally stable and have small crystallites (Cavani ***et al.***, 1991). The LDH is subjected to thermal treatment at a temperature of 400–450 °C (see Figure 2.6). At this temperature, it is believed that dehydroxylation and decarbonation occur, leading to an amorphous mixed oxide of the LDH. The LDO is reconstructed into an intercalated form by treatment with an aqueous solution of the desired anion, carried out in deionised water and with total exclusion of CO_2. The reaction mixture is therefore refluxed under nitrogen (Dimotakis & Pinnavaia, 1990).

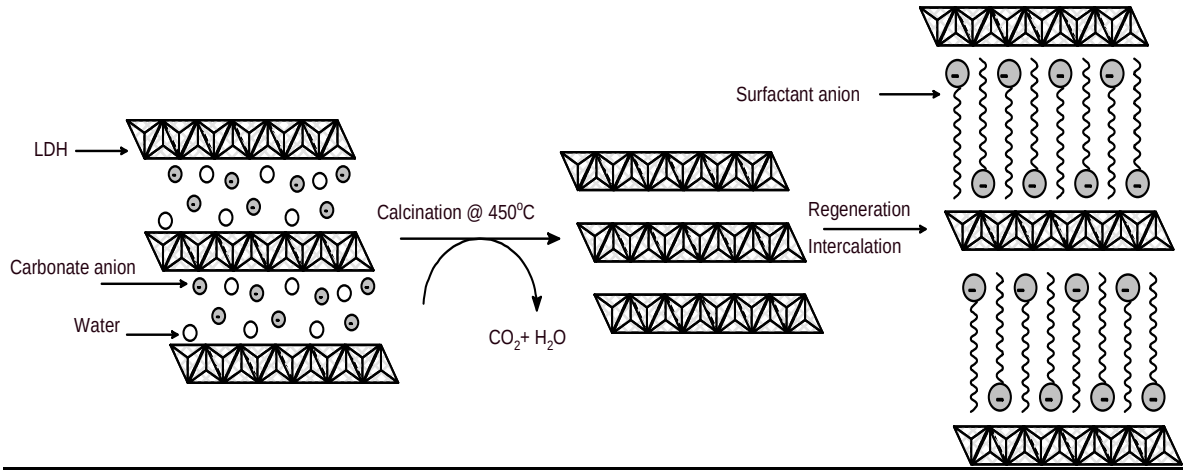

Figure 2.6: Schematic representation of the regeneration process

The regeneration process follows a fast rehydration mechanism of the oxide with intercalation of the hydroxyl anions, and finally the exchange of the latter with the desired anions (Crepaldi ***et al.***, 2002; Sato ***et al.***, 1988). The process is typical of the topotactical nature of regeneration. Stanimirova & Kirov (2001) argue that regeneration occurs through dissolution of Mg/Al-solid solution and successive LDH recrystallisation.

Chibwe & Jones (1989) synthesised polyoxymetalate-pillared LDHs by the regeneration method in which the calcined precursor is exposed to a solution of the pillaring anions. On the other hand, Dimotakis & Pinnavaia (1990) describe

exchange into LDH-OH as being facilitated by the presence of glycerol as a swelling agent. Despite all the achievements in this form of intercalation, You ***et al***. (2000b) and Costa ***et al***. (2008) point out the shortcomings of the reconstruction method such as strange surface morphologies and loss of crystallinity. With regard to the intercalation of organic anions, mixed phases may be synthesised (Chibwe & Jones, 1989) and the formation of the carbonate form is almost unavoidable. Hibino & Tsunashima (1998) proved that reconstruction of the calcined LDH is not totally reversible, evidenced by the fact that the intercalated carbonate content reduces with each successive calcination and regeneration in a solution of Na_2CO_3. The surface morphology of the intercalates appears perforated or shows signs of secondary growth of smaller layers (Costa ***et al.***, 2008). However, when one examines the XRD data it is plain to see that in the regeneration method there is a loss of crystallinity, as reflected by the broadening of peaks. Such a loss was observed by Costa ***et al***. (2008), You ***et al***. (2000b), Stanimova ***et al.*** (2001) and Hibino & Tsunashima (1998). It is also evident from the present study that the reconstruction method holds additional drawbacks for the intercalation of SDS.

2.6.3 Elimination

This method entails the elimination of the interlamellar anion and ultimately, replacement with desired anion. The interlamellar anion in this instance must be susceptible to acid attack. Carlino & Hudson (1994, 1995), Carlino ***et al.*** (1996), Crepaldi ***et al***. (2000) and Iyi ***et al***. (2005) cite the removal of the carbonate anion by acid attack. Carlino & Hudson (1995) found that the mechanism relies heavily on the concentration of the organic acid when used in the thermal melt method. Iyi ***et al***. (2005) postulated a two-step mechanism involving protonation of the carbonate ions into hydrogen carbonate with the instantaneous inclusion of anions in solution. Iyi ***et al***. (2005) deintercalated carbonate ions using salt-HCl mixed solutions with sodium salt containing various monovalent ions.

The negative aspects of the method that have been brought to light include the strong acidity of HCl, the low acid tolerance of MgAl-LDH and difficulty with the handling of HCl in large-scale experiments. This led Iyi & Sasaki (2008) to explore the deintercalation of the carbonate anion using an acetate buffer (sodium acetate

and acetic acid/NaCl mixed solution). The use of an acetate buffer alone did not yield the desired results. Nevertheless, the addition of NaCl resulted in decarbonation, with the reaction proceeding with no morphological change at 25 ºC. It was concluded that the charge density of the LDH and the acid species play a vital role in the ease of decarbonation (Iyi ***et al.***, 2005; Iyi & Sasaki, 2008). Deintercalation was achieved with ease for the LDH with Mg/Al~3 as compared with the LDH with Mg/Al~2 (Iyi & Sasaki, 2008). Constantino ***et al***. (1998) deintercalated carbonate anions by allowing gaseous HCl to flow over hydrotalcite-like compounds at 150 °C.

This method has, as far as could be ascertained, not yet been used to intercalate anionic surfactants of the sulphate or sulphonate type.

2.7 Orientation of Intercalated Anions

The anions orient themselves in such a way that they maximise their interaction with the positively charged hydroxide layer. This feature is reflected in the interlayer spacing and is normally valid for 3R stacking, also denoted by the $\boldsymbol{d}_{003}$ value. In pristine LDH, CO_3^{2-} anions lie parallel to the hydroxide layer to ensure utmost interaction between the oxygen atoms and the layer by forming hydrogen bonds. Hence, the electrostatic interaction between the anion and the brucite-like layer is optimised (Braterman ***et al.***, 2004). Carboxylate and sulphate/sulphonate heads attach to the hydroxide layer, whilst the alkyl chains are tilted at an angle. The preferred tilt angle is approximately 55° for optimal contact between the head and the layer (Kopka ***et al.***, 1988; Braterman ***et al.***, 2004).

There are three possible assemblies: monolayer, bilayer and partial overlap packing (see Figure 2.7). The monolayer arrangement in surfactant-intercalated LDH is actually interdigitated anti-parallel half-monolayers (Xu & Braterman, 2003; Takagi ***et al.***, 1993). Generally, the monolayer assembly is easily formed when the ratio of the anion/M^{3+} approaches unity, whereas the bilayer formation is dictated by the presence of excess carboxylate, incorporated as free acids at higher pH (Braterman ***et al.***, 2002). Clearfield ***et al***. (1991) noted the partial overlap in alkyl-sulphates as a result of an increase in the intercalation pH. In contrast, Xu &

Braterman (2003) found that this conformation is linked to non-linear geometry of the alkenyl chain, as in the case of LDH cis-oleate (Braterman ***et al.***, 2004).

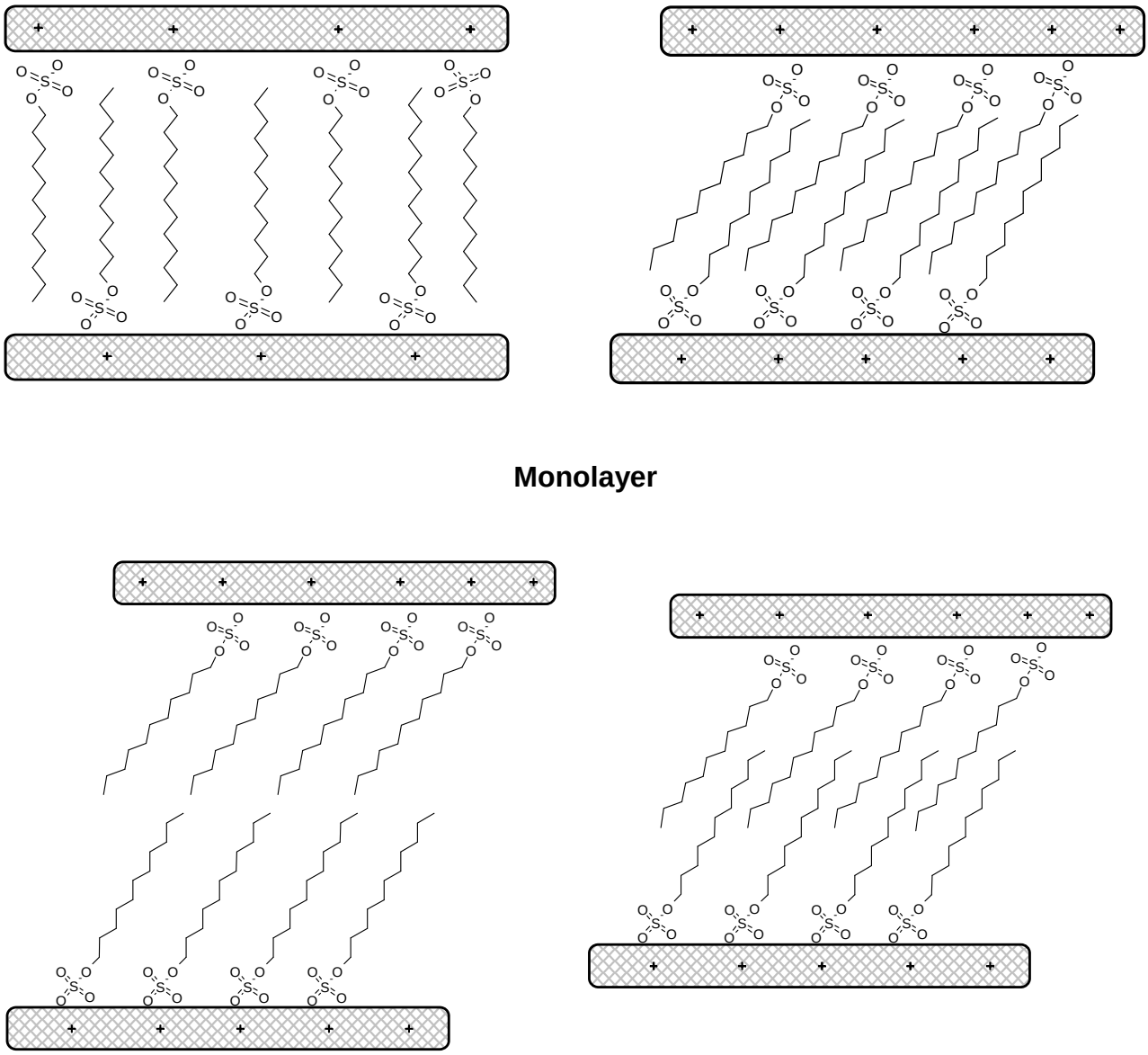

Monolayer

Bilayer **Partial overlap**

Figure 2.7: Orientation of anions in the interlayer

The basal spacing estimation equation for mono- and bilayer intercalated clays was derived by Kopka ***et al***. (1988) based on the following assumptions: (i) alkyl chain substituents assume an extended chain conformation; (ii) the methylene bond length equals 0.127 nm; and (iii) the slant angle is independent of the chain length.

Monolayer: $d_L = d_0 + d_1 + d_2 + 0.127\boldsymbol{n}\cos\alpha$ (5)

Bilayer: $d_L = 2d_0 + 2d_1 + d_3 + 0.254\boldsymbol{n}\cos\alpha$ (6)

where:

d_L is the basal spacing

n is the number of carbon atoms in the alkyl chain

α is the chain tilt angle to the hydroxyl layer

d_0 is the vertical dimension of the head group, taking into account its intercalated orientation

d_1 and ***d_2*** are the distances between the two facing terminal (ionised) head groups and tail ends respectively, although these are subject to change due to absorbed water, solvents or ions in the interlayer

d_3 is the distance between the two facing terminal methyl groups in bilayer structures

In the intercalation of alkyl arylsulphonates, e.g. dodecylbenzene sulphonate (DBS), Meyn ***et al.*** (1990) and You ***et al***. (2000b) suggest that the benzene ring is tilted towards the layer, with the extended alkyl chain in a perpendicular position (see Figure 2.8).

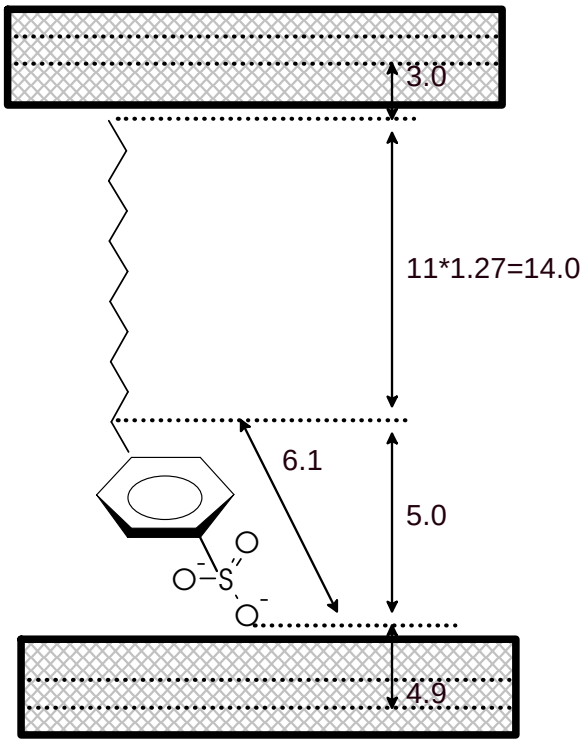

Figure 2.8: Schematic presentation of the theoretical calculation of the d-spacing (adapted from Meyn et al., 1990)

Conversely, Xu & Braterman (2003) and Zhao & Nagy (2004) contend that (i) the benzene rings are oriented perpendicularly to allow for three-point attachment of the sulphonate group to the hydroxide layer, and (ii) that the alkyl chains are tilted at ca. 56° with respect to the layer planes in order to facilitate their close packing. These authors state that such an anti-parallel arrangement reduces the electrostatic repulsion between the anion head groups and effectively maintains the hydrophobic interactions between the hydrocarbon chains. The two different proposals were examined by plotting the basal spacing against the chain carbon number (see Figure 2.9).

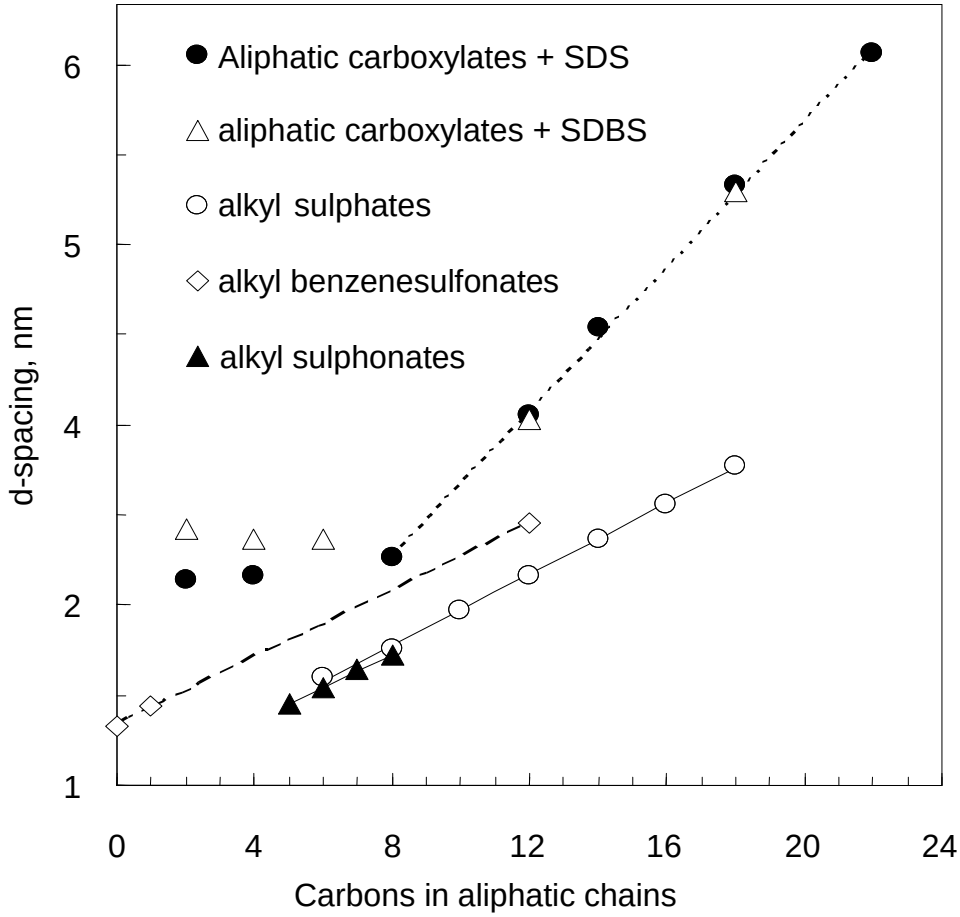

Figure 2.9: Effect of alkyl chain length on the basal spacing: (▲) Alkyl sulphonates in Mg_2Al-LDH (Xu & Braterman, 2007); (○) alkyl sulphates in Zn_2Al-LDH (Kopka ***et al.***, 1988); (◊) alkylbenzene sulphonates in Mg_2Al-LDH (Meyn ***et al.***, 1990); LDH-"carboxylates" prepared in the presence of SDS (•) or SDBS(Δ) this work and Nhlapo ***et al***. (2008) and Moyo ***et al.***, 2008)

The tilt angle can be calculated from knowledge of the type of intercalation and the slope of the d_L versus carbon number plot (see equations (5) and (6)). Using the least squares method for fitting the data shown in Figure 2.9 yields α values of 60.0°, 68.8° and 61.8° for alkylsulphonates in Mg_2Al-LDH (Xu & Braterman, 2007), alkyl sulphates in Zn_2Al-LDH (Kopka ***et al.***, 1988) and alkylbenzene sulphonates in Mg_2Al-LDH (Meyn ***et al.***, 1990) respectively. Although the values obtained are higher than the expected angle of 56°, the result substantiates Xu & Braterman's (2003) theory.

Table 2.4: Effect of the intercalation method and Mg:Al ratio on the d-spacing of LDH-DS and LDH-DBS

Intercalation method	**d-spacing[1] (nm)**		**Reference**
LDH Mg:Al ratio	**LDH-DS**	**LDH-DBS**	
Reconstitution			(Chibwe & Jones, 1989)
0.250		2.64	(You ***et al.***, 2000a)
0.250		3.01	(Ulibarri ***et al.***, 2001)
0.330	2.68	2.95	(Costa ***et al.***, 2008)
0.333	2.62	2.95	(Bouranda ***et al.***, 2008)
0.340	2.6		(Pavan ***et al.***, 2000)
Co-precipitation			
0.171	4.03		(Zhao & Nagy, 2004)
0.205	3.66		(pH = 10)
0.250	2.63		(Drezdon, 1998)
0.250		2.68	(Wang ***et al.***, 2005)
0.254	2.54		(Zhao & Nagy, 2004) (pH = 10)
0.290	2.63		(Jobbágy & Regazzoni, 2004)
0.301	2.60		(Zhao & Nagy, 2004) (pH = 10)
Ion exchange			
0.171	2.92		(Zhao & Nagy, 2004))
0.175		2.74	(You ***et al.***, 2000a)
0.204		2.74	
0.205	2.78		(Zhao & Nagy, 2004)
0.250	2.27	2.66	(You ***et al.***, 2000b)
0.250		2.95	(Meyn ***et al.***, 1990)
0.254	2.43		(Zhao & Nagy, 2004)
0.256		2.66	(You ***et al.***, 2000b)
0.301	2.58		(Zhao & Nagy, 2004)
0.323	2.09	Failed[2]	(Anbarasan ***et al.***, 2005)
0.333	2.42	2.96	(Venugopal ***et al.***, 2006)
0.333	2.6		(Hu & O'Hare, 2005)
0.333		2.87	(You ***et al.***, 2000a)
0.333		3.05	(Xu & Braterman, 2003)

[1]Where applicable as prepared before drying. [2] Intercalation failed.

Table 2.4 shows a considerable spread in the basal spacings of LDH-DS and LDH-DBS that have been reported in the literature. From the data collected it is evident that the d-spacing of LDH-CO_3 and its intercalated derivatives is due to a number of factors. The main disparity is caused by the degree of hydration, which is simply related to the presence and absence of water in the interlayer (Kopka ***et al.***, 1988; Meyn ***et al.***, 1990; Newman & Jones, 1998; Pesic ***et al.***, 1992). This includes variation caused by the drying technique used, together with the effect of temperature on drying. Vacuum drying at 65 °C was discovered to reduce the basal spacing by 0.3 nm owing to removal of the adsorbed water from the interlayer (Meyn ***et al.***, 1990). The presence of interlayer water was found also to affect the tilt angle of the aliphatic chain (Newman & Jones, 1998). Zhao & Nagy (2004) investigated the influence of pH on the d-spacing of intercalates prepared by co-precipitation. LDH-DS interlayer spacing is said to be affected by the method of synthesis (Newman & Jones, 1998), the LDH Mg:Al ratio (Zhao & Nagy, 2004) and the intercalation pH (Clearfield ***et al.***, 1991; Zhao & Nagy, 2004). Clearfield ***et al***. (1991) found that as the exchange pH increased, so did the basal spacing, although the amount of SDS in the interlayer decreased. The mentioned anomalous behaviour has been explained as the hydrolysis of the sulphate substituent to an alcohol, in alkaline conditions (Moyo ***et al.*** 2008).

2.8 Characterisation Techniques

There are several analytical techniques available for the characterisation of LDHs. These include powder X-ray diffraction, Fourier transform infrared spectroscopy (FT-IR), thermogravimetry (TG), differential scanning calorimetry (DSC), scanning electron microscopy (SEM) and transmission electron microscopy (TEM). Other analyses are Raman spectroscopy, differential thermal analysis (DTA), nuclear magnetic resonance (NMR), electron spin resonance (ESR), extended X-ray absorption fine structure (EXAFS), X-ray absorption near edge structure (XANES), Mössbauer spectroscopy, UV/VIS spectroscopy, neutron scattering, TG coupled with mass spectrometry (TG-Mass Spec) and BET, just to mention a few. The use of a combination of techniques helps in the elucidation of the LDH structure and composition, and the orientation of the interlayer anions. The techniques discussed below are those that were used in the present study.

2.8.1 X-ray diffraction (XRD)

Powder X-ray diffraction is the main technique used for the characterisation of LDHs. X-rays interacts with the LDH material, creating secondary diffraction beams of the X-rays, and these are related to the interplanar spacing of the powder sample. When the scattered waves interfere constructively, the relationship is summed up mathematically by Bragg's Law (see Figure 2.10):

$$n\lambda = 2d\sin\theta \qquad (7)$$

where:

n is an integer

λ is the wavelength of the X-rays

d is the interplanar spacing generating the diffraction

θ is the diffraction angle

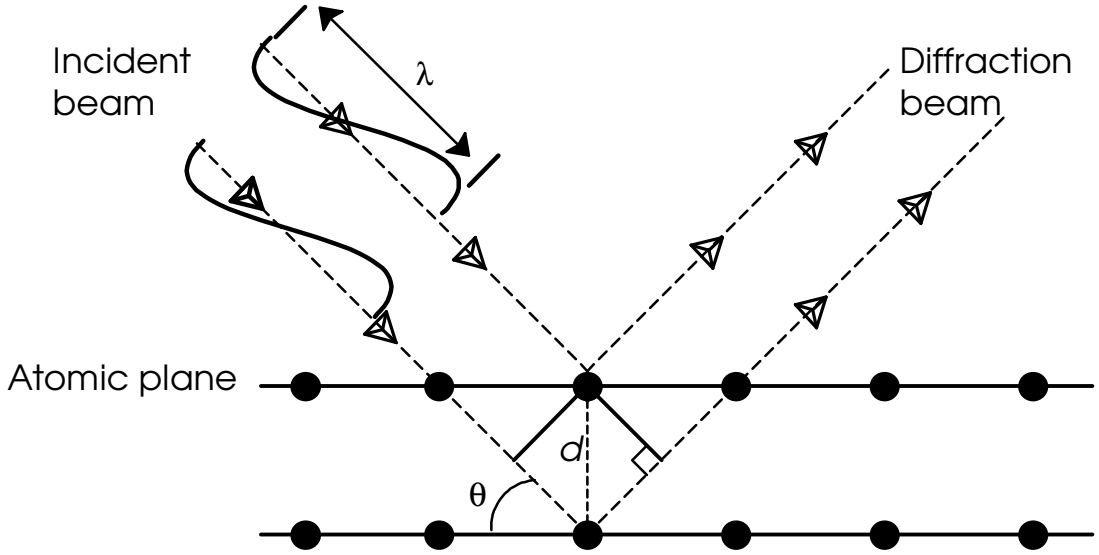

Figure 2.10: X-ray diffraction according to Bragg's Law

The X-ray diffraction pattern is unique for every crystalline structure. In essence crystallinity, is a direct function of the organisation within the hydroxide layer. The basal reflections for LDHs are strong and normally assume a rhombohedral structure, indexed as 003, 006, 009 etc. (Braterman ***et al.***, 2004). The reflections correspond to successive orders of the basal spacing (***d).*** Hence, the average d-spacing is usually calculated as (Xu and Braterman, 2004):

$$d = 1/n\ [d_{003} + 2d_{006} + 3d_{009} + \ldots . nd_{00(3n)}] \qquad (8)$$

The ***d***-spacings relate to the peaks observed, with repeating distances between planes of atoms in the structure, while the intensities denote the types of atom in the repeating planes.

Technical hitches are as a result of the poor crystallinity of the materials prepared, resulting in very broad and asymmetrical diffraction lines. Peak broadening arises from strain and defects within crystallites (Braterman ***et al***., 2004). Disorder in the stacking sequence lowers the symmetry, consequently giving considerable differences in relative intensities.

2.8.2 Fourier transform infrared (FT-IR) spectroscopy

Vibrational spectroscopy of LDHs involves vibration in the octahedral lattice, the hydroxyl groups and the interlayer anions. The region 250–1 000 cm^{-1} is indicative of lattice vibrations in Mg_2-Al-LDH, with five characteristic peaks. The hydroxyl groups in brucite-like sheets show two stretching modes: δ(OH) at 3 400–3 500 (OH···HOH) and at 3 000–3 100 cm^{-1} ($HO\cdots CO_3^{2-}$). Two librational modes (δ_{OH}) are observed at 650–900 cm^{-1} (Braterman ***et al***., 2004).

Interlayer-water bending vibration of δ_{H2O} occurs at 1 600–1 650 cm^{-1}. The interlayer anions may be identified by this technique, including the types of bond they form and their orientation within the interlayer. In the 1 000–1 800 cm^{-1} range, the absorption bands observed are due to the existence of anions. The application of this procedure in the analysis of organo-LDHs is appropriate in that IR is more specific for organic anions. Details are presented in Section 4.2.

2.8.3 Thermal analysis

Thermogravimetric (TG) methods are useful in studying the thermal stabilities/behaviour of both intercalated LDHs and pristine LDH. The decomposition pathways of LDHs are understood by making use of this analytical tool. Decomposition of LDHs normally entails endothermic processes of

dehydration, dehydroxylation and elimination of anions. In Mg-Al-LDHCO_3^{2-}, dehydration occurs between 100 and 300 °C, and dehydroxylation at 350–500 °C simultaneously with the decarbonation of the carbonate anion. At temperatures above 700 °C, the decomposition products are mixed oxides of M (II) and M (III).

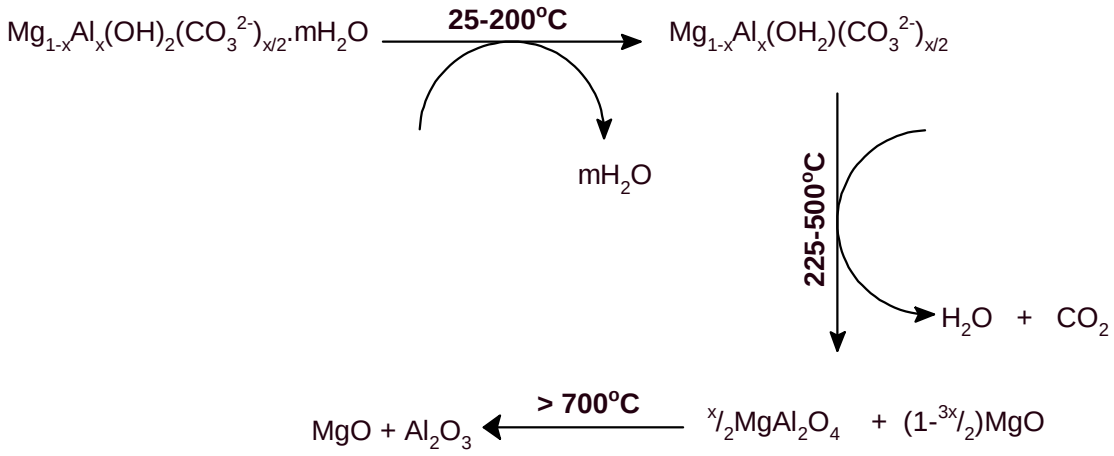

Scheme 2.5: Decomposition pathway of (Mg-Al)-LDH-CO_3 (Bera, 2000)

TG may be coupled with FT-IR and mass spectrometry for more conclusive interpretations.

2.9 Scanning Electron Microscopy (SEM)

This characterisation technique gives an appreciation of the shape and aggregation of LDH crystallites. When inorganic anions are intercalated, crystallites typically have hexagonal platelets. On the other hand, organic intercalated LDHs have ribbon-like or bar-like morphologies. The differences in the crystal habits are attributed to intermolecular interactions. With organo-LDHs, the structure is affected by hydrophobicity, critical micelle concentration (CMC) and charge density (Braterman ***et al.***, 2004).

2.9.1 Other techniques

Other techniques that have been used in this study include BET, DSC, high-temperature XRD, TG-MS and TG-FT-IR, so as to provide informed interpretation.

2.10 LDH Applications

LDHs combine properties such as low toxicity, basicity and high specific area (100 ± 300 m^2/g). As mentioned earlier, they are very flexible with regard to what anions may be used for modification, and hence their properties can be tailored to suit the desired application. Calcined derivatives of LDHs have a 'memory effect' property and can be reconstructed under mild conditions. These calcined derivatives have an even wider spectrum of application for current and future use. The areas of application have been divided into five groups, namely industry, catalysis, catalyst support, medicine and adsorbents.

LDHs have potential application as flame retardants (Costa ***et al.***, 2005, 2006 & 2008), molecular sieves and ion exchangers. Catalytic activity is noted in areas such as hydrogenation, basic catalysis in aldol condensation reactions, reforming of hydrocarbons, oxidation and catalyst supports for Ziegler-Natta (Cavani ***et al.***, 1991; Hetterley ***et al.***, 2008). Seftel ***et al***. (2008) reported investigations into the photocatalytic properties of Zn-Al LDHs and it was discovered that the catalytic activity increases with an increase in the cationic ratio and calcination temperature.

Polymer-LDH nanocomposites are prepared from the delamination of the hydroxide sheets in a polymer matrix (Costa ***et al.***, 2005 & 2006; Khan & O'Hare, 2002; Leroux ***et al.***, 2001; Fischer, 2003). Generally, these nanocomposites show improved properties compared with virgin polymer. Specific parameters, such as improved strength and heat resistance, reduced gas permeability and flammability, and improved biodegradability of biodegradable polymer have been noted (Fischer, 2003; Zhu ***et al.***, 2008). They are also used in polymer technology as halogen scavengers, flame retardants and PVC stabilisers.

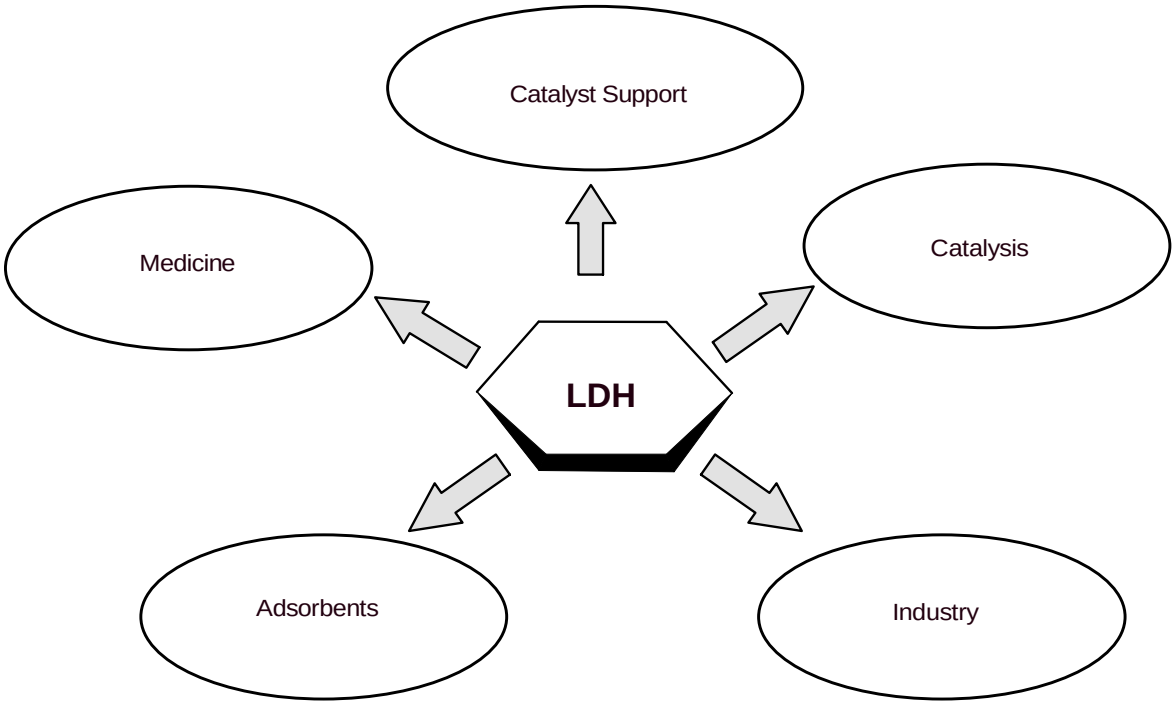

Scheme 2.6: Layered double hydroxide application areas (Cavani ***et al.***, 1991)

LDHs are biocompatible and have found many medicinal applications. They have been utilised as antacids and antipeptins. A number of researchers (Zhu ***et al.***, 2008; Darder ***et al.***, 2005; Carja ***et al.***, 2007; Del Arco ***et al.***, 2009; Shi ***et al.***, 2007; Trikeriotis & Ghanotakis, 2007) have explored their use in drug-delivery systems; this application is made possible by the high anionic exchange and large surface area of LDHs. In addition, the encapsulation of the drug within the interlayer isolates it from the immediate environment, and improves its long-term stability and storage. Pesticides and genes have been protected, carried and delivered by intercalated LDHs and the active compounds have been released controllably to target sites (Choy ***et al.***, 1999; Wang ***et al.***, 2005).

In the field of environmental remediation, LDHs have been reportedly used for the sorption of non-ionic organic compounds, e.g. trichloroethylene and tetrachloroethylene (You ***et al.***, 2000a). LDHs have also been used as adsorbents to remove contaminants from water (Zhao & Nagy, 2004; Bouranda ***et al.***, 2008). Their membrane-like nature makes them of significance in separation and membrane technologies (Newman & Jones, 1998; Tseng ***et al.***, 1996; Borja ***et al.***, 1992).

The incorporation of surfactants leads to the hydrophobisation of the LDHs (Dèkány ***et al.***, 1997; Mohanambe & Vasudevan, 2005). This results in hybrid layered materials that can be used as thickening agents. Surfactant-LDHs are capable of sorption of non-ionic molecules (Dèkány ***et al.***, 1997; You ***et al.***, 2000a and 2000b; Mohanambe & Vasudevan, 2005).

Owing to the extensive use and convenience of LDH intercalates, it is of importance to consider environmentally friendly and energy-efficient methods of intercalation that will yield products of a satisfactory quality. LDH-CO_3 is currently available as a bulk raw material owing to growing PVC stabiliser applications. Therefore, it is of interest to upgrade this basic starting material by using suitable intercalation procedures.

CHAPTER 3: EXPERIMENTAL

3.1 Materials

LDH-CO_3 was the starting material for all the elimination and reconstruction experiments. Magnesium and aluminium nitrates were used for the co-precipitation reactions, while magnesium and aluminium chloride were used to prepare LDH-Cl for ion exchange. LDH-CO_3 (Hydrotalcite Grades HT-325 and HT-5) was obtained from Chamotte Holdings, South Africa. Both silica and magnesium carbonate were found to be sources of minor contamination. The theoretical anion exchange capacity of the LDH-CO_3 was calculated to be 213 meq/100 g. The molecular mass of the compound is ca. 234.66 g.

Table 3.1 gives a list of reagents, suppliers and their specifications. The reagents were used without further purification. In all experiments, distilled water was used unless otherwise stated.

Table 3.1: List of reagents used in the experiments, suppliers and their specifications

Reagent	Formula	Supplier	Purity
Sodium dodecyl sulphate	$C_{12}H_{25}OSO_3Na$	Fluka	≥ 99%
Sodium dodecylbenzene sulphonate	$C_{18}H_{29}OSO_2Na$	Fluka	~ 88%
Glacial acetic acid	$C_2H_4O_2$	Saarchem UnivAR	99.5%
Butyric acid	$C_4H_8O_2$	Merck-Schuchardt	≥ 99%
Hexanoic acid	$C_6H_{12}O_2$	Merck-Schuchardt	-
Octanoic acid	$C_8H_{16}O_2$	Croda Chemicals	-
Lauric acid	$C_{12}H_{24}O_2$	Croda Chemicals	-
Dodecyl alcohol	$C_{12}H_{25}O$	Croda Chemicals	-
Acetone	C_3H_6O	Saarchem UnivAR	99.5%
Aluminium nitrate	$Al(NO_3)_3 \cdot 9H_2O$	Merck	≥ 98.5%
Aluminium chloride	AlCl	Merck	≥ 98%
Magnesium nitrate	$Mg(NO_3)_3 \cdot 6H_2O$	Merck	99-102%
Magnesium chloride	$MgCl_2 \cdot 6H_2O$	Saarchem-Merck	98-101%
Sodium hydroxide	NaOH	Saarchem	≥ 98%

3.2 Sample Preparation

The detailed experimental procedures for all the samples are given in Appendix I. The general experimental set-up used is as shown in Figure 3.1.

3.2.1 Elimination (acid-mediated ion exchange)

Surfactant intercalation experiments were carried out using variations of the following representative procedure: 75 g sodium dodecyl sulphate (SDS) (0.26 mol) and 15 g acetic acid (0.25 mol) were dispersed in 1.5 L of distilled water and the pH adjusted to 10. Then 20 g of HT-325 (LDH-CO_3 approximating $[Mg_{0.66}Al_{0.34}(OH)_2](CO_3)_{0.17}.½H_2O$ (ca. 0.10 mol Al) were added slowly while stirring. The emulsion-suspension was left to stir overnight. The pH was again adjusted to 10 each morning by adding dilute ammonia or NaOH solution if required. It was noted that the pH dropped to as low as 7.2 overnight. The mixture was allowed to react at ambient temperature for a total of two days. The product was recovered by centrifugation, washed four times with distilled water and once with acetone. After each washing the solids were separated from the liquid by centrifugation. The product was allowed to dry at room temperature.

This experiment was repeated leaving out the acetic acid or the SDS. The effect of raising the reaction temperature to 65 or 80 °C, as well as using reduced amounts of the SDS and/or the acetic acid was also investigated. Similar experiments were conducted using sodium dodecylbenzene sulphonate (SDBS) in place of the SDS.

3.2.2 Surfactant-mediated exchange

The procedure used in the preparation of LDH-laurate was as follows: 20 g LDH-CO_3 (0.10 mol Al), 40 g SDS (0.26 mol), 76.9 g lauric acid (0.38 mol) and 20 g HT-325 were dispersed in 1 L of distilled water at 70 °C and allowed to stir continuously for 3 days. The lauric acid was divided into three equal portions. One part was added at the beginning of the experiment and the two other portions added each subsequent day. When required, dilute NH_4OH was added to the mixture in order to maintain the pH at 10±0.5.

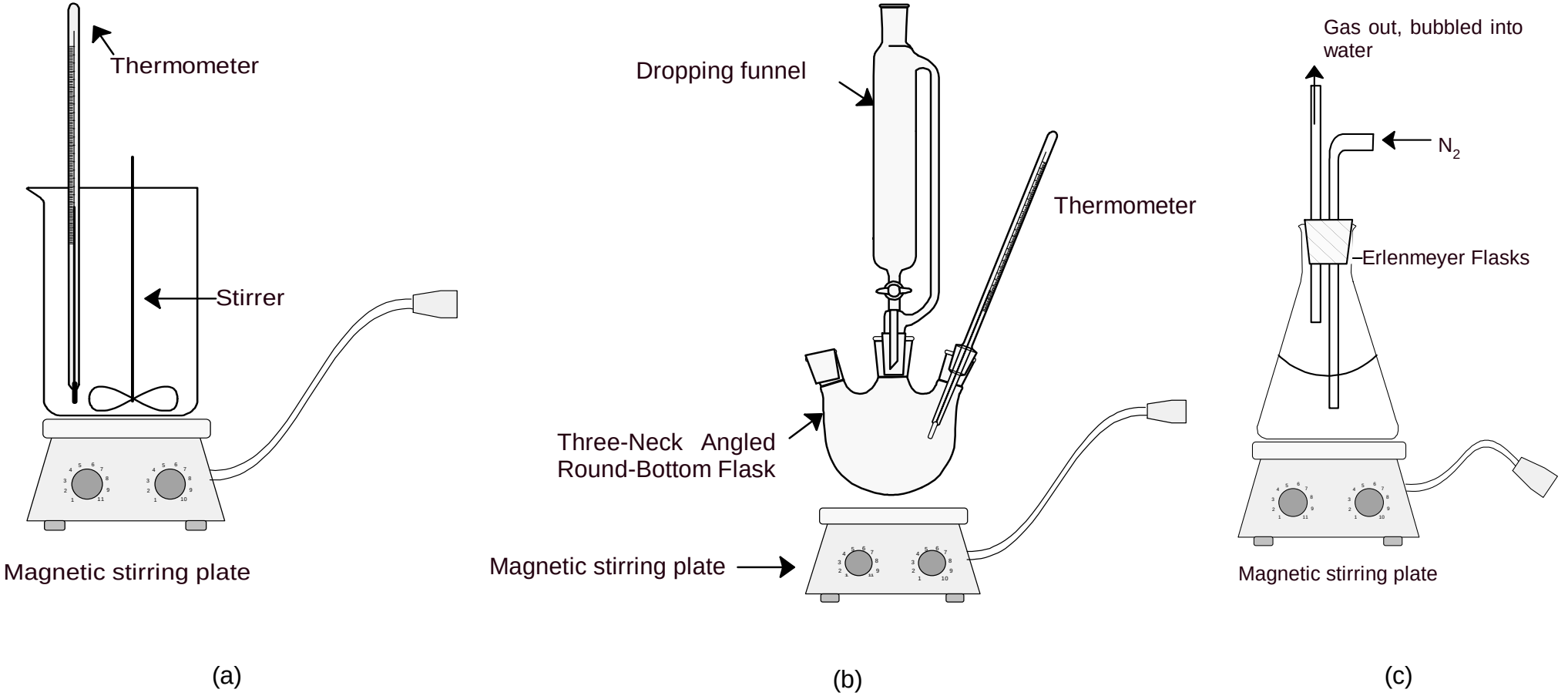

Figure 3.1: Basic experimental set-up for the (a) elimination and regeneration, (b) co-precipitation and (c) intercalation reactions carried out in an inert atmosphere

3.2.3 Regeneration

The regeneration method followed is similar to that described by Costa ***et al***. (2008), but under normal laboratory conditions. The LDH-CO_3 was first calcined at 450 °C for 3 h. The calcined LDH (LDO) was added to a solution of the desired surfactant anion. 2M sodium hydroxide solution was used for pH correction whenever required. The LDO was left to stand in the surfactant solution for two days. The regenerated LDO was separated by centrifugation and washed four times with water. The product was oven-dried at 60 °C.

Additional LDH-DS and LDH-DBS samples prepared using an LDH with $\boldsymbol{x} \approx 0.33$ were donated by Dr Costa and analysed as provided without further purification or modification.

3.2.4 Ion exchange

Initially, the LDH-Cl precursor was prepared. Mg-Al-LDH in the ratio 2:1 was made by dissolving 50 mmol of $AlCl_3$ and 150 mmol of $MgCl_2$. Deionised water, 15MΩ cm, was used. The mixed metal solution was added to the NaOH solution, corrected to a pH of 8.20 using 2M NaOH. The product was washed with distilled water at least six times and once with acetone, and then left to dry at room temperature.

The dry LDH-Cl was then reacted with the 0.2M surfactant solution. The mixture was refluxed for 24 h and nitrogen gas was sparged through the solution for an additional 24 h. The sample was then put in the oven and left to age for 24 h at 65 °C. The pH of the mixture was maintained at approximately 9. The sample was recovered by centrifugation and washed at least six times with water. Washing was stopped once the silver nitrate solution gave negative test results for the detection of residual chloride ions. The same procedure was used for the preparation of LDH-DS and LDH-DBS.

3.2.5 Co-precipitation

This was carried out in a set of three experiments:

- In the first experiment the mixed metal salt solution was added slowly to an alkaline solution of the surfactant; the suspension was left to stir under an inert atmosphere. The pH was corrected to 7.0±0.5
- The second experiment was carried out under ambient conditions; the pH was corrected to 7±0.5 and the temperature kept at 25 °C.
- Thirdly, the conditions of the above experiment were altered by increasing the temperature to 65 °C and the pH to 10.0±0.5

Generally, the precipitation was carried out in a similar way to that given by Zhang ***et al.*** (2007) and Crepaldi ***et al***. (2002). The nitrate salts were dissolved in ~ 500 ml of distilled water. A separate solution of the surfactant was prepared in 300 ml of distilled water. An additional 100 ml was added to the surfactant solution. The resulting solution was added to the mixed nitrate solution, which was corrected to a pH of ~ 7 using 2M NaOH. The mixture was left to stir at 25 °C for three days. Both SDS and SDBS were intercalated in this manner. The sample used for comparison with the other methods is the sample prepared in inert atmosphere.

3.3 Characterisation

3.3.1 BET and particle size

The particle size distribution and BET surface area of the precursor LDH were determined using a Malvern Mastersizer Hydro 2000MY instrument and a Micromeritics Flowsorb II 2300 instrument respectively.

3.3.2 X-ray fluorescence (XRF) analysis

The elemental composition was determined by XRF analysis. The intercalated materials were ashed before analysis in order to reduce their bulk. These samples were ground to < 75 μm in a tungsten carbide mill and roasted at 1 000 °C. Then 1 g of sample was added to 9 g of $Li_2B_4O_7$ and fused into a glassed bead. Major element analysis was executed on the fused bead using an ARL9400XP+ spectrometer.

3.3.3 Scanning electron microscopy (SEM)

Powder samples were viewed on a JEOL 840 SEM under low magnification. They were prepared as follows: a small quantity of the powder product of the LDH-CO_3 precursor/intercalate was placed to carbon tape on a metal sample holder. Excess powder was removed using a single blast of compressed air. The samples were then coated five times with gold under argon gas using the SEM autocoating unit E5200 (Polaron Equipment Ltd).

3.3.4 Thermogravimetric analysis (TG)

Thermogravimetric analysis was conducted on a Mettler Toledo A851 TGA/SDTA machine. Powder samples of ca. 10 mg were placed in 70 µl alumina open pans. The temperature was scanned at 10 °C/min in the range from 25 to 800/1200 ^{o}C.

3.3.5 Fourier transform infrared (FT-IR) analysis

FT-IR spectra were recorded on a Bruker Opus Spectrophotometer. Samples were finely ground and combined with spectroscopic-grade KBr in a ratio of 1:50, i.e. approximately 2 mg of sample and 100 mg of KBr. The mixture was pressed into a pellet with a 13 mm diameter. The reported spectra were obtained over the range 400 - 4 000 cm^{-1} and represent the average of 32 scans at a resolution of 2 cm^{-1}.

3.3.6 X-ray diffraction (XRD) analysis

Phase identification was carried out by XRD analysis on a PANalytical X-pert Pro powder diffractometer. The instrument features variable divergence and receiving slits and an X'celerator detector using Fe-filtered Co K-α radiation (0.17901 nm). The X'Pert High Score Plus software was used for data manipulation.

3.3.7 Gas chromatography/mass spectrometry (GC/MS)

Small samples (3 – 4 mg) were analysed on an Agilent GC/MS system fitted with a DB-17MS intermediate polarity GC column (30 m x 0.25 mm I.D.), an Agilent MSD 5971 mass spectrometer and a CDS Instruments Pyroprobe 2000 pyrolyzer. Helium was used as carrier gas (1 ml/min; split 1:20).

CHAPTER 4: RESULTS AND DISCUSSION

The Malvern particle size analysis of the LDH-CO_3 precursor revealed a bimodal particle size distribution with d (0.1) = 1.0 µm; d (0.5) = 3.5 µm and d (0.99) = 260 µm. The measured BET surface areas were 21.6, 17.0, 15.7 and 5.3 m^2/g for the LDH-CO_3, LDH-DS, LDH-DBS and LDH-laurate respectively. All samples refered to here were prepared by the elimination method, with the exception of LDH-laurate which was prepared by surfactant mediated exchange.

Table 4.1 shows the chemical composition of the precursor LDH and the intercalated products as determined by XRF analysis. The results are presented as atom ratios relative to the aluminium present. The data for the precursor indicates a value for ***x*** of 0.346 in the chemical formula $[Mg_{1-x}Al_x(OH)_2](CO_3)_{x/2}.nH_2O$. XRF analysis points to values for ***x*** of 0.278, 0.349 and 0.317 for LDH-laurate, LDH-DS and LDH-DBS respectively for samples obtained from the elimination method. Cavani ***et al.***, (1991) suggest that for pure hydrotalcites the ***x*** values range between $0.22 \leq x \leq 0.33$. From this perspective, the x-values obtained in this study are in good agreement with those obtained from the literature for pure hydrotalcites (Brindley & Kikkawa, 1979; Mascolo & Marino, 1980; Miyata, 1980). It is clear from the collated data that in the regeneration and co-precipitation methods there is substantial co-intercalation of sodium ions together with the surfactant anions.

Table 4.1: XRF results with composition expressed as atom ratios relative to aluminium

Intercalation method			Elimination		Regeneration		Co-precipitation	
Atom	LDH	LDH-laurate	LDH-DS	LDH-DBS	LDH-DS	LDH-DBS	LDH-DS	LDH-DBS
Mg	1.89	2.31	1.87	2.16	2.27	2.13	2.02	1.81
S	0.02	0.03	0.36	0.27	0.47	0.13	0.26	0.70
Na	0.01	0.02	0.01	0.00	0.04	0.04	0.25	0.74
Si	0.05	0.05	0.04	0.05	0.05	0.06	0.04	0.04
Ca	0.00	0.02	0.00	0.00	0.02	0.02	0.00	0.00
x	0.35	0.28	0.35	0.32	0.30	0.32	0.33	0.36

x refers to the M(II)/M(III) ratio calculated as: $$x = \frac{M(III)}{M(II) + M(III)}$$

4.1 Thermogravimetric Analysis

The thermal decomposition of LDH-CO_3 occurs in three distinct steps: removal of interlayer water; dehydroxylation; and an overlap of both the dehydroxylation and decarbonation reactions (Miyata, 1977; Rey, 1992; Reichle, 1985). Generally, the first step is due to the loss of interlayer water and is assumed to be complete at a temperature of 150 °C (Carlino & Hudson, 1995; Frost ***et al.***, 2003; Kandare & Hossenlopp, 2006; Evans & Duan, 2005). Mass loss is effectively complete at 700 °C. The x-value of the LDH-CO_3 was found to be 0.346. For this value the exact formula of the compound is considered to be $[Mg_{0.65}Al_{0.35}(OH)_2](CO_3)_{0.17}.0.48H_2O$. Hence, the theoretical mass losses each of organic substituents in LDH-CO_3 are 11, 44 and 13% for the H_2O, OH and CO_3 groups respectively. Figure 4.1 shows three decomposition steps at 237, 321 and 426 °C.

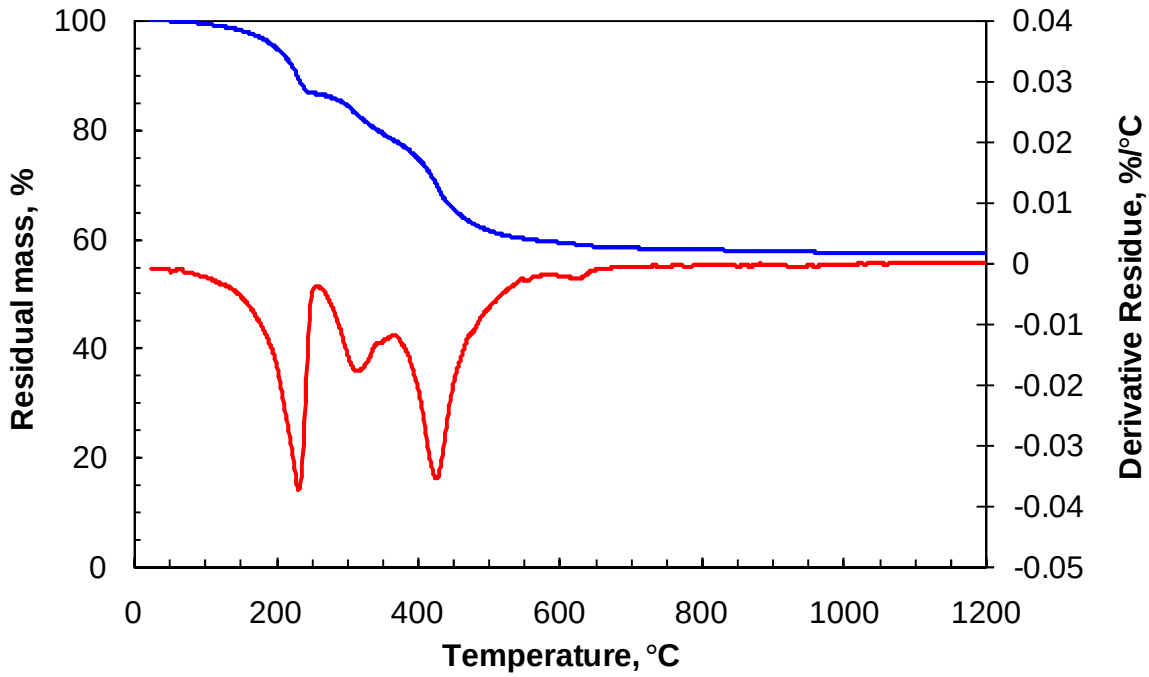

Figure 4.1: Thermogravimetric (TG) and derivative mass loss curves of LDH-CO_3

For the other LDH precursors prepared, the LDH nitrate and chloride showed two-step weight loss (see Figure 4.2 and Appendix II). This thermal profile is in agreement with those of Reichle (1986) and Bera ***et al.*** (2000), who assigned the low-temperature (25–220 °C) mass loss to water being adsorbed or intercalated,

and the loss at higher temperatures (225–450 °C) to decomposition or deanation. This variation is explained by the difference in the Mg^{2+}/Al^{3+} ratio. High-temperature decomposition occurs in two distinct steps for an Mg^{2+}/Al^{3+} ratio of 2, as seen with the LDH-CO_3, the first peak being attributed to partial dehydroxylation and the second to dehydroxylation plus decarbonation (Cavani ***et al.***, 1991; Miyata, 1980; Zhao ***et al.***, 2002). The LDH-Cl rapidly loses large amounts of water at temperatures below 100 °C, as compared with the other LDHs.

The final residues may, to a first approximation, be assumed to have the same composition as the ash of the precursor, provided the sodium ions did not co-intercalate. This assumption allows calculation of a rough estimate for the organic content of the initial sample.

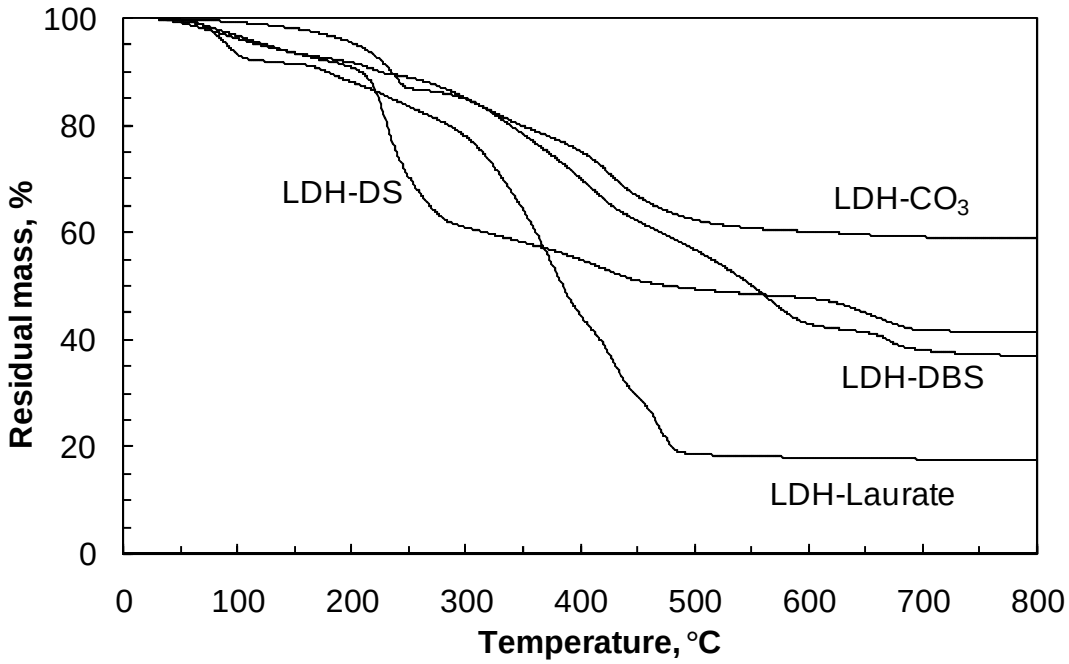

Figure 4.2: Thermogravimetric (TG) mass loss curves for LDH-CO_3, LDH-DS, LDH-DBS and LDH-laurate

The surfactant-intercalated LDH follows a similar decomposition path. Generally, mass loss has its onset from temperatures above 50 °C. In the elimination method, the mass loss of samples accelerates above 170, 210, 250 and 270 °C for LDH-laurate, LDH-DS, LDH-CO_3 and LDH-DBS respectively (see Fig 4.2). Below

550 °C the mass loss of LDH-DS exceeds that of LDH-DBS. The point at which the mass loss rate accelerates cannot be regarded as a threshold limit for the stability of the LDH. Pyrolysis GC/MS of LDH-SDBS performed at 200 °C already reveals the liberation of a range of branched alkyl benzene compounds, i.e. typical SDBS degradation products.

The degree of aluminium substitution of the clay, characterised by the value that ***x*** assumes in the formula $[Mg_{1-x}Al_x\ (OH)_2](CO_3)_{x/2}.zH_2O$, also indicates the anion exchange capacity of the material. If intercalation had proceeded to completion, the expected residue levels when dry, i.e. dehydrated clay basis, are 63.4, 29.0, 26.9 and 34.3% for LDH-CO_3, LDH-DS, LDH-DBS and LDH-laurate respectively. This may be compared against the experimentally determined values of 60.0, 44.1, 39.1 and 18.9. The degree of intercalation was estimated using the values for ***x*** from the Al:Mg ratios indicated by XRF analysis (see Table 4.1), together with the residue levels determined by TG (see Table 4.2). The calculated values are 0.37, 0.46 and 2.51 for LDH-DS, LDH-DBS and LDH-laurate. Thus the extent of laurate intercalation exceeded the anionic exchange capacity of the clay by ca. 1.5 times. This high value is attributed to concomitant intercalation of non-ionised lauric acid and/or sodium laurate by which tight packing of the alkyl chains inside the clay galleries was achieved (Kanoh ***et al.***, 1999; Itoh ***et al.***, 2003; Nhlapo ***et al.***, 2008).

Table 4.2: Sample designations, XRD determined basal spacings and thermogravimetric data

Intercalated compound (carboxylic acid)	Method	d_L	TG residual mass, %			Clay	Organic
		nm	150 °C	700 °C	800 °C	%	%
Inorganic precursors							
LDH-CO_3 (HT 325)		0.763	98.09	59.15	58.82	100	-
LDH-CO_3 (Costa)		0.759	99.03	56.16	55.77	100	-
LDH-NO_3			97.29	56.64	56.17	100	-
LDH-Cl			80.76	53.22	52.27	100	-
SDS experiments							
LDH + SDS (no acid)	e[1]	0.760	98.41	58.68	-	98.9	1.1
LDH-DS (Costa)	r[2]	2.69	94.09	65.03	64.70	na	Na
LDH-DS (This study)	r	2.69	92.92	55.26	55.01	98.7	1.3
LDH-DS (acetic acid)	e	2.60	93.52	41.71	41.37	73.8	26.2
LDH-DS (butyric acid)	e	2.59	92.52	33.33	33.02	59.5	40.5
LDH-octanoate	e	2.72	91.92	23.62	-	42.6	57.4
LDH-laurate	e	3.66	90.67	14.71	-	26.9	73.1
LDH-DS	c[3]	3.78	95.27	35.94	35.76	49.4	50.6
LDH-DS	I[4]	2.62	93.40	52.20	51.91	75.4	24.6
SDBS experiments							
LDH-DBS (Costa)	r	3.07	91.57	41.06	40.85	74.4	25.6
LDH-DBS (this study)	r	3.04	92.41	45.77	45.50	81.5	18.5
LDH-DBS (acetic acid)	e	2.88	93.55	37.99	36.92	65.8	34.2
LDH-DBS (butyric acid)	e	2.84	92.52	33.33	33.02	59.5	40.5
LDH-DBS (hexanoic acid)	e	2.84	92.99	38.68	38.24	68.6	31.4
LDH-DBS (lauric acid)	e	3.64	91.69	18.56	18.30	33.0	67.0
LDH-DBS	c	3.07	92.27	42.62	23.45	42.6	57.4
LDH-DBS	I	3.05	93.45	44.59	44.35	64.3	35.7
LDH-(DBS+dodecyl alcohol)	e	3.15	93.64	36.17	35.84	63.1	36.9

[1] e = elimination
[2] r = regeneration method
[3] c = co-precipitation
[4] I = ion exchange

The sulphur-to-aluminum atom ratio should also provide an indication of the degree of intercalation of the anionic surfactants. Certainly, the S/Al value for LDH-DS is in good agreement with the degree of intercalation estimated from the TG data. However, the S/Al = 0.266 value determined via XRF analysis for LDH-DBS is significantly lower than expected (see Table 4.1). It is possible that some sulphur may have been lost during the de-intercalating heat treatment of the samples.

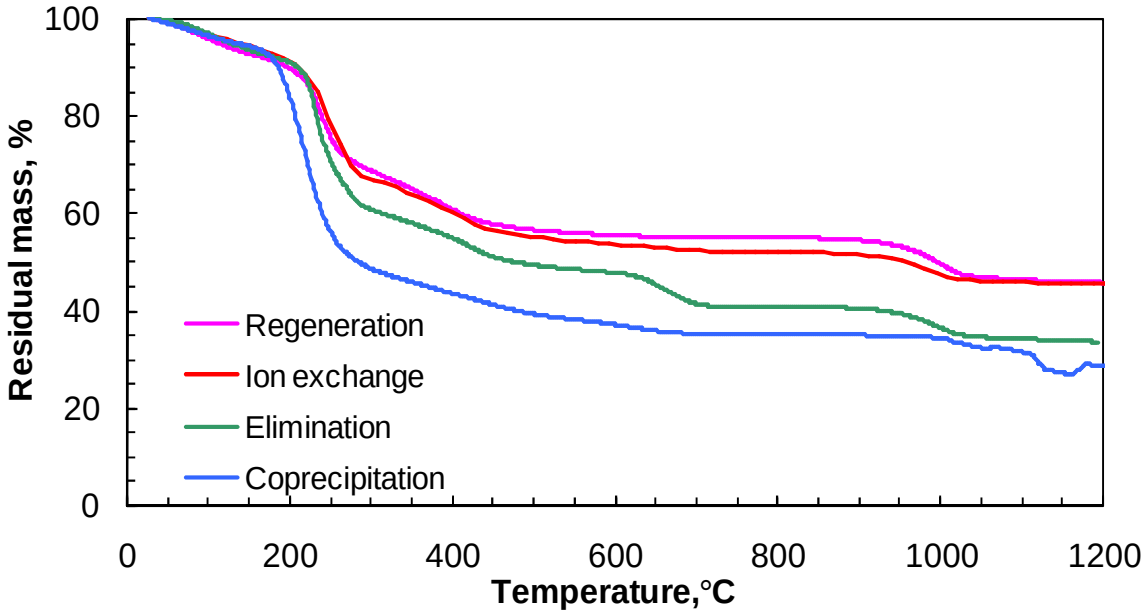

Figure 4.3: Thermogravimetric (TG) mass loss curves for the different preparative methods as indicated for LDH-DS intercalates

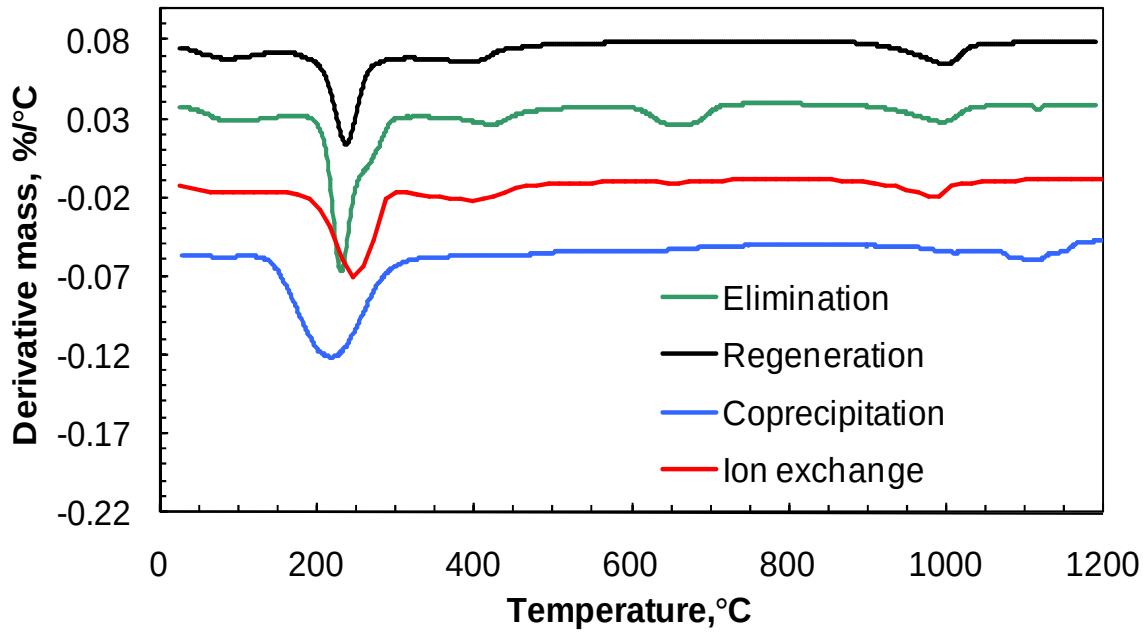

Figure 4.4: Derivative mass loss curves of LDH-DS intercalates prepared by different methods

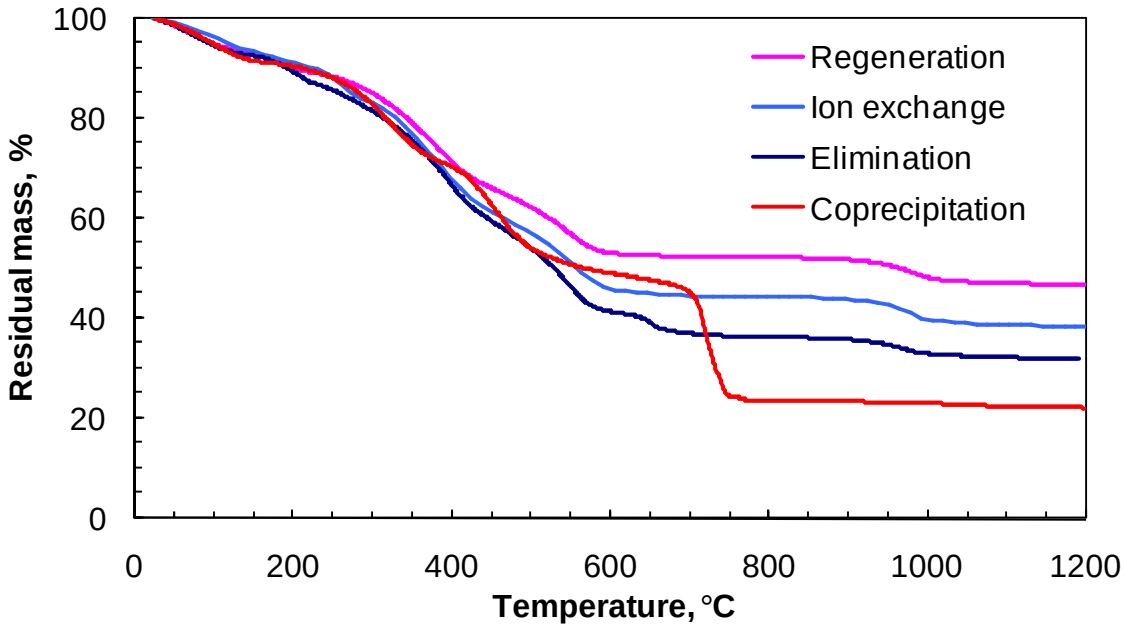

Figure 4.5: Thermogravimetric (TG) mass loss curves for the different preparative methods as indicated for LDH-DBS intercalates

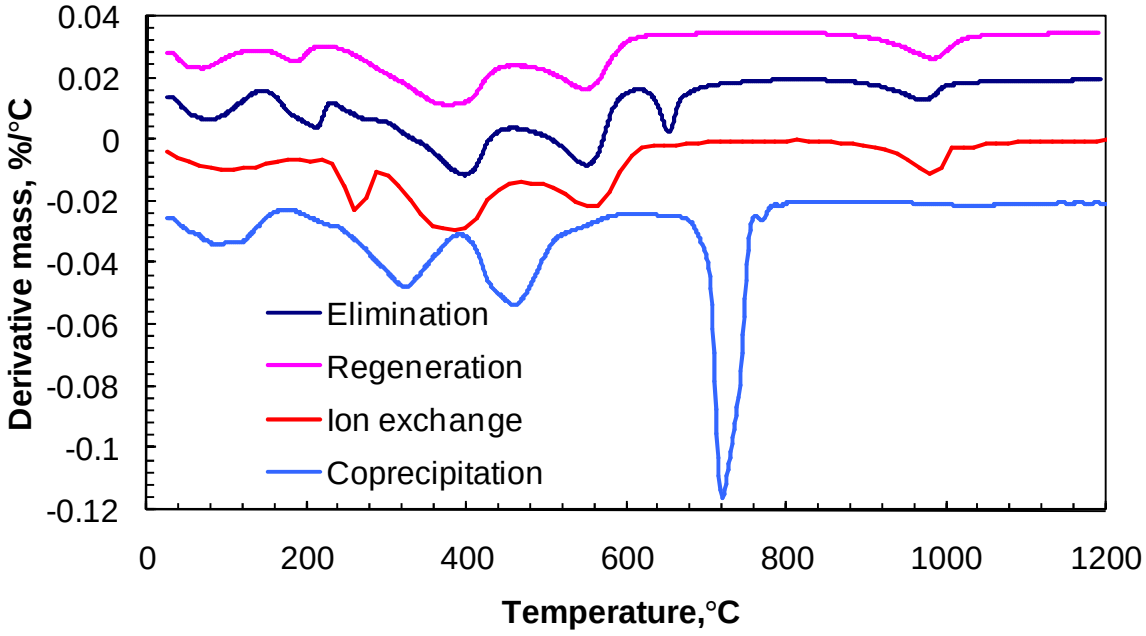

Figure 4.6: Derivative mass loss curves of LDH-DBS intercalates prepared by different methods

The derivative mass loss curves for the LDH-DS show at least two endothermic peaks (see Figure 4.4). The largest mass loss, which occurs between 150 and 300 °C, could be interpreted as an overlap of all three expected thermal events, i.e. dehydration, dehydroxylation and deanation/decarbonation. On the other hand, the curve for LDH-DBS (Figure 4.6) shows several decomposition steps, indicating a progressive disintegration of the dodecylbenzene sulphonate anion. The LDH-DS co-precipitation product becomes less thermally stable as it undergoes substantial mass loss between 180 and 250°C (see Figure 4.3). The regeneration and ion exchange products show similar decomposition patterns and are stable at the above-mentioned temperatures.

An additional decomposition event is observed, occurring at temperatures above 700 or 900°C depending on the individual intercalation products. The event is assumed to be desulphurisation, clearly seen for all elimination, regeneration and ion exchange samples above 900 °C. If the intermediate decomposition product of the LDH-surfactant is LDH-SO_4, this assumption is validated by Constantino ***et al.*** (1995). They found that thermal decomposition of Mg-Al-LDH-sulphate at 900 °C resulted in the formation of a mixture of MgO, $MgAl_2O_4$ and $MgSO_4$. Marino &

Mascolo (1982) discovered mass loss above 950 °C to be associated with the decomposition of the magnesium sulphate phase and the liberation of SO_3.

With regard to the amount of organic anion intercalated, it would appear that the co-precipitation method achieves the greatest intercalation percentage (see Figures 4.3 and 4.5). The theoretical residual clay content is 63.4, 29.0 and 26.9% for LDH-CO_3, LDH-SDS and LDH-SDBS respectively. Chart 4.1 represents the percentage of organic content present in each of the LDH-surfactants prepared in this study.

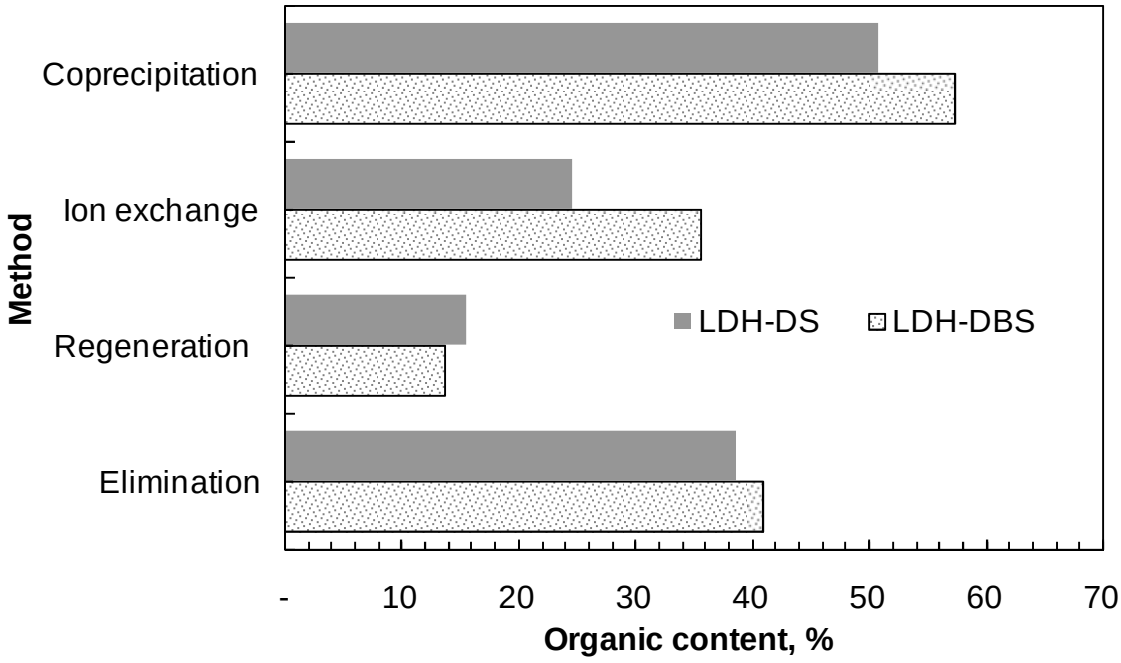

Chart 4.1: Comparison of percentage organic content achieved with the various preparative methods

As mentioned earlier, the anion exchange capacity is directly proportional to the degree of Al substitution in the Al-Mg LDH. It is likely that the incomplete intercalation in the ion exchange and elimination method can be attributed to the partial removal of the pre-existing anions (e.g. Cl and CO_3^{2-}). In the regeneration and co-precipitation methods, it could be due to the preparative procedures, which tend to alter the anticipated structure of the Mg-Al LDH. The co-precipitation method that was used results in a continuous change in the pH of the solution and the formation of $M(OH)_2$ and/or $M(OH)_3$ phases, which results in an LDH with an

undesired M(II)/M(III) ratio. Such changes, in turn, result in a change in the anionic exchange capacity of the LDH (He ***et al.***, 2005), which ultimately alters the degree of intercalation.

In the regeneration method, the memory effect is not fully satisfied, which is consistent with the literature and also what was observed in this study. On intercalating organic anions, mixed phases may be synthesised (Chibwe & Jones, 1989) and the formation of the carbonate form is unavoidable, as evidenced by the presence of the carbonate peak (see Figures 4.7 to 4.9). Hibino & Tsunashima (1988) proved that reconstruction of the calcined LDH is not totally reversible; this claim is substantiated by the fact that the intercalated carbonate content reduces with each successive calcination. In the article on the thermal decomposition of hydrotalcite-like compounds in the 1998 annual report of the National Institute for Resources and Environment (NIRE) it is stated that when LDH-CO_3 with an ***x*** value of 0.33 is calcined at 500 °C, 20–30% of the carbonates remain. Decarbonation is deemed to be complete at 600–900 °C. At this temperature, the Al ions go into MgO and spinel forms, suggesting that the process is complete when the Al ions migrate. An increase in the calcination temperature causes solid-state diffusion of the divalent cations into tetrahedral positions, resulting in a progressive formation of stable MgO and of $MgAl_2O_4$ spinel, ultimately causing a reduction in the memory effect (He ***et al.***, 2005; Labajos ***et al.***, 1992; Marchi & Apesteguýa, 1998).

You ***et al.*** (2000b) used anion exchange to intercalate SDS and SDBS in LDH-Cl. They obtained AEC levels of ca. 72% using this method, even though the solutions were sparged with nitrogen. Zhao & Nagy (2004) observed partial intercalation for LDH-DS samples prepared by both ion exchange and co-precipitation. Costa ***et al.*** (2008) also obtained partially substituted LDH-surfactant intercalates from the regeneration method. Actually, their data shows for their purported LDH-DS, a TG residue value that is higher than that found for the precursor LDH-CO_3. This indicates that the product obtained could not have been a pure LDH-DS. To investigate this anomalous finding further in this study, the intercalation was repeated by regeneration experiments and the samples supplied by Dr Costa were reanalysed. The TG and XRD results obtained for these samples are presented in

Tables 4.1 and 4.2 and compared with the samples prepared using acetic acid as intercalation aid (elimination). The regeneration product continues to show a very small degree of intercalation, even in the current study.

4.2 FT-IR Results

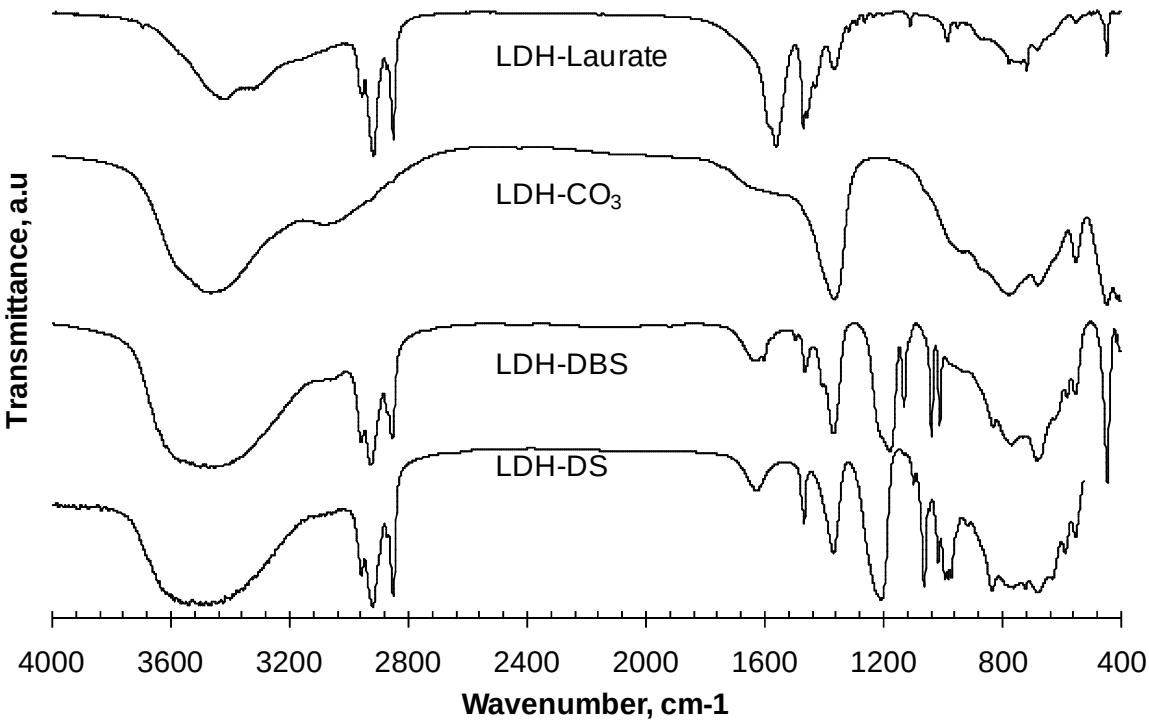

Figure 4.7: FT-IR spectra of LDH-surfactant prepared by elimination compared with LDH-CO_3

Figure 4.7 compares the FT-IR spectra of the unmodified layered double hydroxide (LDH-CO_3) with the LDH-surfactant intercalates. Costa ***et al.*** (2008) provide a comprehensive analysis of the infrared absorption bands relevant to the present compounds. The spectra are unique for every material; moreover, in LDHs, information regarding the interlayer anions and mixed metal hydroxide structure may be obtained. In the 3200–3700 cm^{-1} region, OH stretching vibrations and interlayer water are observed in all compounds (Labajos ***et al.***, 1992; Coates, 2000). The shoulder present at 3000–3100 cm^{-1} in LDH-CO_3 indicates a hydrogen bonding interaction between $CO_3^{2-}\cdots H_2O$ within the interlayer (Perez-Ramirez ***et al.***, 2001; Kloprogge & Frost, 1999 and 2000). Its presence in the LDH-laurate indicates the unreacted LDH-CO_3 as an impurity. As expected, the carbonate

peak located at 1367 cm^{-1} is well developed in LDH-CO_3. There are three carbonate assignments that can be observed, i.e. bending non-planar mode, γ_2 (850–880 cm^{-1}), asymmetric stretching mode, γ_3 (1350-1380 cm^{-1}), and bending angular mode, γ_4 (670-690 cm^{-1}). The γ_3 vibration is the most sensitive and prominent carbonate peak. However, the position may differ from one LDH to the next as a result of varying M^{II}/M^{III} ratio. A decrease in the M^{II}/M^{III} ratio has the effect of shifting the γ_3 vibration to lower wavenumber values and the reverse is also true (Hernandez-Mareno ***et al.***, 1985). This helps to explain the varying peak position of γ_3 CO_3^{2-} vibrations. For LDHs with an ***x***-value of 0.33, the peak position is predicted to be at 1357 cm^{-1} (Costa ***et al.***, 2008).

The triple peaks observed in the range 2850–2965 cm^{-1} are due to C-H stretching. They confirm the presence of the alkyl chains of the surfactant anions in the intercalated LDH derivatives (Costa ***et al.***, 2008; Clearfield ***et al.***, 1991; Bouranda ***et al.***, 2008; Rajamathi et al., 2005). Generally, organic sulphate and sulphonate groups exhibit frequencies at 1200–1180 cm^{-1} (Clearfield ***et al.***, 1991; Crepaldi ***et al.***, 2002) and 1420–1370 cm^{-1} (Bouranda ***et al.***, 2008; Anbarasan ***et al.***, 2005; Wang ***et al.***, 2005). The former band is evidently absent in the LDH-laurate spectrum. This indicates that the LDH preferentially intercalated the laurate and that DS was not co-intercalated (see Appendix III). The incorporation of the SDS ions is also confirmed by the 1204 cm^{-1} peak attributed to -S=O vibrations (Nethravathi ***et al.***, 2005). The double peaks observed at 1229 and 1216 cm^{-1} are assigned to C-H twist and SO_4 respectively (Clearfield ***et al.***, 1991; Crepaldi ***et al.***, 2002).

In the LDH-DBS intercalates, the peaks at 1186 and 1038 cm^{-1} are due to the symmetrical and asymmetrical S=O vibrations. The $\gamma_{C=C}$ of the benzene ring is visible at 1602, 1496 and 1409 cm^{-1} and as a weak shoulder at 1450 cm^{-1}. A weak peak at 1637 cm^{-1} is assigned to the H_2O bending vibration of interlayer water, while a strong peak at 1359 cm^{-1} is assigned to the vibration of the carbonate species (Bouranda ***et al.***, 2008). The characteristic vibration bands of the sulphonate group are 1186, 1130, 1039, 1011 and 832 cm^{-1} (Bouranda ***et al.***, 2008; Anbarasan ***et al.***, 2005; Wang ***et al***., 2005). The above-mentioned bands are present in all LDH-DBS intercalates, whatever the preparation method used.

The characteristic 446 cm^{-1} M-O lattice vibration band is present in all the samples. This is consistent with an intact LDH sheet structure. The Mg-OH translation mode and Al-OH translation mode are observed at 763 and 549 cm^{-1} respectively (Kloprogge ***et al.***, 2002 and 2004). The shoulder at 917cm^{-1} is a result of the M-OH deformation mode.

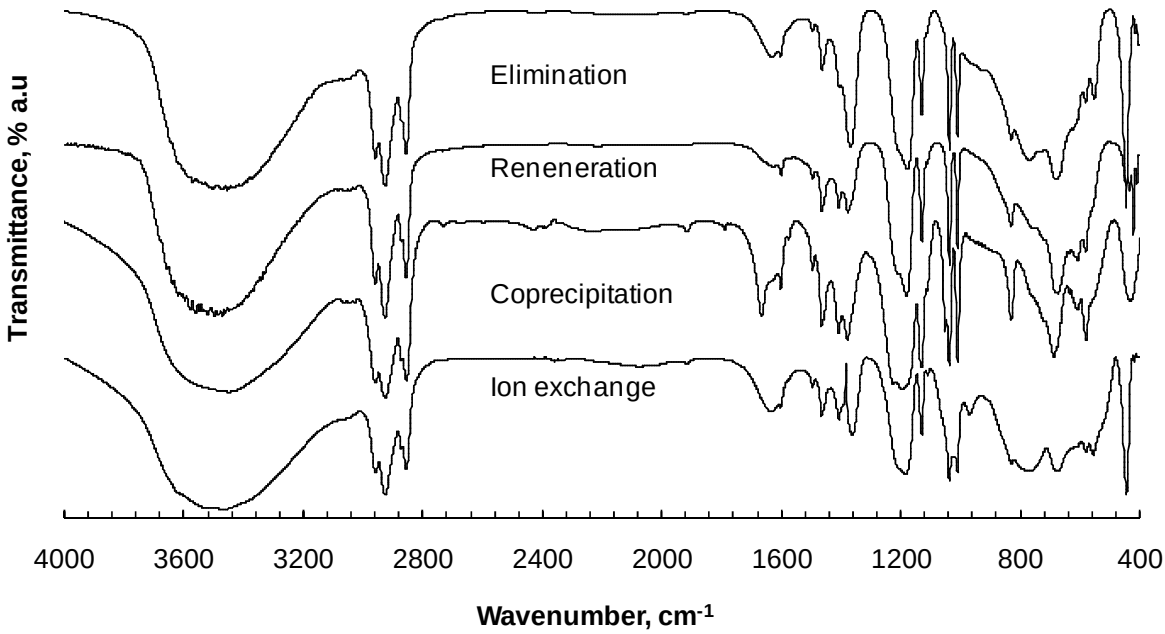

Figure 4.8: Comparison of FT-IR spectra of LDH-DBS from different methods

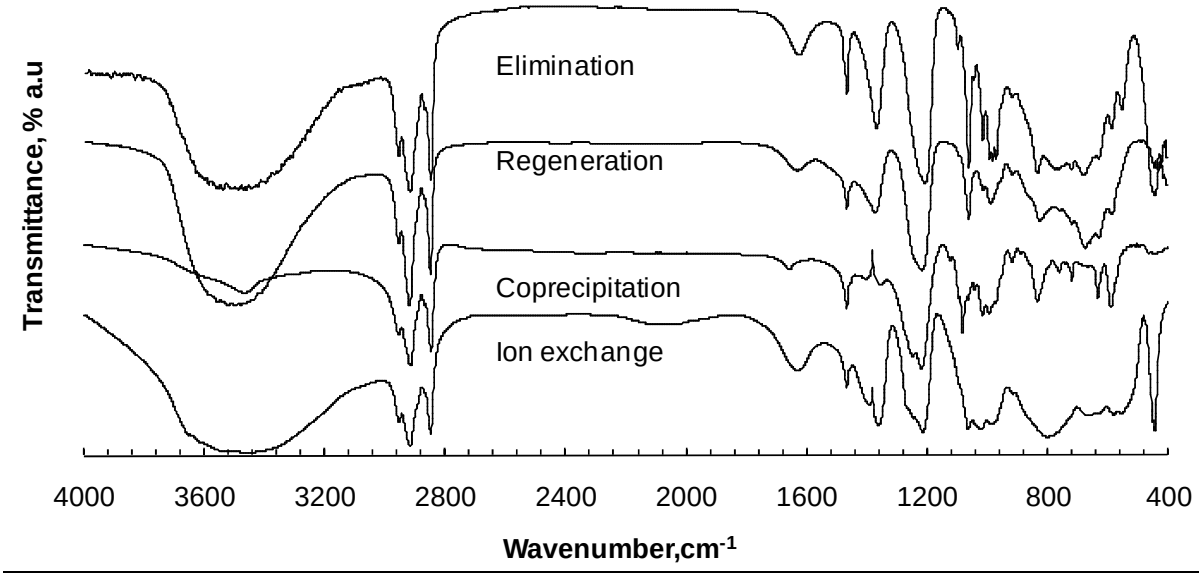

Figure 4.9: Comparison of FT-IR spectra of LDH-DS from different methods

Generally, the spectra show no marked difference, indicating that similar end-products were obtained. The elimination, regeneration and ion exchange spectra showed trace contamination by carbonate ions, confirmed by the presence of the 1365–1370 cm^{-1} peak in both the LDH-DBS and LDH-DS samples.

4.3 XRD

In this study, it was established that intercalation favours the incorporation of long-chain carboxylic acids above the anionic surfactants SDS and SDBS (see Figure 2.9). The observed basal spacings (d_L) for the products obtained with either surfactant (SDS or SBS) are the same, provided the aliphatic acid chain is sufficiently long. The dependence of d_L on the number of carbons in the carboxylic acid (n) was determined by a least squares curve fit to the SDS data and yielded:

$$d_L = 0.810 + 0.241\, n \qquad (7)$$

The magnitude of the observed basal spacing values implies bilayer intercalation. The slope $\Delta d_L/\Delta n = 0.241$ is consistent with a chain tilt angle of ca. 71.6° to the plane of the clay sheets (Nhlapo ***et al.***, 2008).

Anbarasan and co-workers (2005) found that SDBS on its own does not intercalate in LDH in aqueous suspension, even when the reaction temperature is raised to 70 °C. Although they claim that some intercalation of SDS occurs under similar conditions, the basal spacing of the product was anomalously low (d_L = 2.09 nm cf. 2.67 nm). In the present study, intercalation of neat SDS and SDBS, as well as acetic acid on its own, was attempted under ambient conditions and a pH of 10. The experimental basal spacing and TG data obtained for these products are presented in Table 4.2. They are in substantial agreement with the values determined for the precursor compounds and thus indicate that no discernible intercalation occurred. However, the results were markedly different when the LDH was suspended in an aqueous medium in the presence of mixtures of one of the surfactants together with a lower acid. Figure 2.9 shows that the basal spacing of the products obtained with acetic, butyric or hexanoic acid deviate considerably from the straight-line dependence predicted by equation (7). For LDH-DBS, the corresponding d-values agree with each other to within experimental error ($d_L \approx 2.86$ nm), while for LDH-DS, the $d_L \approx 2.58$ nm for acetic and butyric acids. The experimental d_L values are in reasonable agreement with the basal spacing values reported for LDH-DS and LDH-DBS as prepared by other methods (see Table 4.1). This implies that the presence of lower aliphatic acids facilitates intercalation of SDBS and SDS in LDH-CO_3 under mild conditions, i.e. ambient temperature and aqueous medium at pH < 10.

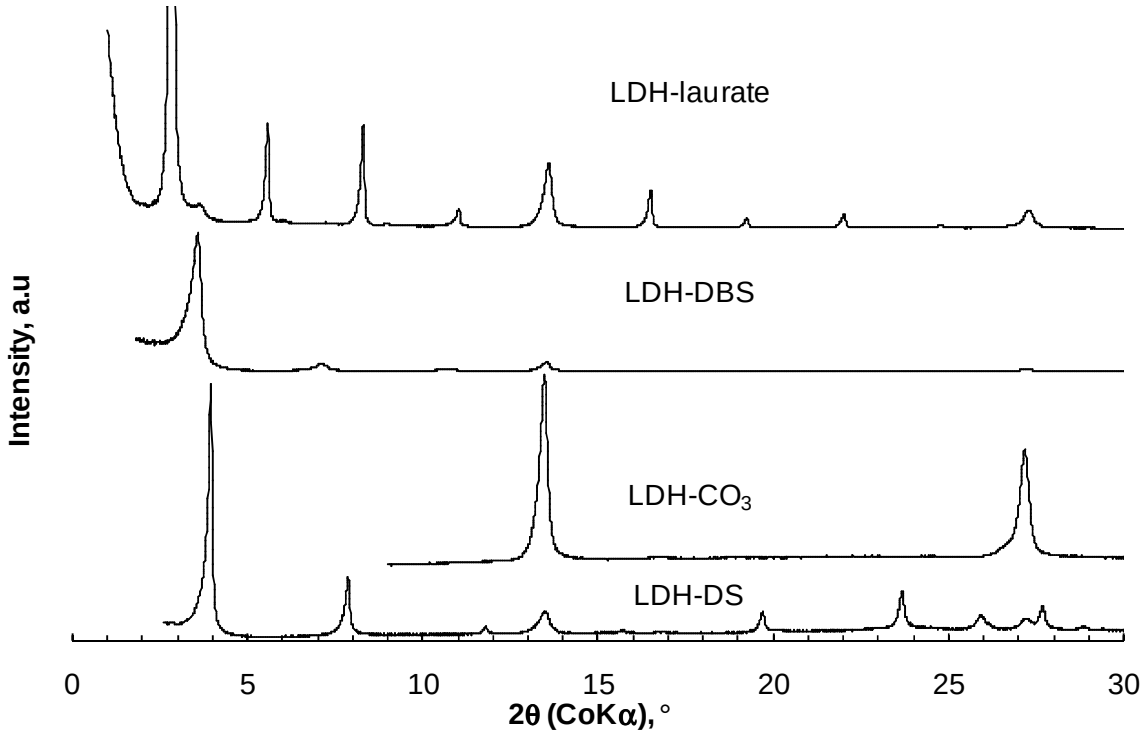

Figure 4.10: X-ray diffractograms for LDH-CO3, LDH-DS, LDH-DBS and LDH-laurate

Figure 4.10 compares the X-ray diffractograms recorded for LDH-DS, LDH-DBS (both prepared in the presence of acetic acid) and LDH-laurate, with that for LDH-CO_3. The reflections at 0.76 nm ($2\theta = 13.2^{\circ}$) and 0.38 nm ($2\theta = 27.2^{\circ}$) are characteristic of LDH-CO_3. They are also present in the LDH-surfactant compounds, indicating that they contain LDH-CO_3 as an impurity. The shift of the 0.76 nm basal reflection to higher orders is indicative of interlayer expansion, hence the incorporation of the respective surfactant anions.

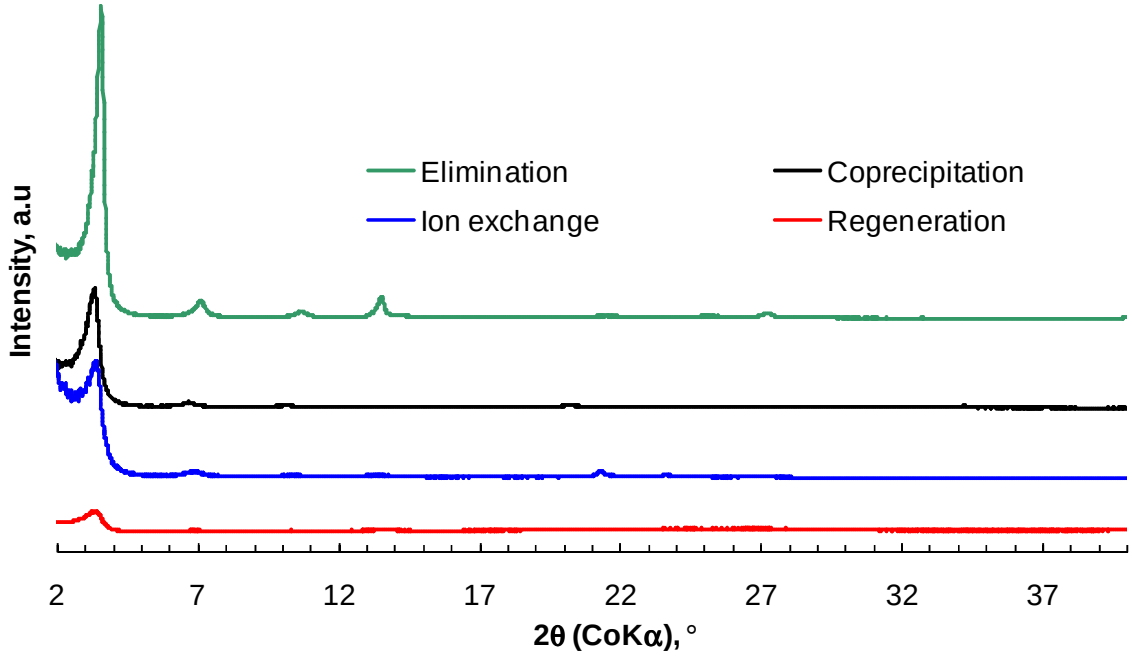

Figure 4.11: X-ray diffractogram of LDH-DBS prepared from the methods indicated

Generally, the peaks observed for LDH-DBS are sharp and distinct, indicating better ordering as seen in the elimination method (see Figure 4.11). The broadening of the peaks in the regeneration method is an indication of an amorphous LDO, which does not completely revert to its original structure.

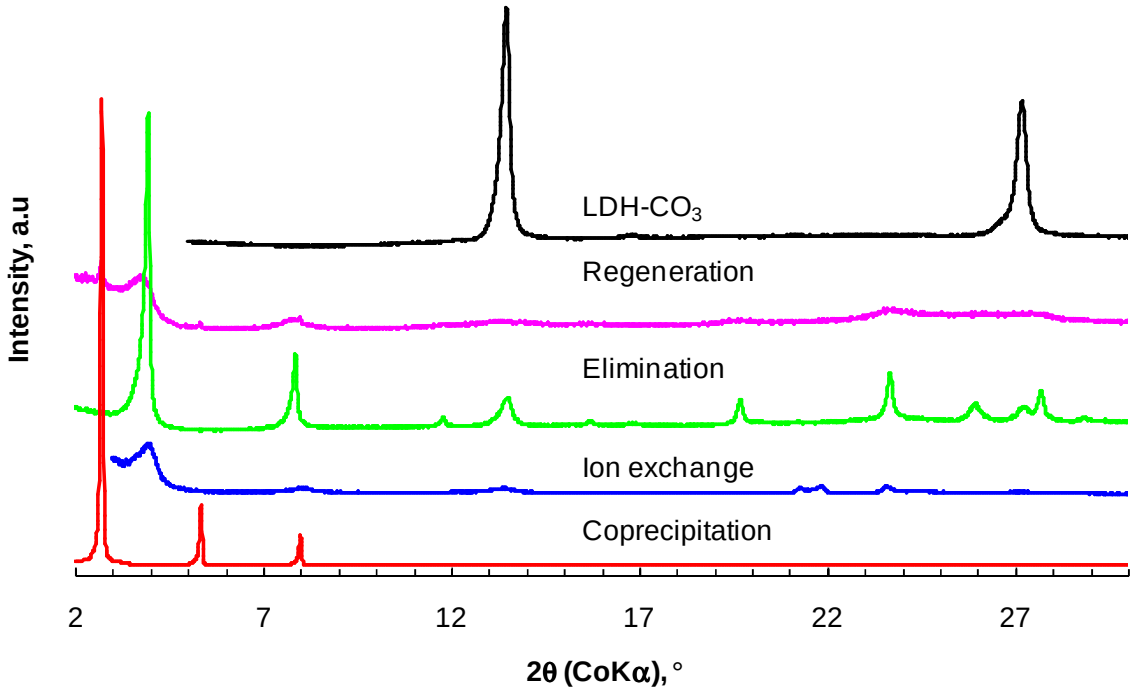

Figure 4.12: X-ray diffractogram of LDH-DS prepared by various methods

Focusing on the LDH-DS obtained by the regeneration method, the broad peaks centred at 3.82°, 7.81° and 8.00° (2.64 nm) in Figure 4.10 are characteristic for monolayer intercalated SDS. The 0.74 nm basal spacing indicated by the peak at 14.0° is attributable to unreacted LDH-CO_3. A close look at the XRD spectrum for the regeneration-based LDH-DS reveals two additional series of XRD peaks. The large basal spacing (3.83 nm) indicated by the low-intensity, but sharp, series of peaks at 2.70°, 5.34° and 8.00° points to bilayer intercalation (see Figures 4.12 and 4.13). This can be explained by the co-intercalation of dodecanol with the dodecyl sulphate. Greater interlayer separation is also observed with the LDH-DS based on co-precipitation (3.8 nm). However, the peaks in the diffractogram are distinct and sharp, indicating better ordering.

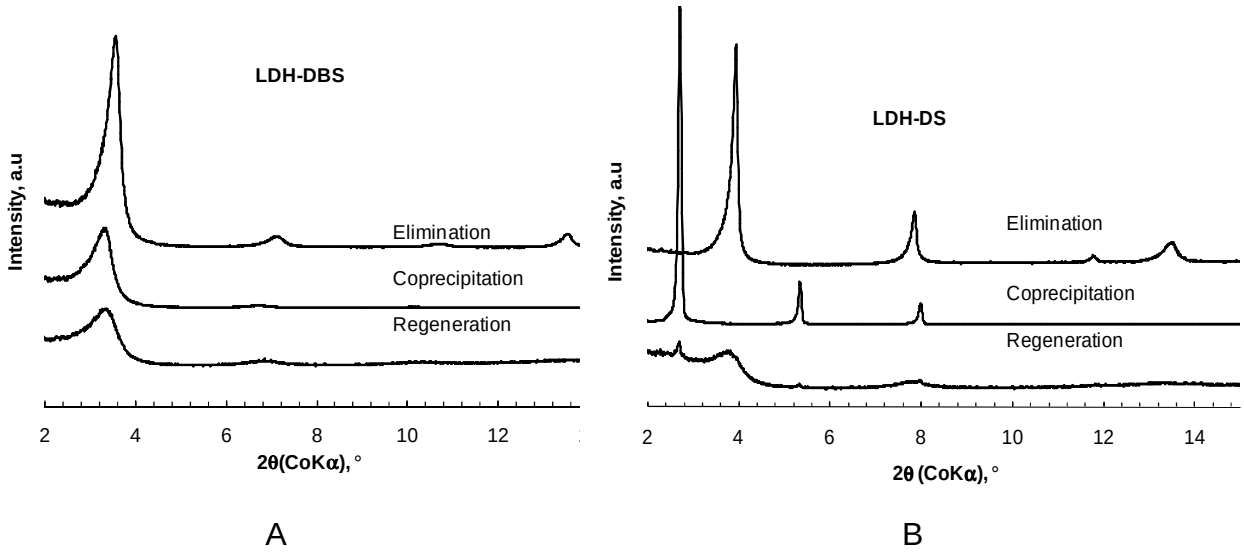

Figure 4.13: Comparison of X-ray diffractograms for LDH-surfactants prepared by regeneration, co-precipitation and ion exchange by elimination method

The assumption mentioned explains several anomalies in the experimental data for LDH-DS prepared by the regeneration method, as well as observations by other investigators (You ***et al***., 2000b; Zhao & Nagy, 2004; Costa ***et al.***, 2008, Clearfield ***et al.***, 1991; Anbarasan ***et al.***, 2005). Firstly, although the LDH-DS has a high sulphur content (atom ratio S/Al = 0.467), the data on the TG residue at 800 °C indicate a very low organic content (see Table 4.2), thus indicating insufficient dodecyl sulphate present to account for the high concentration of sulphur in the sample. Considering the solubility of both magnesium and aluminium sulphate, it is likely that the excess sulphur could be accounted for by the formation of LDH-SO_4. Indeed, the peaks at 11.8° and 23.9° (basal spacing of 0.87 nm) are consistent with the presence of this phase as an impurity. Kopka ***et al.*** (1988) found that the alkanols co-intercalate with alkyl sulphates into Zn_2Cr-LDH, forming a bilayer arrangement. They observed a basal spacing of 4.15 nm for the combination of SDS and dodecanol in this LDH matrix. Thus, the present value for Mg_2Al-LDH is at least within the right approximation/estimation.

To demystify the origin of the dodecanol and excess of sulphate ions, it is well documented that sodium dodecyl sulphate hydrolyses at low pH (Bethell ***et al.***, 2001; Nakagaki & Yokoyama, 1985). Conversely, Angarska ***et al***. (1998) found that

hydrolysis also occurs under highly basic conditions. Such hydrolysis yields both the required sulphate ions and the dodecanol according to the following reaction:

Scheme I: $CH_3(CH_2)_{11}OSO_3^- + OH^- \rightarrow CH_3(CH_2)_{11}OH + SO_4^{2-}$

Clearfield and co-workers (1991) undertook an extensive study of the effect of pH on the intercalation of SDS in Ni_4Al-LDH-Cl. Their reactions seem to have been conducted under ambient conditions with reaction times varying from 4 to 24 h. They found that an increase in the reaction pH resulted in a corresponding increase in the interlayer spacing. However, surprisingly, the amount of dodecyl sulphate that was intercalated decreased. The suggestion made in this study provides a rationalisation of the pH effect observed by Clearfield ***et al.*** (1991). Hydrolysis of the surfactant releases sulphate ions that are preferentially intercalated. This reduces the ability of the clay to absorb SDS. The co-intercalation of the resultant dodecanol with the dodecyl sulphate explains the drastic increase in the basal spacing. Interestingly, at pH = 9 and pH = 10, Clearfield ***et al.*** (1991) observed basal spacing values of 36.6 and 42 nm respectively. The latter value is just slightly larger that that found by Kopka ***et al.*** (1988) for the co-intercalation of dodecanol and dodecyl sulphate.

Zhao & Nagy (2004) made similar observations with respect to a pH effect in Mg_4Al-LDH-DS and Mg_5Al-LDH-DS prepared by co-precipitation. When prepared at pH = 10, basal spacing values of 36.6 and 40.3 nm were found for these two compounds respectively. These researchers used SDS in stoichiometric excess (1.5 times) and long reaction times at elevated temperatures (3 days at 65 °C). The degree of ion exchange was estimated from the total organic content. They observed a decrease in the apparent degree of ion exchange with an increase in the reaction pH. The possible deduction is again that the high basal spacing is caused by the partial hydrolysis of the SDS and the subsequent co-intercalation of dodecanol with SDS. If this were indeed the case, the actual degree of ion exchange would be even lower and attributable to concomitant sulphate intercalation. Similar arguments may be relevant to explain the low degree of intercalation, as well as the reported bilayer nature of sodium octyl sulphate (SOS) intercalation, reported by You ***et al***. (2000b).

Co-intercalation of the sodium salts was found to accompany that of the surfactant anions when the anion exchange or the direct precipitation methods were used to prepare LDH-DS (Clearfield ***et al.***, 1991; Xu & Braterman, 2003) or LDH-DBS (Xu & Braterman, 2003). However, the amounts tend to be small, e.g. Na/Al < 0.065 (Clearfield ***et al.***, 1991). Table 4.1 indicates that even lower amounts of sodium were found in the present samples prepared using acetic acid as mediating agent. Quite the opposite is true for the sodium content of the samples prepared by the regeneration method. Considering Scheme I, rehydration of the calcined clay (LDO) oxide initially results in rapid formation of LDH-OH (Angarska ***et al.***, 1998) according to Scheme II. Some magnesium (and aluminum) hydroxide will also dissolve. Both scenarios introduce excess hydroxyl anions and the pH of the water phase increases. In this study it was found that the hydration of the present LDO caused an initial rapid increase to pH = 10.7, with a slower rise to pH = 12 over a 24-h period. By comparison, pH = 9.8 when the same amount of LDH-CO_3 was suspended in distilled water and this decreased to pH = 9.2 after 24 h.

Scheme II: $\{LDO\} + 3.5\ H_2O \rightarrow \{LDH\}^{+}OH^{-}$

Next, these OH^- anions may be exchanged with other anions that are present in the mixture, e.g. intercalation of the dodecyl sulphate ion according to Scheme III:

Scheme III: $R\text{-}OSO_3^-Na^+_{(aq)} + \{LDH\}^+OH^- \xrightarrow{Kf} R\text{-}OSO_3^-\{LDH\}^+ + Na^+_{(aq)} + OH^-_{(aq)}$

Parker ***et al.*** (1995) measured the amount of anion that was absorbed by freshly calcined LDH after 24 h. They found that the relative preference for anions follows the sequence:

Sequence A: $SO_4^{2-} > F^- > HPO_4^{2-} > Cl^- > B(OH)_4^- > NO_3^-$.

This matches the order of preferred affinity of anions in LDH (with $x \approx 0.3$) reported by Miyata (1983):

Sequence B: $CO_3^{2-} >> SO_4^{2-} >> OH^- > F^- > Br^- > Cl^- > NO_3^- > I^-$

Bontchev ***et al.*** (2003), instead, found that $Br^- > Cl^-$ for an LDH with $x \approx 0.25$. This suggests that the exact order of anion preference may depend to some extent on the Mg/Al ratio. In either case it is clear that LDH has a high affinity for the divalent sulphate ions and that they will easily replace the hydroxyl ions present in the clay.

4.4 SEM

LDH-CO_3, as seen in the SEM micrographs below, consists of small crystals that have a sand rose arrangement formed by numerous inter-grown small crystallites (Adachi-Pagano ***et al.***, 2000). On average, the crystallite diameter for LDH-CO_3 is found to be 1 μm (Braterman ***et al.***, 2004). Generally, the particle size and lateral dimensions will differ according to the preparation conditions.

The platelets in the LDH-DBS appear to be agglomerated; this can be explained by hydrophobic interactions. The products from the elimination method have small sheets and less sharp edges as compared with their LDH precursor. The intercalates obtained by the regeneration method have an unusual surface morphology in which the surface appears perforated; this is consistent with the findings of Costa ***et al.*** (2008).

Of profound interest is the fact that all the intercalation methods studied yield products with varying morphological properties. Co-precipitation LDH-DS showed very large crystallites with three different growth habits and crystallite behaviour ranging from plain platelets to ribbon-like and bar-like materials. Xu & Braterman (2003) observed this particular characteristic in LDH-DBS. Normally, in inorganic LDHs “the crystallite growth is along the ***a*** and ***b*** axes to maximise the exposure of the hydroxyl groups to the aqueous phase, given that the hydroxides of the metal hydroxide layer are found in the ***ab*** plane” (Xu & Braterman, 2003). However, in LDH-surfactant the ***ab*** plane is hydrophobic in nature, leading to a simplistic nucleation of new sheets which form antiparallel structures. Hence, growth along the c-axis is energetically and kinetically favourable, consequently forming bar-like structures (Braterman ***et al.***, 2004). The ribbon-like particles exhibit twists and

bends owing to hydrophobic interactions of the internal and external surfactant anions.

From these arguments, one could conclude that the morphology of organo-LDH is greatly affected by aspects such as hydrophobicity (Xu & Braterman, 2003), critical micelle concentration (Pavan ***et al.***, 1999) and charge density (Braterman ***et al.***, 2004).

Table 4.3: SEM micrographs of LDH-surfactants prepared by various methods

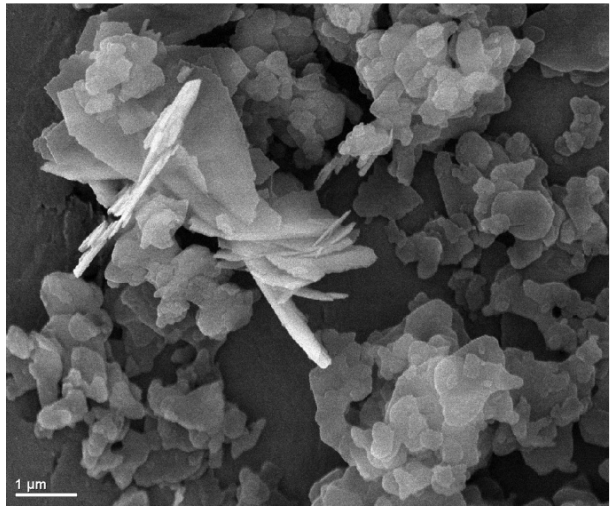

LDH-CO_3

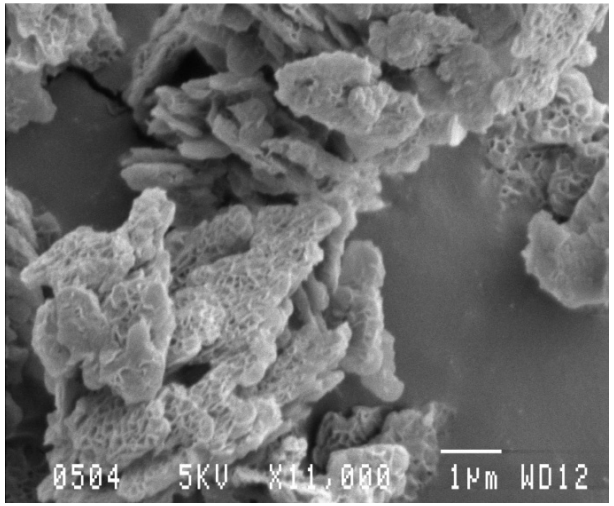

Regeneration LDH-DBS

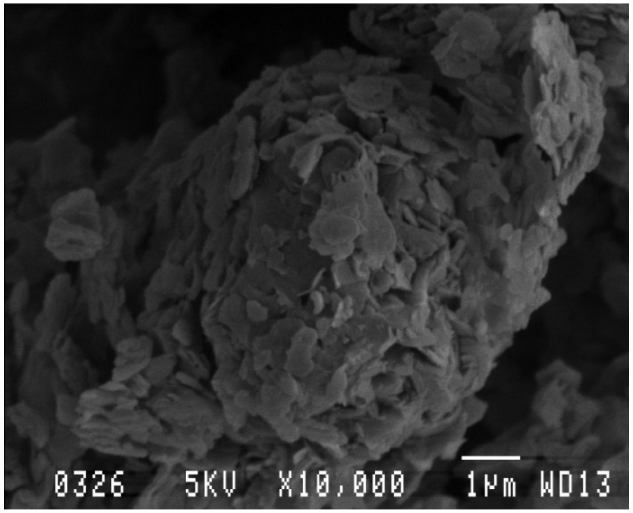

Elimination LDH-DBS

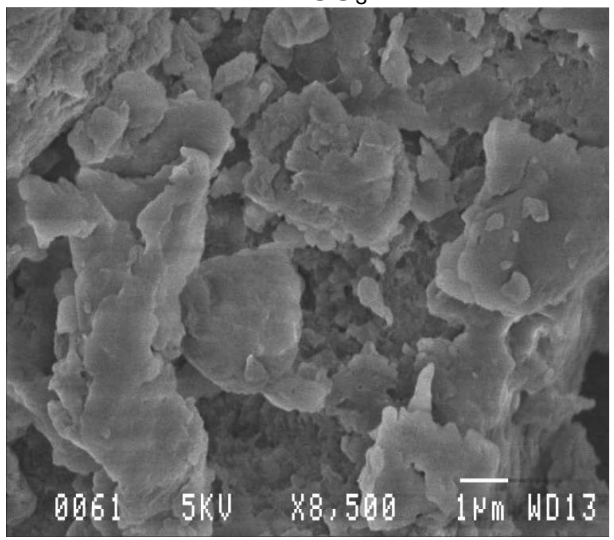

Co-precipitation LDH-DBS

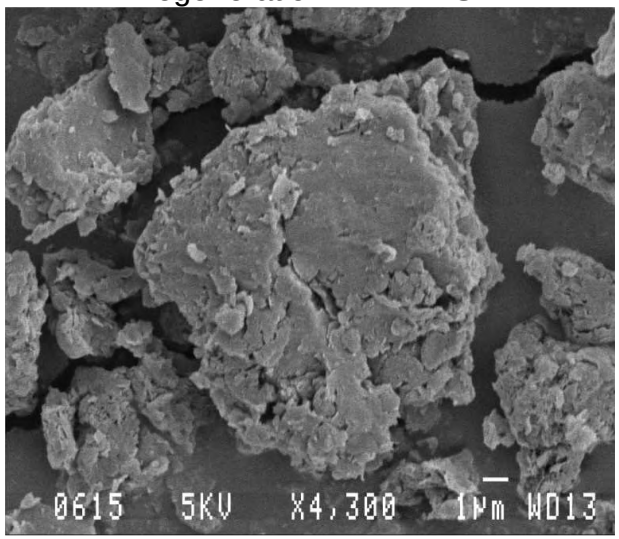

Ion exchange LDH-DBS

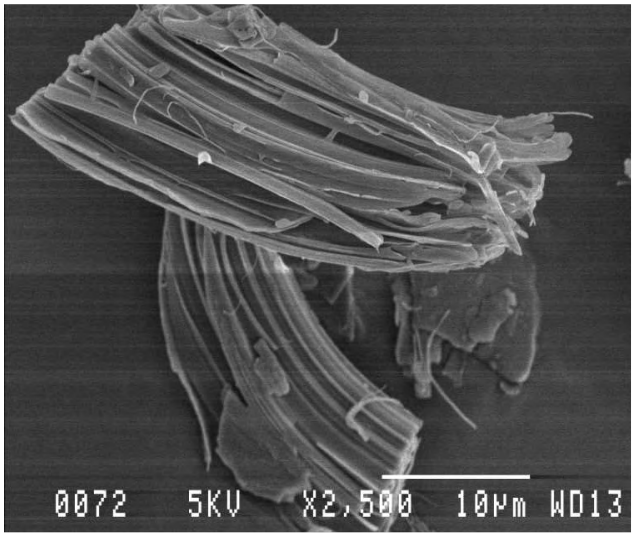

Co-precipitation LDH-DS

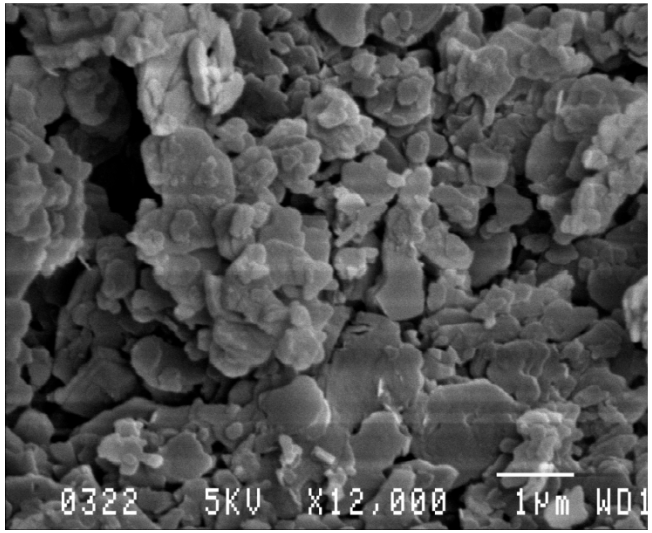

Elimination LDH-DS

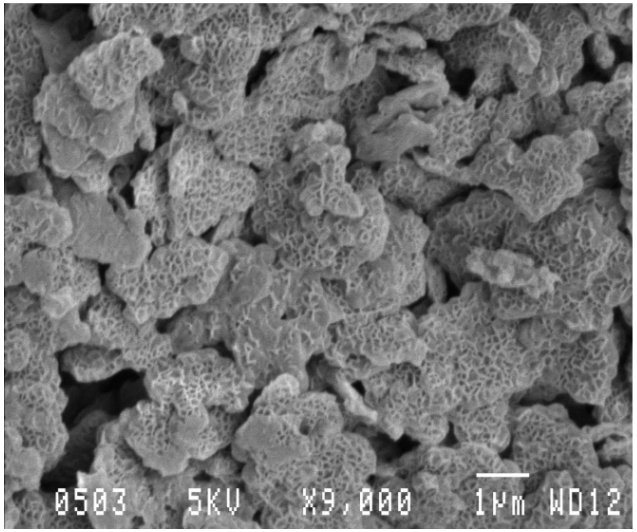

Regeneration LDH-DS

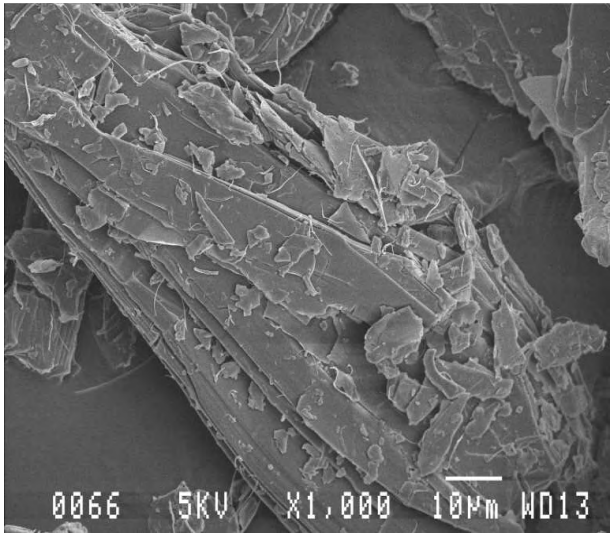

Co-precipitation LDH-DS

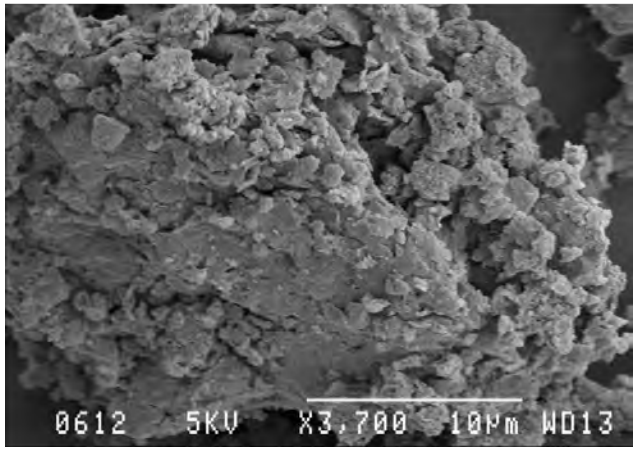

Ion exchange LDH-DS

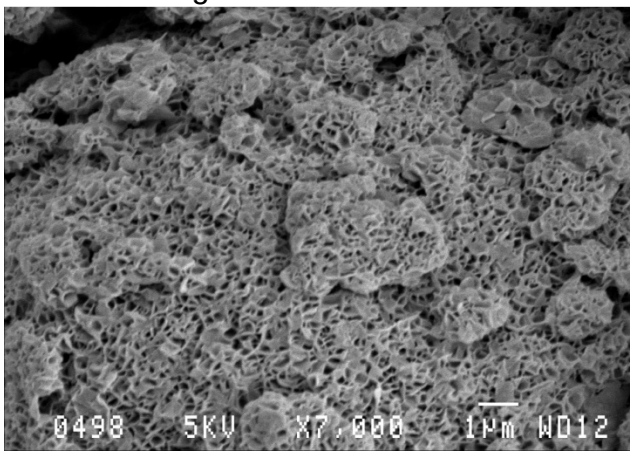

Surface of regenerated LDH-DS

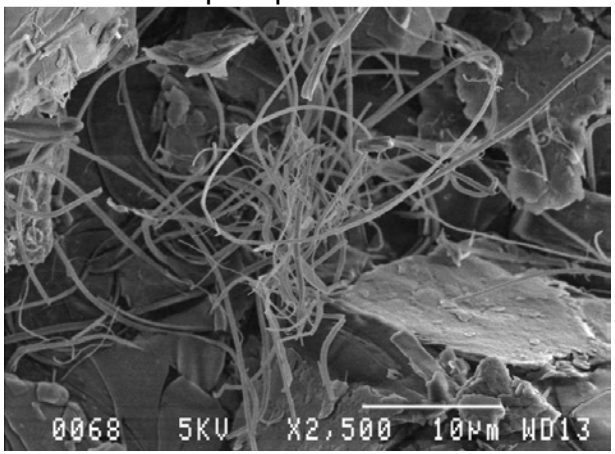

Co-precipitation LDH-DS

4.5 Mechanism of Acid-Mediated Decarbonation and Intercalation

Bish (1980) pioneered the decarbonation of LDH-CO_3 by treatment with dilute aqueous solutions. Decarbonation was followed by exchange with Cl^-, NO_3^- and SO_4^{2-} using the corresponding inorganic acids. Iyi ***et al.*** (2004 and 2005) proposed a plausible two-step process to explain the decarbonation of LDH-CO_3 in the presence of dilute acid or acid-sodium salt mixtures. The initial step consists of protonation of the carbonate and its conversion to the hydrocarbonate.

$$CO_3^{2-}{}_{(aq)} + H^+{}_{(aq)} \leftrightarrow HCO_3^-{}_{(aq)} + H_2O_{(l)} \quad (8)$$

In this study, it was established that the presence of short-chain carboxylic acids facilitates the intercalation of surfactant anions. In the absence of these acids, no intercalation is observed. These acids play the role of eliminating the carbonate anion, with the simultaneous incorporation of the surfactant anion into the interlayer region. It could even be argued that the conversion of the interlayer carbonate ions into monovalent ions is a prerequisite: it allows the interlayer spacing to increase, hence accommodating the much larger surfactant molecules. Iyi et al. (2005) found that the degree of substitution is affected by the presence of the counterion and the ***x***-value. A high degree of substitution is associated with a large excess of the counterion in high concentrations (> 4 mol/L). The ease of substitution also decreases with an increase in ***x***, the fractional aluminium substitution in the layers. These two factors may explain why only partial replacement of carbonate was achieved in the present study.

CHAPTER 5: CONCLUSION

Direct intercalation of surfactant into LDH-CO_3 precursor is difficult, owing to the tenacity with which the carbonate anion is held within the hydroxide layers. In an effort to overcome this difficulty, either thermal or acid treatments have been employed. Iyi ***et al.*** (2004 and 2005) demonstrated that the conversion of LDH-CO_3 in LDH-A, where A is another inorganic anion, is facilitated by the presence of dilute acids as decarbonation aids. In the current study, the concept was extended to the intercalation of LDH-CO_3 with dodecyl sulphate (DS) and dodecylbenzene sulphonate (DBS). Intercalation was found to proceed smoothly under mild conditions of pH and temperature when water-soluble carboxylic acids were added to aqueous suspensions of LDH-CO_3 and surfactant. In comparison with the regeneration technique, well-crystallised products with improved purity were obtained. However, the degree of carbonate substitution that was achieved did not exceed 50%.

In the regeneration method, the LDH-CO_3 is heated and converted into an essentially carbonate-free layered double oxide (LDO). The resulting LDO is then suspended and stirred in an aqueous medium containing the desired anion. Several researchers have successfully employed this method. This study showed that although the method works for DBS, problems are encountered when applying it to DS. The anomalous behaviour of the latter surfactant is attributed to its hydrolysis in a highly basic medium, forming sulphate ions and dodecanol. Thus, LDH-DS prepared by the regeneration method contains LDH-SO_4 as an impurity. In addition, the liberated dodecanol may co-intercalate with DS in a bilayer format to give an extra impurity phase. These insights elucidate the anomalous pH effect on the d-spacing reported for LDH-DS. Interestingly, the bilayer orientation is also observed with the co-precipitation product prepared at essentially neutral pH. Amidst all the success in the implementation of the regeneration method, metal uniformity of the LDH is altered by calcination; as a result less organic anions are incorporated within the interlayer.

Purer products showing a high degree of anion intercalation have been obtained

using (i) direct synthesis by co-precipitation (Zhang ***et al.***, 2007), or (ii) ion exchange starting with LDH- (Xu & Braterman, 2003), i.e. LDH precursors with more easily exchangeable monovalent anions, e.g. Cl^- or NO_3^-. The high crystallinity obtained by the coprecipitation method, has been assumed to be due to direct formation of the LDH-surfactant from solution, rather than transformation of a pre-existing solid (Braterman 2004). However, in this study the co-precipitation products were found to have a substantial amount of sodium ions. Nonetheless, these methods should be considered when high-purity LDH-DS or LDH-DBS is sought.

REFERENCES

Adachi-Pagano, M., Forano, C. and Besse J-P. (2003). Synthesis of Al-rich hydrotalcite-like compounds by using the urea hydrolysis reaction – control of size and morphology. ***J. Mater. Chem.,*** 13: 1988-1993.

Adachi-Pagano, M., Forano, C. and Besse, J-P. (2000). Delamination of layered double hydroxides by use of surfactants. ***Chem. Commun***., 91-92.

Allmann, R. (1970) Doppelscheichtstruktchen mit brucitahnlichen Schitionen $[Me(II)_{1-x}Me(III)_x(OH)_2]^{x+}$. ***Chimia***, 24: 99-108.

Allmann, R. (1968). The crystal structure of pyroaurite. ***Acta Cryst***. 24: 972-977

Aminoff, G. and Broome, B. (1930). Contribution to the knowledge of mineral pyroaurite. ***Kungl. Sven. Vetensk. Handl.*** 5: 23

Anbarasan, R., Lee, W. and Im, S. S. (2005). Adsorption and intercalation of anionic surfactants onto layered double hydroxides – XRD study. ***Bull. Mater. Sci.,*** 28: 145-149.

Angarska, J. K., Tachev, K. D., Kralchevsky, P. A., Mehreteab, A. and Broze, G. (1998). Effects of counterion and co-ions ondrainage and stability of liquid films and foams. ***J. Colloid Interface Sci.***, 200: 31- 45.

Aramendia, M. A., Borau, V., Jimenez, C., Marinas, J. M., Ruiz, J. R. and Urbano, F. J. (2002). Comparative study of Mg/M(III) (M=Al, Ga, In) layered double hydroxides obtained by coprecipitation and the sol-gel method, ***J. Solid State Chem***., 168:156-161.

Beekman, S.M., (1960). Preparation and properties of new gastric antiacids. I. Aluminium hydroxide-magnesium carbonate dried gels. ***J. Am Pharm Assoc***. 49: 191-200

Bera, P., Rajamathi, M., Hegde, M. S. and Kamath, P. V. 2000. Thermal behaviour of hydroxides, hydroxysalts and hydrotalcites. ***Bull. Mater. Sci.***, 23(2): 141-145.

Bethell, D., Fessey, R. E., Namwindwa, E. and Roberts, D. W. 2001. The hydrolysis of C_{12} primary alkyl sulphates in concentrated aqueous solutions. Part 1. General features, kinetic form and mode of catalysis in sodium dodecyl sulphate hydrolysis. ***J. Chem. Soc. Perkin Trans***., 2: 1489- 1495.

Bhattacharyya, A., Hall, D. B. and Barnes, T. J. (1995). Novel oligovanadate-pillared hydrotalcite. ***Appl. Clay Sci***., 10: 57-67.

Bish, D. L. (1980). Anion exchange in the pyroaurite group mineral takovite. Application to other hydroxide minerals. ***Bull Mineral***., 103: 170 -175.

Bitting, D. and Harwell, J. H. (1987). Effects of counterions on surfactant surface aggregates at the alumina/aqueous solution interface. ***Langmuir,*** 3: 500-511.

Boclair J. W. and Braterman, P. S. (1999). Layered double hydroxide stability. 1. Relative stabilities of layered doule hydroxides and their simple counterparts. ***Chem. Mater.***, 11: 298-302.

Boehm, H-P., Steinle, J. and Vieweger, C. (1977). Zuschrift $[Zn_2Cr(OH)_6]^x \cdot 2H_2O$, neu schichtverbindungen mit anionenaustausch-und quellvermogen. ***Angew. Chem.,*** 89: 259-260.

Bontchev, R. P., Liu, S., Krumhansl, J. L., Voigt, J. and Nenoff, T. M. (2003). Snythesis, characterization, and ion exchange properties of hydrotalcite $Mg_6Al_2(OH)_{16}(A)_x(A^I)_{2-x} \cdot 4H_2O$ (A,A^I = Cl^-, Br^-, I^- and NO_3^-, $2 \geq x \geq 0$) derivatives. ***Chem. Mater.,*** 15: 3669- 3675.

Borja, M. and Dutta, P. K. (1992). Fatty acids in layered metal hydroxides: Membrane-like structure and dynamics. ***J. Phys. Chem.*** 96: 5434-5444.

Bouranda, M., Lafjah, M., Ouali, M. S. and De Menorval, L. C. 2008. Basic dye removal from aqueous solutions by dodecylsulfate- and dodecylbenzene sulfonate-intercalated hydrotalcite. ***J. Hazard. Mater.,*** 153: 911-918.

Braterman, P. S., Xu, Z. P. and Yarberry, F. (2004). Layered double hydroxides. In: Auerbach, S. M. and Dutta, P. K. (Eds), ***Handbook of Layered Materials***. New York: Taylor & Francis, pp. 373-474.

Brindley, G. W. and Kikkawa, S. (1979). A crystal-chemical study of Mg,Al and Ni,Al hydroxy-perchlorates and hydroxy-carbonates. ***Am. Mineral.***, 64: 836-843.

Bröckner FJ, Kaempfer K. (1975). ***Chemie Ing. Techn.*** 47:513

Caillere, S. and Henin, S. (1944). New observation of faratsihite. ***Compt. Rend.***, 219: 256

Carja, G., Chiriac, H. and Lupu, N. (2007). New magnetic organic–inorganic composites based on hydrotalcite-like anionic clays for drug delivery. ***J. Magn. Magn. Mater.,*** 311: 26-30.

Carlino, S. (1997). The intercalation of carboxylic acids into layered double hydroxides: A critical evaluation and review of different methods. ***Solid State Ionics***, 98: 73-84.

Carlino, S. and Hudson, M. J. (1994). The reaction of molten sebacic acid with a layered (Mg/Al) double hydroxide. ***J. Mater. Chem.,*** 4: 99-104.

Carlino, S. and Hudson, M. J. (1995). Thermal intercalation of layered double hydroxides: Capric acid into an Mg-Al LDH. ***J. Mater. Chem.,*** 5(9): 1433-1442.

Carlino, S., Hudson, M. J., Husain, S. W. and Knowles, J. A. (1996). The reaction of molten phenylphosphonic acid with a layered double hydroxide and its calcined oxide. ***Solid State Ionics***, 84: 117-I29.

Cavani, F., Trifirò, F. and Vaccari, A. (1991). Hydrotalcite-type anionic clays: Preparation, properties and applications. ***Catal. Today***, 11: 173-301.

Chibwe, K. and Jones, W. (1989). Intercalation of organic and inorganic anions into layered double hydroxide. ***J. Chem. Soc., Chem. Commun.,*** 926-927.

Choy, J-H. (2004). Intercalative route to heterostructured nanohybrids. ***J. Phys. Chem. Solids,*** 65: 373-383.

Choy, J-H., Kwak, S-Y., Park, J-S., Jeong, Y-J. and Portier, J. (1999). Intercalative nanohybrids of nucleoside monophosphates and DNA in layered metal hydroxide. ***J. Am. Chem. Soc.***, 121: 1399-1400.

Clearfield, A., Kieke, M., Kwan, J., Colon, J. L. and Wang, R. C. (1991). Intercalation of dodecyl sulfate into layered double hydroxides. ***J. Inclusion Phenom. Mol. Recognit. Chem.,*** 11: 361-378.

Coates, J. (2000). Interpretation of infrared spectra, a practical approach. In: Meyer (R. A. (Ed.) ***Encyclopedia of Analytical Chemistry***. Chichester: Wiley, p. 10815 - 10837.

Colvin, V. L., Goldstein, A. N. and Alivisatos, A. P. (1992). ***J. Am. Chem. Soc.,*** 114: 5221-5230.

Constantino, V. R. L. and Pinnavaia, T. J. (1995). Basic properties of $Mg^{2+}_{1-x}Al^{3+}_{x}$ layered double hydroxides intercalated by carbonate, hydroxide, chloride and sulfate anions. ***Inorg. Chem.,*** 34: 883-892.

Corma, A., Fornes, V., Martin-Aranda, R. M. and Rey, F. (1992). Determination of base properties of hydrotalcites: Condensation of benzaldehyde with ethyl acetoacetate. ***J. Catal.***, 134: 58-65.

Costa, F. R., Abdel-Goad, M., Wagenknecht, U. and Heinrich, G. (2005). Nanocomposites based on polyethylene and Mg-Al layered double hydroxide. Part I: Synthesis and characterization. ***Polymer,*** 46: 4447-4453.

Costa, F. R., Leuteritz, A., Wagenknecht, U., Jehnichen, D., Häusler, L. and Heinrich, G. (2008). Intercalation of Mg-Al layered double hydroxides by anionic surfactants: Preparation and characterization. ***Appl. Clay. Sci.***, 38(3-4): 153-164.

Costa, F. R., Wagenknecht, U., Jehnichen, D., Abdel-Goad, M. and Heinrich, G. (2006). Nanocomposites based on polyethylene and Mg-Al layered double hydroxide. Part II: rheological characterization. ***Polymer,*** 47: 1649-1660.

Constantino, U., Marmottini, F., Nocchetti, M. and Vivani, R. (1998). New synthetic routes to hydrotalcite-like compounds – Characterisation and properties of the obtained materials. ***Eur. J. Inorg. Chem.,*** 1439-1446.

Crepaldi, E. L., Pavan, P. C. and Valim, J. B. (1999). A new method of intercalation by anion exchange in layered double hydroxides. ***Chem. Commun.,*** 155-156.

Crepaldi, E. L., Pavan, P. C. and Valim, J. B. (2000). Anion exchange in layered double hydroxides by surfactant salt formation. ***J. Mater. Chem.,*** 10: 1337-1343.

Crepaldi, E. L., Pavan, P. C., Tronto, J., Cardoso, L. P. and Valim, J. B. (2002). Chemical, structural and thermal properties of Zn(II)-Cr(III) layered double hydroxides intercalated with sulfated and sulfonated surfactants. ***J. Colloid Interface Sci.,*** 248: 429-442.

Crepaldi, E. L., Tronto, J., Cardoso, L. P. and Valim, J. B. (2002). Sorption of terephalate anions by calcined and uncalcined hydrotalcite-like compounds. ***Colloids Surf. A.***, 211: 103-114.

Crespo, I., Barriga, C., Rives, V. and Ulibarri, M. A. (1997). Intercalation of iron hexacyano complexes in Zn,Al-hydrotalcite. ***Solid State Ionics,*** 101-103: 729-735.

Darder, M., Lopez-Blanco, M., Aranda, P., Leroux, F. and Ruiz-Hitzky, E. (2005). Bio-nanocomposites based on layered double hydroxides. ***Chem. Mater.***, 17: 1969-1977.

Dèkány, I. and Haraszti, T. (1996). Layered solid particles as self-assembled films .***Colloid Surf A.,*** 391: 123-124.

Dèkány, I., Berger, F., Imrik, K. and Lagaly, G. (1997). Hydrophobic layered double hydroxides (LDHs): Selective adsorbents for liquid mixtures. ***Colloid. Polym. Sci.,*** 275: 681-688.

Del Arco, M., Fernández, A., Martín, C. and Rives, V. (2009). Release studies of different NSAIDs encapsulated in Mg,Al,Fe-hydrotalcites. ***Appl. Clay Sci.,*** 42(2-3): 538-344.

Delmas, C. and Borthomieu, Y. (1993). Chimie Douce Reaction: A new route to obtain well crystallized layered double hydroxides. ***J. Solid State Chem.,*** 104: 345-352.

Dimotakis, E. D. and Pinnavaia, T. J.(1990). New route to layered double hydroxides intercalated by organic anions: Precursors to polyoxometalate-pillared derivatives. ***J. Am. Chem. Soc.,*** 29(13): 2393-2394.

Dos Reis, M. J., Silverio, F., Tronto, J. and Valim, J. B. (2004). Effects of pH, temperature, and ionic strength on adsorption of sodium dodecylbenzenesulfonate into Mg–Al–CO3 layered double hydroxides. ***J. Phys. Chem. Solids,*** 65: 487-492.

Drezdzon, M. A. (1988). Synthesis of isopolymetalate-pillared hydrotalcite via organic-anion-pillared precursors. ***Inorg. Chem.,*** 27: 4628-4632.

Evans, D. G. and Duan, X. (2005). Preparation of layered double hydroxides and their applications as additives in polymers, as precursors to magnetic materials and in biology and medicine. ***Chem. Commun.,*** 485-496.

Feitknecht, W. (1938). Über die α- form der hydroxide zweiwertiger metalle. ***Helv Chim Acta.*** 21: 766-784.

Feitknecht, W. and Gerber, M. (1942). Zur kenntnis de doppelhydroxide und der basichen doppelsalze. (III). ***Helv Chim Acta.***, 25: 131-137.

Feitknecht, W. (1936). ***Z Angew Chem.*** 49:24

Fendler, J. H. and Meldrum, F. C. (1995). The colloid chemical approach to nanostructured materials. ***Adv. Mater.,*** 7: 607-632.

Fischer, H. (2003). Polymer nanocomposites: From fundamental research to specific applications. ***Mat. Sci. Engng C.,*** 23: 763-772.

Flink G. (1910). Bidrag till sveriges mineralogi. ***Arkiv Kemi Min Geol.*** 3:1-166

Flink G. (1914). ***Z Kryst Min.,*** 53: 409-420

Foshag WF. (1920). The chemical composition of hydrotalcite and hydrotalcite minerals. ***Proc. US Nat Museum.*** 58: 147-153

Frondel, C. (1941). Constitution and polymorphism of the pyroaurite and sjögrenite groups. ***Am. Mineral.,*** 26: 295-315.

Frost, R. L., Martens, W., Ding, Z. and Kloprogge, J. T. (2003). DSC and high-resolution TG of synthesized hydrotalcites of Mg and Zn. ***J. Therm. Anal. Calorim.,*** 71: 429-438.

Fudala, A., Palinko, I. and Kiricsi, I. (1999). Preparation and characterization of hybrid organic-inorganic composite materials using the amphoteric property of amino acids: Amino acid intercalated layered double hydroxide and montmorillonite. ***Inorg. Chem.,*** 38: 4653-4658.

Gardner, E. A., Yun, S. K., Kwon, T. and Pinnavaia, T. J. (1998). Layered double hydroxides pillared by macropolyoxometalates. ***Appl. Clay Sci.***, 13: 479-494.

Harwell, J., Hoskins, J. C., Schechter, R. S. and Wade, W. H. (1985). Pseudophase separation model for surfactant adsorption: Isomerically pure surfactants. ***Langmuir,*** 1: 251-262.

He, J., Wei, M., Li, B., Kang, Y., Evans, D. G. and Duan, X. (2005). Preparation of layered double hydroxides. In: Evans, D. G. and Duan, X. (Eds). ***Layered Double Hydroxides***, Heidelberg, Germany: Springer, pp. 89-119.

Hernandez-Mareno, M. J., Ulibarri, M. A., Rendon, J. L. and Serna, C. J. (1985). IR characteristics of hydrotalcite-like compounds. ***Phys. Chem. Miner.***, 12: 34-38.

Hetterley, R. D., Mackey, R., Jones, J. T. A., Khimyak, Y. Z., Fogg, A. M. and Kozhevnikov, I. V. (2008). One-step conversion of acetone to methyl isobutyl ketone over Pd-mixed oxide catalysts prepared from novel layered double hydroxides. ***J. Catal***., 258: 250-255.

Hibino, T. and Tsunashima, A. (1998). Characterization of repeatedly reconstructed Mg-Al hydrotalcite-like compounds: Gradual segregation of aluminum from the structure. ***Chem. Mater.***, 10: 4055-4061.

Hu, G. and O'Hare, D. (2005). Unique layered double hydroxide morphologies using reverse microemulsion synthesis. ***J. Am. Chem. Soc.***, 127: 17808-17813.

Hussein, M. Z. B., Zainal, Z. and Ming, C. Y. (2000). Microwave-assisted synthesis of Zn-Al-layered double hydroxide-sodium dodecyl sulfate nanocomposites. ***J. Mater. Sci. Lett.***, 19: 879-883.

Itoh, T., Ohta, N., Shichi, T., Yui, T. and Takagi, K. (2003). The self-assembling properties of stearate ions in hydrotalcite clay composites. ***Langmuir,*** 19: 9120-9126.

Iyi, N. and Sasaki, T. (2008). Decarbonation of MgAl-LDHs (layered double hydroxides) using acetate-buffer/NaCl mixed solution. ***J. Colloid Interface Sci.***, 322: 237-245.

Iyi, N., Matsumoto, T., Kaneko, Y. and Kitamura, K. (2004). Deintercalation of carbonate ions from a hydrotalcite-like compound: Enhanced decarbonation using acid-salt mixed solution. ***Chem. Mater.***, 16: 2926-2932.

Iyi, N., Okamoto, K., Kaneko, Y. and Matsumoto, T. (2005). Effects of anion species on deintercalation of carbonate ions from hydrotalcite-like compounds. ***Chem. Lett.***, 34: 932-933.

Jobbágy, M. and Regazzoni, A. E. (2004). Delamination and restacking of hybrid layered double hydroxides assessed by in situ XRD. ***J. Colloid Interface Sci.***, 275: 345-348.

Kandare, E. and Hossenlopp, J. M. (2006). Thermal degradation of acetate-intercalated hydroxy double and layered hydroxy salts. ***Inorg. Chem.***, 45: 3766-3773.

Kanoh, T., Shichi, T. and Takagi, K. (1999). Mono- and bilayer equilibria of stearate self-assembly formed in hydrotalcite interlayers by changing the intercalation temperature. ***Chem. Lett.***, 117-118.

Khan, A. and O'Hare, D. (2002). Intercalation chemistry of layered double hydroxides: Recent developments and applications. ***J. Mater. Chem.***, 12: 3191-3198.

Kloprogge, J. T. and Frost, R. L. (1999). Infrared emission spectroscopic study of the dehydroxylation of synthetic Mg/Al and Mg/Zn/Al- hydrotalcites. ***Phys. Chem. Chem. Phys.***, 11641-1647.

Kloprogge, J. T. and Frost, R. L. (2000). Reply on Comments on 'Infrared emission spectroscopic studies of the thermal transformation of Mg-, Ni- and Co-hydrotalcite catalysts' by Pérez-Ramirez, J. Mul, G., Kapteijn, F. and Moulijn, J. A. ***Appl. Catal., A: Gen.***, 204: 269-270.

Kloprogge, J. T., Hickey, L. and Frost, R. L. (2004). FT-Raman and FT-IR spectroscopic study of synthetic Mg/Zn/Al-hydrotalcites. ***J. Raman Spectrosc.***, 35: 967-974.

Kloprogge, J. T., Wharton, D., Hickey, L. and Frost, R. L. (2002). Infrared and Raman study of interlayer anions CO_3^{2-}, NO_3^-, SO_4^{2-} and ClO_4^- in Mg/Al hydrotalcite. ***Am. Mineral.***, 87: 623-629.

Kooli, F., Holgado, M. J., Rives, V., Sanroman, S. and Ulibarri, M. A. (1997). A simple conductivity study of decavanadate intercalation in hydrotalcite. ***Mater. Res. Bull.***, 32(8): 977-982.

Kooli, F., Kosuge, K. and Tsunashima, A. (1995). New Ni-Al-Cr and Ni-Al-Fe carbonate hydrotalcite-like compounds: Synthesis and characterization. ***J. Solid State Chem***., 118: 285-291.

Kopka, H., Beneke, K. and Lagaly, G. (1988). Anionic surfactants between double metal hydroxide layers. ***J. Colloid Interfac. Sci.***, 123: 427-436.

Labajos, F. M. Rives, V. and Ulibarri, M A. (1992). Effects of hydrothermal and thermal treatments on the physicochemical properties of Mg-Al hydrotalcite-like materials. ***J.Mater. Sci.***, 27: 1546-1552.

Leroux, F., Adachi-Pagano, M., Intissar, M., Chauvière, S., Forano, C. and Besse, J-P. (2001). Delamination and restacking of layered double hydroxides. ***J. Mater. Chem.,*** 11: 105-112.

Li, F. and Duan, X. (2005). Application of layered double hydroxides. In: Evans, D. G. and Duan, X. (Eds), ***Layered Double Hydroxides***. Heidelberg, Germany: Springer, pp. 173-223.

Lopez, T., Bosch, P., Asomoza, M., Gomez, R. and Ramos, E. (1997). DTA-TG and FTIR spectroscopies of sol-gel hydrotalcites: Aluminum source effect on physicochemical properties. ***Mater. Lett.***, 31: 311-316.

Lopez-Salinas, E. and Ono, Y. (1993). Intercalation chemistry of a Mg-Al layered double hydroxide ion-exchanged with complex MCI;- (M = Ni, Co) ions from organic media. ***Microporous Mater.***, 133-142.

Marchi, A. J. and Apesteguýa, C. R. (1998). Impregnation-induced memory effect of thermally activated layered double hydroxides. ***Appl. Clay Sci.***, 13: 35-48.

Marino, O. and Mascolo, G. (1982). Thermal stability of Mg,Al double hydroxides modified by anionic exchange. ***Thermochim. Acta.,***55: 377-383

Mascolo, G. (1995). Synthesis of anionic clays by hydrothermal crystallization of amorphous precursors. ***Appl. Clay Sci.***, 10: 21-30.

Mascolo, G. and Marino, O. (1980). A new synthesis and characterization of magnesium-aluminium hydroxides. ***Miner. Mag.***, 43: 619-621.

Messersmith, P. B. and Stupp, S. I. (1995). High-temperature chemical and microstructural transformation of a nanocomposite organic. ***Chem. Mater.***, 7: 454-460.

Meyn, M., Beneke, K. and Lagaly, G. (1990). Anion-exchange reactions of layered double hydroxides. ***Inorg. Chem.***, 29: 5201-5207.

Miyata, S and Okada A .(1977). Synthesis of hydrotalcite-like compounds and their Physico-chemical properties – the systems $Mg^{2+}Al^{3+}$-SO_4^{2-} and $Mg^{2+}Al^{3+}$-CrO_4^{2-}. ***Clays Clay Miner.,*** 25: 14-18

Miyata, S. (1980). Physico-chemical properties of synthetic hydrotalcites in relation to composition. ***Clays Clay Miner***., 28: 50-56.

Miyata, S. (1983). Anion-exchange properties of hydrotalcite compounds. ***Clay Clays Miner.***, 31(4): 305-311.

Miyata, S. and Kumura, T. (1973). Synthesis of new hydrotalcite-like compounds and their physico-chemical properties. ***Chem. Lett.***, 843-848.

Mohanambe, L. and Vasudevan, S. (2005). Structure of a cyclodextrin functionalized anionic clay: XRD analysis, spectroscopy, and computer simulations. ***Langmuir***, 21: 10735-10742.

Morioka, H., Tagaya, H., Karasu, M., Kadokawa, J. and Chiba, K. (1995). Preparation of new useful materials by surface modification of inorganic layered compounds. ***J. Solid State Chem.***, 117: 337-342.

Moyo, L., Nhlapo, N. S. and Focke, W. W. (2008). A critical assessment of the methods for intercalating anionic surfactants in layered double hydroxides. ***J. Mater. Sci.***, 43: 6144-6158.

Nakagaki, M. and Yokoyama, S. (1985). Acid catalyzed hydrolysis of sodium dodecyl sulphate. ***J. Pharm. Sci.***, 74: 1047-1052.

Nayak, M., Kutty, T. R. N., Jayaraman, V. and Periaswamy, G. (1997). Preparation of the layered double hydroxide (LDH) $LiAl_2(OH)7{\cdot}2H_2O$, by gel to crystallite conversion and a hydrothermal method, and its conversion to lithium aluminate. ***J. Mater. Chem.***, 7(10): 2131-2137.

Nethravathi, C., Harichandran, G., Shivakumara, C., Ravishankar, N. and Rajamathi, M. (2005). Surfactant intercalated á-hydroxides of cobalt and nickel and their delamination-restacking behaviour in organic media. ***J. Colloid Interface Sci.***, 288: 629-633.

Newman, S. P. and Jones, W. (1998). Synthesis, characterization and layered double hydroxides containing organic guests. ***New J. Chem.***, 105-115.

Nhlapo, N., Motumi, T., Landman, E., Verryn, S. M. C. and Focke, W. W. (2008). Hydrotalcite: Surfactant-assisted fatty acid intercalation of layered double hydroxides. ***J. Mater. Sci.***, 43(3): 1033-1043.

NIRE annual report, (1995). Thermal decomposition of hydrotalcite-like compounds.

O'Hare, D. (1991). Inorganic intercalation compounds. In: Bruce, D. W. and O'Hare, D. (Eds), ***Inorganic Materials***, New York: Wiley, pp. 166-228.

Oriakhi, C. O., Farr, I. V. and Lerner, M. M. (1996). Incorporation of poly(acrylic acid), poly(vinylsulphonate) and poly(styrenesulphonate). ***J. Mater. Chem.***, 6(1): 103-107.

Palmer, S. J., Frost, R. L. and Nguyen, T. (2009). Hydrotalcites and their role in coordination of anions in Bayer liquors: Anion binding in layered double hydroxides. ***Coord. Chem. Rev.***, 253(1-2): 250-267.

Parker, M. L., Milestone, N. B. and Newman, R. H. (1995). Use of hydrotalcite as an anionic absorbent. ***Ind. Eng. Chem. Res***., 34: 1196.

Pavan, P. C., Crepaldi, E. L. and Valim, J. B. (2000). Sorption of anionic surfactants on layered double hydroxides. ***J. Colloid Interface Sci.***, 229: 346-252.

Pavan, P. C., Crepaldi, E. L. de A., Gomes, G. and Valim, J. B. (1999). Adsorption of sodium dodecyl sulfate on a hydrotalcite-like compound. Effect of temperature, pH and ionic strength. ***Colloids Surf. A: Physicochem. Eng. Aspects***, 154: 399-410.

Pavan, P. C., Gomes, G. A, Valim, J. B. (1998). Adsorption of sodium dodecyl sulfate on layered double hydroxides. ***Microporous Mesoporous Mater.***, 21: 659-665.

Perez-Ramirez, J., Mul, G., Kapteijn, F. and Moulijn, J. A. (2001). A spectroscopic study of the effect of the trivalent cation on the thermal decomposition behaviour of Co-based hydrotalcites. ***J. Mater. Chem.***, 11: 2529-2536.

Pesic, L., Salipurovic, S., Markovic, V., Vucelic, D., Kagunya, W. and Jones, W. (1992). Thermal characteristics of a synthetic hydrotalcite-like material. ***J. Mater. Chem.***, 2(10): 1069-1073.

Prinetto, F., Ghiotti, G., Graffin, P. and Tichit, D. (2000). Synthesis and characterization of sol-gel Mg/Al and Ni/Al layered double hydroxides and comparison with co-precipitated samples. ***Microporous Mesoporous Mater.***, 39: 229-247.

Rajamathi, J. T., Ravishankar, N. and Rajamathi, M. (2005). Delamination-restacking behaviour of surfactant intercalated layered hydroxy

double salts, $M_3Zn_2(OH)_8(surf)_2 \cdot 2H_2O$ [M= Ni, Co and surf = dodecyl sulphate (DS), dodecyl benzene sulphonate (DBS)]. ***Solid State Sci***., 7: 195-199.

Ramos, E., Lopez, T., Gomez, R., Bosch, P. and Asomoza, M. (1997). Thermal stability of sol-gel hydrotalcites. ***J. Sol-Gel Sci. Technol.***, 8: 437-442.

Rao, M. M., Reddy, B. R., Jayalakshmi, M., Jaya, V. S. and Sridhar, B. (2005). Hydrothermal synthesis of Mg–Al hydrotalcites by urea hydrolysis. ***Mater. Res. Bull.***, 40: 347-359.

Reichle, W. T. (1986). Anionic clay minerals. ***Chemtech***., 58-63.

Reichle, W. T. (1985). Catalytic reactions by thermally activated, synthetic, anionic clay minerals. ***J. Catal.***, 94: 547-557.

Reichle, W. T. (1986). Synthesis of anionic clay minerals (mixed metal hydroxides, hydrotalcite). ***Solid State Ionics***, 22: 135-141.

Rey, F., Fornes V. and Rojo J.M. (1992). Thermal decomposition of hydrotalcites, an infrared and nuclear magnetic resonance spectroscopic study. ***J. Chem. Soc., Faraday Trans.*** 88: 2233-2288

Robins, D. S. and Dutta P. K. (1996). Examination of fatty acid exchanged layered double hydroxides as supports for photochemical assemblies. ***Langmuir***, 12: 402-408.

Sato, T., Tezuka, M., Endo, T. and Shimada, M. (1988). Removal of sulfuroxyanions by magnesium aluminium oxides and their thermal decomposition. ***J. Chem. Tech. Biotechnol.***, 39: 275-285.

Schollhorn, R. (1980). Intercalation chemistry. ***Physica B***, 99: 89-99.

Seftel, E. M., Popovici, E., Mertens, M., De Witte, K., Van Tendeloo, G., Cool, P. and Vansant, E. F. (2008). Zn–Al layered double hydroxides: Synthesis, characterization and photocatalytic application ***Microporous Mesoporous Mater.***, 113: 296–304.

Shi, W., Wei, M., Jin, L. and Li, C. (2007). Calcined layered double hydroxides as a “biomolecular vessel” for bromelain: Immobilization, storage and release. ***J. Mol. Catal. B: Enzym.***, 47: 58-65.

Smyth J. R. and Bish, D. L. (1988). Crystal structures and cation sites of the rock-forming minerals. London: Allen and Unwin, p. 69.

Soma, I., Wakano, H., Takahashi, H. and Yamaguchi, M. (1975) Flame resistant vinyl chloride resin compositions. Jap. Patent 50 063 047.

Stanimirova, T. S., Kirov, G. and Dinolova, E. (2001). Mechanism of hydrotalcite regeneration. ***J. Mat. Sci. Lett***., 20: 453-455.

Tadros, T. (2005). ***Applied surfactants: Principles and applications***. Heppenheim, Germany: Wiley-VCH Verlag, pp. 1-61

Takagi, K., Shichi, T., Usami, H. and Sawaki, Y. (1993). Controlled photocycloaddition of unsaturated carboxylates intercalated in hydrotalcite clay interlayers. ***J. Am. Chem. Soc.***, 115: 4339-4344.

Taylor, H.F.W. (1969). Segregation and cation ordering in sjögrenite and pyroaurite. ***Miner. Mag.*** 37: 377-389

Texter, J. (1999). Characterization of surfactants. In: Lange, K. R. (Ed.), ***Surfactants: A Practical Handbook.*** Cincinnati: Hanser/Gadner, pp. 1-68.

Treadwell, WD. and Bernasconi, E. (1930). Versuche zur elektrometrischen titration von aluminium-und-magnesium ion nebeneinander. ***Helv Chim Acta.*** 13: 500-509

Trifiro, F. and Vaccari, A. (1996). Hydrotalcite-like anionic clays (Layered double hydroxides). In: Davies, J. E. D., Atwood, J. L., MacNicol, D. D. and Vogtle, F. (Eds), ***Comprehensive Supramolecular Chemistry***, Oxford, UK: Pergamon Press, pp. 251-291.

Trikeriotis, M. and Ghanotakis, D. F. (2007). Intercalation of hydrophilic and hydrophobic antibiotics in layered double hydroxides. ***Int. J. Pharm.***, 332: 176-184.

Trujillano, R., Holgado, M. J., González, J. L. and Rives, V. (2005). Cu-Al-Fe layered double hydroxides with CO32- and anionic surfactants with different alkyl chains in the interlayer. ***Solid State Sci.***, 7: 931-935.

Tseng, W-Y., Lin, J-T., Mou, C-Y., Cheng, S., Liu, S-B., Chu, P.P. and Liu, H-W. (1996). Incorporation of C_{60} in layered double hydroxide. ***J. Am. Chem. Soc.***, 118(18): 4411-4418.

Ulibarri, M. A., Pavlovic, I., Barriga, C., Hermosín, M. C. and Cornejo, J. (2001). Adsorption of anionic species on hydrotalcite-like compounds: Effect of interlayer anion and crystallinity. ***Appl. Clay. Sci.***, 18: 17-27.

Utraki, L. A. (2004). ***Clay-Containing Polymeric Nanocomposites***, Vol. 1. Shropshire, UK: Rapra Technologies Ltd, p. 434.

Vaccari, A. (1998). Preparation and catalytic properties of cationic and anionic clays. ***Catal. Today***, 41: 53-71.

Venugopal, B. R., Shivakumara, G. and Rajamathi, M. (2006). Effect of various factors influencing the delamination behavior of surfactant intercalated layered double hydroxides. ***J. Colloid Interface Sci.***, 294: 234-239.

Wang, B., Zhang, H., Evans, D. G. and Duan, X. (2005). Surface modification of layered double hydroxides and incorporation of hydrophobic organic compounds. ***J. Mater. Chem. and Physics***, 92: 190-196.

Whilton, N. T., Vickers, P. J. and Mann, S. (1997). Bioinorganic clays: Synthesis and characterization of amino- and polyamino acid intercalated layered double hydroxides. ***J. Mater. Chem.***, 7(8): 1623-1629.

Whitesides, G. M., Mathias, J. P. and Seto, C. T. (1991). Molecular self-assembly and nanochemistry: a chemical strategy for the synthesis of nanostructures. ***Science***, 254: 1312-1319.

Whittingham, M. S. (1979). Intercalation chemistry and energy storage. ***J. Solid State Chem.***, 29: 303-310.

Williams, G. R., Norquis, A. J. and O'Hare, D. (2004). Time-resolved, in situ x-ray diffraction studies of staging during phosphonic acid intercalation into [LiAl2(OH)6]Cl.H2O. ***Chem. Mater.***, 16: 975-981.

Xiang, X., Zhang, L., Hima, H. I., Li, F. and Evans, D. G. (2009). Co-based catalysts from Co/Fe/Al layered double hydroxides for preparation of carbon nanotubes, ***Appl. Clay Sci.***, 42 (3-4): 404-409.

Xu, Z. P. and Zeng, H. C. (2001). Decomposition pathways of hydrotalcite-like compounds $MgAl_x(OH)_2(NO_3)_x \cdot nH_2O$ as a continuous function of nitrate anions. ***Chem. Mater***., 13: 4555-4563.

Xu, Z. P. and Braterman, P. S. (2007). Competitive intercalation of sulfonates into layered double hydroxides (LDHs): The key role of hydrophobic interactions. ***J. Phys. Chem.***, 13: 268-273.

Xu, Z. P. and Braterman, P. S. (2003). High affinity of dodecylbenzene sulfonate for layered double hydroxide and resulting morphological changes. ***J. Mater. Chem.***, 13: 268-273.

Yang, J-F. and Zhou, Z-T. (2008). Use of spray technique to prepare Ni/Al-layered double hydroxides. ***J. Alloys Compd. ,***in press.

You, Y., Zhao, H. and Vance, G. F. (2002a). Hybrid organic-inorganic derivatives of layered double hydroxides and dodecylbenzenesulfonate: Preparation and adsorption characteristics. ***J. Mater. Chem.***, 12: 907-912.

You, Y., Zhao, H. and Vance, G. F. (2002b). Surfactant-enhanced adsorption of organic compounds by layered double hydroxides. ***Colloids Surf., A: Physicochem. Eng. Aspects***, 205: 161-172.

Zhang, H., Wen, X. and Wang, Y. (2007). Synthesis and characterization of sulfate and dodecylbenzenesulfonate intercalated zinc–iron layered double hydroxides by one-step coprecipitation route. ***J. Solid State Chem.***, 180: 1636-1647.

Zhao, H. and Nagy, K. L. (2004). Dodecyl sulfate-hydrotalcite nanocomposites for trapping chlorinated organic pollutants in water. ***J. Colloid Interface Sci.***, 274: 613-624.

Zhao, Y., Li, F., Zhang, R., Evans, D. G. and Duan, X. (2002). Preparation of layered double-hydroxide nanomaterials with a uniform crystallite size using a new method involving separate nucleation and aging steps. ***Chem. Mater.***, 14: 4286-4291.

Zhu, J., Yuan, P., He, H., Frost, R., Tao, Q., Shen, W. and Bostrom, T. (2008). In situ synthesis of surfacant/silane-modified hydrotalcites. ***J. Colloid Interface Sci.***, 319: 498-504.

APPENDIX I: DETAILED EXPERIMENTAL PROCEDURE

The intercalative methods used in this study are elimination, regeneration, ion exchange and co-precipitation.

The percentage yield was calculated with respect to the masses of the surfactant and the HT used. However, in the instances where dodecyl alcohol and lauric acid were used, their respective masses were included in the calculation under the assumption that they co-intercalate with the surfactant.

$$Mg_2Al(OH)_6(CO_3^{2-})_{0.5}\cdot 2H_2O + NaDS \leftrightarrow Mg_2Al(OH)_6(DS)\cdot 2H_2O + 0.5Na_2CO_3$$

Surfactant is in large excess to ensure 100% ion exchange reaction at equilibrium.
1 mole reacts with 1mole of surfactants
Molecular weight of HT = 234.66g

In 20g HT the number of moles = 20/234.66
= 0.0852moles

Moles of HT in reaction = Moles of surfactant

$\therefore$ theoretical yield = [Moles of HT * M_{HT}] + [Moles of Surf * M_{Surf}]
= 20 + 24.57
= 44.57g

The % Yield is therefore calculated as;

% Yield = [Actual yield/ Theoretical yield]*100
= [25.289/44.57]*100
= 57%

Elimination (acid-mediated ion exchange)

Lower carboxylic acids, such as acetic, butyric and hexanioic acid, mediated the exchange. In the elimination procedure various aspects of intercalation, such as an increase in the anion exchange capacity (AEC) of the surfactant used; co-intercalation with other anions (namely dodecyl alcohol and lauric acid); and the effect of temperature and pH were also investigated. Reactions were conducted in

1.5 L of distilled water.	
LDH-DS (also used in partial pH control)	20 g HT 325 + 75 g SDS + 0.25 mol (15 g) of acetic acid 3 AEC of SDS Glacial acetic acid used – Saarchem AR grade 1021020 LC Sample was run at room temperature at 25 °C for two days. pH = 9-10 Mass ratio of acid:surfactant - 1:4.8 Mole ratio: 1:1 Sample was separated by centrifugation, washed three times with water, three times with ethanol and once with acetone. Mass of product = 25.589 g % Yield = 57%
LDH-DS (Acid/salt mixture)	No pH control 20.00 g HT-5 + 49.05 g SDS + 5.4 g acetic acid + 1M ammonium acetate Sample was left to run for five days at 25 °C. pH = 6.31 Sample was recovered by centrifugation, washed four times with water and once with acetone. Mass of product = 24.72 g % Yield = 55%
LDH-DS (dodecyl alcohol)	No pH control 20.00 g HT-5 + 51.17 g SDS + 15 g acetic acid + 30.12 g dodecyl alcohol Sample was left to run for five days at 65 °C pH = 5.39 Sample was recovered by centrifugation, washed four times with water and once with acetone. Mass of product = 25.5 g % Yield = 63%
LDH-DS (lauric acid)	20 g HT + 54 g lauric acid + 26 g SDS + 5.1 g acetic acid

	Sample was left to run for two days. Reaction temperature = Room temperature at 25 ^{o}C Mole ratio – acetic acid:SDS:lauric acid = 1:1:3 pH = 5.74 (initial pH) 9.87 (adjusted pH using ammonia) Sample was recovered by centrifugation, washed once in water, three times with ethanol and once with acetone. Mass of product = 59.087 g % Yield = 98% (If it is assumed that precisely all the carbonate is replaced by the laurate. Note, this is unrealistic because the products are impure and a greater amount of laurate is actually intercalated.)
LDH-DBS (also used in partial pH control)	20 g HT + 30 g SDBS + 5.1 g acetic acid Sample was left to run for two days. Reaction was carried out at room temperature ~ 25 °C Mole ratio – acetic acid:SDBS = 1:1 pH = 9.45 (ammonia solution added to maintain the pH of the solution > 9) Sample was recovered by centrifugation, washed three times in water and twice with acetone. Mass of product = 26.412 g % Yield = 53%
LDH-DBS (acid/salt mixture)	No pH control 20.00 g HT-5 + 44.58 g SDBS + 5.4 g acetic acid + 1M ammonium acetate Sample was left to run for seven days at 25 °C. Mole ratio – acetic acid:SDBS = 1:1.5 pH = 6.5 Sample was recovered by centrifugation, washed four times with water and once with acetone. Mass of product = 28.9 g % Yield = 58%

LDH-DBS (pH effect)	Strict pH monitoring 20.04 g HT-5 + 44.41 g SDBS + 5.4 g acetic acid Sample was left to run for two days at room temperature. Mole ratio – acetic acid:SDBS = 1:1.5 pH = 10.01 (ammonia solution added to maintain the pH of the solution > 9) Amount of ammonia added= 12 ml Sample was recovered by centrifugation, washed four times with water. Oven dried at 65 °C Mass of product = 15.30 g % Yield = 30%
LDH-DBS (excess acid)	No pH control 20.00 g HT-5 + 44.32 g SDBS + 20.6 g acetic acid Sample was left to run for five days at 25 °C. Mole ratio – acetic acid:SDBS = 1:4.5 pH = 5.13 Sample was recovered by centrifugation, washed four times with water and once with acetone. Mass of product = 30.1 g % Yield = 61%
LDH-DBS (butyric-acid mediated)	20 g HT + 48.34 g SDBS + 30.838 g butyric acid Sample was left to run for two days. Reaction temperature = 80 °C Mole ratio – butyric acid:SDBS = 1:1 pH = 10.23 (ammonia solution added to maintain the pH of the solution > 9) Sample was recovered by centrifugation, washed four times with water and once with acetone. Mass of product = 33.62 g % Yield = 68%
LDH-DBS (hexanoic-acid mediated)	20 g HT + 48.33 g SDBS + 40.656 g hexanoic acid Sample was left to run for two days.

	Reaction temperature = room temperature at 25 ^{o}C Mole ratio – hexanoic acid:SDBS = 1:1 pH = 10.01(ammonia solution added to maintain the pH of the solution > 9) Sample was recovered by centrifugation, washed four times with water and once with acetone. Mass of product = 29.40 g % Yield = 59%
LDH-DBS (lauric acid)	20 g HT + 30 g SDBS + 5.1 g acetic acid + 34 g lauric acid Sample was left to run for two days. Reaction temperature = room temperature at 25 ^{o}C Mole ratio – acetic acid:SDBS: lauric acid = 1:1:2 pH = 10.01(ammonia solution added to maintain the pH of the solution > 9) Sample was recovered by centrifugation, washed four times with water and once with acetone. Mass of product = 40.645 g % Yield = 93%
LDH-DBS (dodecyl alcohol)	20 g HT + 31 g SDBS + 5.1 g acetic acid + 32 g dodecyl alcohol Sample was left to run for two days. Reaction temperature = room temperature at 25 ^{o}C Mole ratio – acetic acid:SDBS:alcohol = 1:1:2 pH = 10.11 (ammonia solution added to maintain the pH of the solution > 9) Sample was recovered by centrifugation, washed three times with water and once with acetone. Mass of product = 33.949 g % Yield = 79%

LDH-DBS (temperature)	40 g HT + 119 g SDBS + 10.2 g acetic acid Sample was left to run for two days. Reaction temperature = room temperature at 25 °C. Mole ratio – acetic acid:SDBS = 1:2 pH = 10.01 (ammonia solution added to maintain the pH of the solution > 9) Sample was recovered by centrifugation, washed four times with water and once with acetone. Mass of product = 42.840 g % Yield = 86%

Regeneration

The intercalations listed below were carried out as described by Costa ***et al.*** (2008). The following assumption was made:

- In the preparation of the aqueous solution of surfactant, there was 100% theoretical anion exchange.

The LDH (HT-325) used in this instance was calcined prior to the intercalation in a furnace at 450 °C for 3 h. The calcined LDH will be denoted as CLDH.

Regeneration LDH-DS	20.10 g CLDH (HT-5) + 25.13 g SDS CLDH was dispersed in the surfactant solution (1 L) and was left to stir for two days at room temperature. pH = 9.99 (pH was corrected by the addition of NaOH solution) Product was washed four times with water to remove the excess surfactant and solids were separated by centrifugation. Sample was oven-dried at 60 °C Mass of product = 37.4 g % Yield = 84%

Regeneration LDH-DBS	20.08 g CLDH (HT-5) + 29.64 g SDBS CLDH was dispersed in the surfactant solution (1 L) and was left to stir for two days at room temperature. pH = 10.34 (pH was corrected by the addition of NaOH solution) Product was washed four times with water to remove the excess surfactant and solids were separated by centrifugation. Sample was oven-dried at 60 °C Mass of product = 44.5 g % Yield = 90%

Ion exchange

Anion exchange reaction with starting material of LDH-Cl.

<u>Preparation of LDH-Cl</u>

Ion exchange was carried out as described in Xu & Braterman (2003) and Boclair & Braterman (1999). 50 mmol and 150 mmol were used for $AlCl_3$ and $MgCl_2$ respectively.

Mass of $MgCl_2$ used = 31.59 g
Mass of $AlCl_3$ used = 6.69 g

The water used in the experiments was deionised water 15MΩ cm. Metal salts were precipitated in NaOH solution. pH was corrected to 8.20.
The product was separated by centrifugation, washed six times with water and once with acetone. The product was left to dry at room temperature.

LDH-DS (ion exchange)	5 mmol of the LDH-Cl 0.00500 * 321.17 = 1.606 g Assuming that the LDH-Cl formed has the formula $Mg_2Al(OH)_6Cl{\cdot}\boldsymbol{n}(H_2O)$, and using Miyata's equation: $\boldsymbol{n} = 1 - N\boldsymbol{x}/\boldsymbol{c}$ where N is the number of sites occupied by each anion and c is the anionic charge, 3.22 g of clay was added to 100 ml of 0.2M surfactant solution. 5.80 g of SDS was dissolved. The mixture was refluxed for 24 h and nitrogen gas was pumped through the solution for an additional 24 h. The sample was then put in the oven and left to age for 24 h at 65 °C. pH maintained at ≈ 9 The sample was separated by centrifugation, washed five times with water and once with acetone, and then left to dry at room temperature. Mass of product = 2.28 g % Yield = 25%
LDH-DBS (ion exchange)	3.21g LDH-Cl + 7.30g SDBS The clay was added to 100 ml of 0.2M surfactant solution. The mixture was refluxed for 24 h and nitrogen gas was pumped through the solution for an additional 24 h. The sample was then put in the oven and left to age for 24 h at 65 °C. pH maintained at ≈ 9 The sample was separated by centrifugation, washed five times with water and once with acetone, and then left to dry at room temperature. Mass of product = 2.71g % Yield = 26%

Co-precipitation (high supersaturation) The method was adapted from Crepaldi ***et al.***, (2002a) (See also Zhang ***et al.***, 2007). The metal ions used by Crepaldi ***et al.*** were Zn/Cr. Precipitation was carried out under variable pH corrected before and after precipitation.	
LDH-DS (normal co-precipitation)	<u>High temperature</u> 51.30 g magnesium nitrate + 37.75 g aluminum nitrate was dissolved in 1 L of distilled water. 72.54 g of the SDS was pre-dissolved in distilled water and the solution was then added to the mixed nitrate salts solution. On addition of the surfactant solution, a white precipitate was formed. <u>pH</u> – Initial pH was 2.37 and this was corrected to 7.07; pH was corrected by the addition of 2M NaOH. The reaction was allowed to proceed at 25 °C for three days. The sample was recovered by centrifugation, washed four times with water and once with acetone. Mass of product = 20.90 g % Yield = 12.9%
LDH-DBS (normal co-precipitation)	<u>High temperature</u> 51.33 g magnesium nitrate + 37.57g aluminum nitrate was dissolved in 1 L of distilled water. 75.72 g of the SDBS was pre-dissolved in distilled water and the solution was then added to the mixed nitrate salts solution. On addition of the surfactant solution, a white precipitate was formed. <u>pH</u> – Initial pH was 3.31 and this was corrected to 7.42; pH was corrected by the addition of 2M NaOH. The reaction was allowed to proceed at 25 °C for three days. The sample was recovered by centrifugation, washed four times with water and once with acetone.

	Mass of product = 50.72 g % Yield = 30.8%
LDH-DBS (co-precipitation at 65 °C)	High temperature 51.41 g magnesium nitrate + 37.51g aluminum nitrate was dissolved in 1 L of distilled water. 70.06 g of the SDBS was pre-dissolved in distilled water and the solution was then added to the mixed nitrate salts solution. On addition of the surfactant solution, a white precipitate was formed. pH – pH initially ~10±0.5 and this was corrected by the addition of 2M NaOH to 10.88. The reaction was allowed to proceed at 65 °C for three days. The sample was halved into solutions (A) and (B); solution (A) was left to age in the oven for 4 days at 65 °C, while (B) was aged at room temperature. Both samples were recovered by centrifugation and washed seven times with water. The pH of the supernatant was checked after each successive wash using pH paper. Mass of product (A) = 43.3g Mass of product (B) = 33.9 g Total mass = 77.2g % Yield = 48.5%
LDH-DS (co-precipitation at 65 °C)	High temperature 51.39 g magnesium nitrate + 37.56 g aluminum nitrate was dissolved in 1 L of distilled water. 57.84 g of the SDS was pre-dissolved in distilled water and the solution was then added to the mixed nitrate salts solution. On addition of the surfactant solution, a white precipitate was formed. pH – pH initially ~10±0.5 and this was corrected by the addition of 2M NaOH to 10.37. The reaction was allowed to proceed at 65 °C for three

	days. The sample was halved into solutions (A) and (B); solution (A) was left to age in the oven for 4 days at 65 °C, while (B) aged at room temperature. Both samples were recovered by centrifugation and washed seven times with water. The pH of the supernatant was checked after each successive wash using pH paper. Mass of product (A) = 19.43g Mass of product (B) = 17.8 g Total mass = 37.23 g % Yield = 25.3%
LDH-DBS (inert atmosphere)	<u>High temperature</u> 51.344 g magnesium nitrate + 37.652 g aluminum nitrate was dissolved in 300 ml of deionised water. 69.524 g of the SDBS was pre-dissolved in 500 ml of deionised water and the solution was then added to 300 ml of NaOH solution at a pH of 10. The solution was allowed to stir until a clear solution was obtained. The mixed metal nitrates solution was added dropwise to this solution with continuous stirring. <u>pH</u> – After addition of the mixed metal nitrates, the pH was ~ 6 and this was corrected to ~ 8±0.5. The solution was left to stir under an inert atmosphere for 36 h and then aged at 65 °C for 24 h. The sample was separated by centrifugation. It was washed four times with water and the precipitate was left to oven dry at 65 °C. Mass of product = 53.7g % Yield = 33.9%

LDH-DS (inert atmosphere)	High temperature 51.8 g magnesium nitrate + 38.1 g aluminum nitrate was dissolved in 300 ml of deionised water. 57.9 g of the SDS was pre-dissolved in 500 ml of deionised water and the solution was then added to 300 ml of NaOH solution at a pH of 10. The solution was allowed to stir until a clear solution was obtained. The mixed metal nitrates solution was added dropwise to this solution with continuous stirring. pH – After addition of the mixed metal nitrates, the pH was ~ 5 and this was corrected to ~ 8±0.5. The solution was left to stir under an inert atmosphere for 36 h and then aged at 65 °C for 24 h. The sample was separated by centrifugation. It was washed four times with water and the precipitate was left to oven dry at 65 °C. Mass of product = 55.4 g % Yield = 37.4

APPENDIX II: THERMAL ANALYSIS

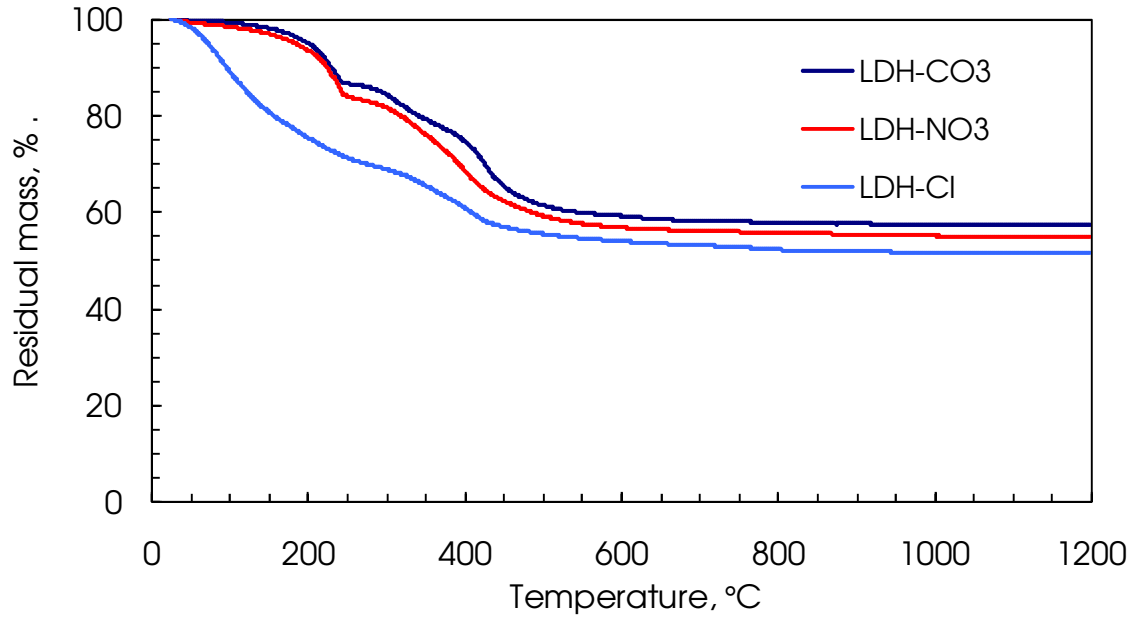

Figure A-1: Comparison of (TG) mass loss curves of LDH precursors

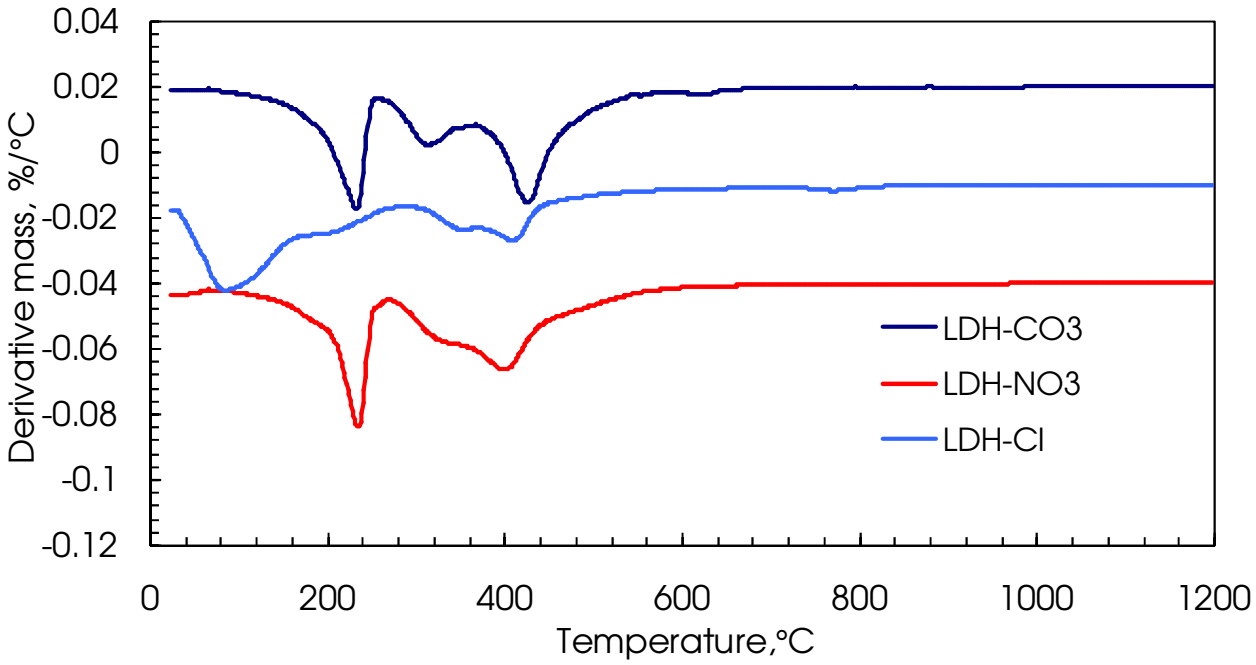

Figure A-2: Comparison of derivative mass loss curves for LDH precursors

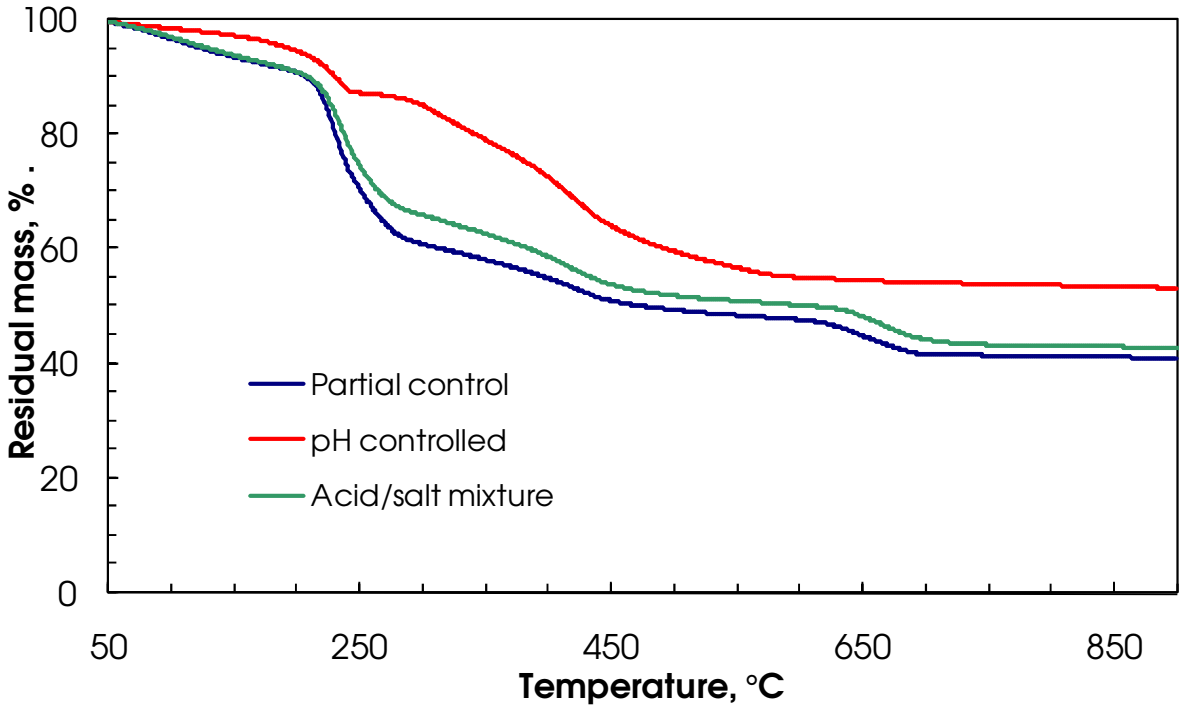

Figure A-3: Mass loss curves of LDH-DS in varying pH environments for the acid-mediated ion exchange

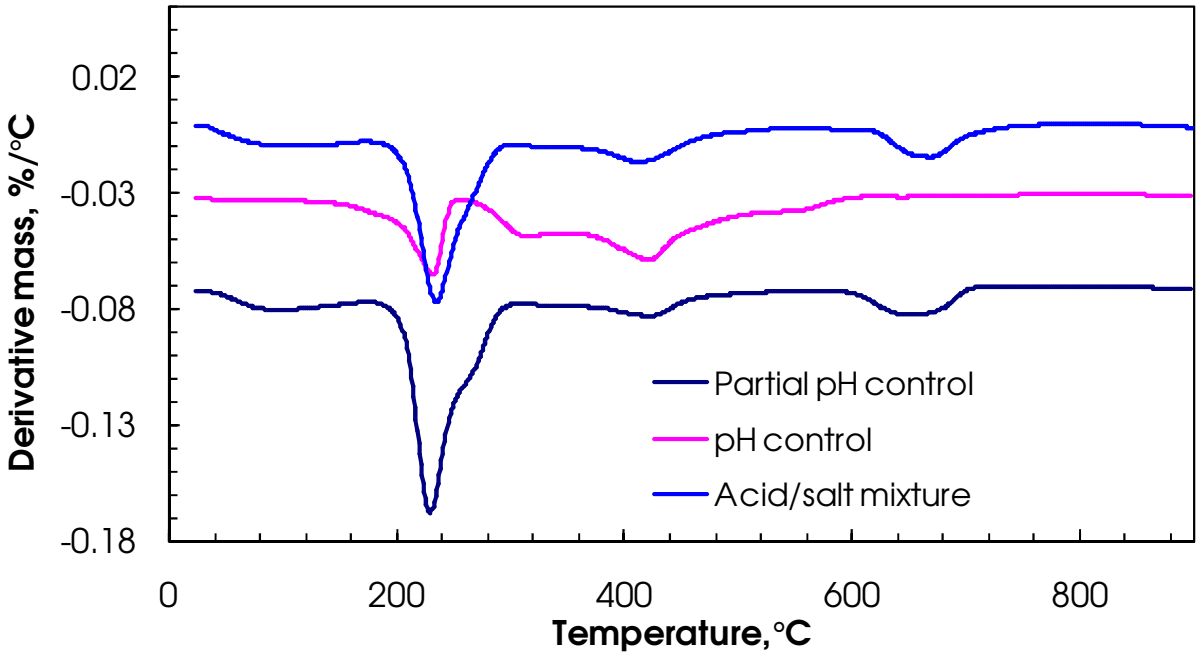

Figure A-4: Comparison of derivative mass loss curves of LDH-DS in varying pH environments for the acid-mediated ion exchange

For the LDH-DS intercalates obtained from the acid-mediated ion exchange (elimination), it is clear that pH has an effect on the level of intercalated anions (see Figure A-3). Figure A-4 shows the similar decomposition patterns followed by the different intercalates.

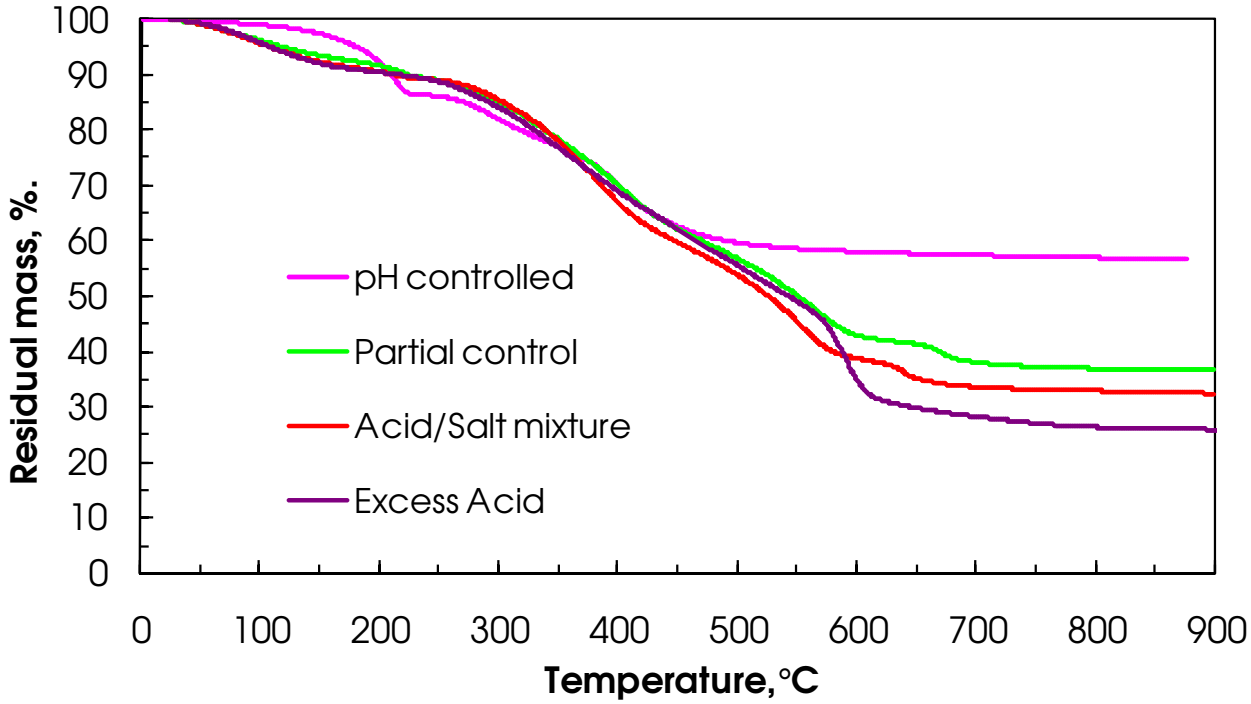

Figure A-5: Mass loss curves of LDH-DBS in varying pH environments for the acid-mediated ion exchange

The same trend is observed in the LDH-DBS as in the intercalates described before.

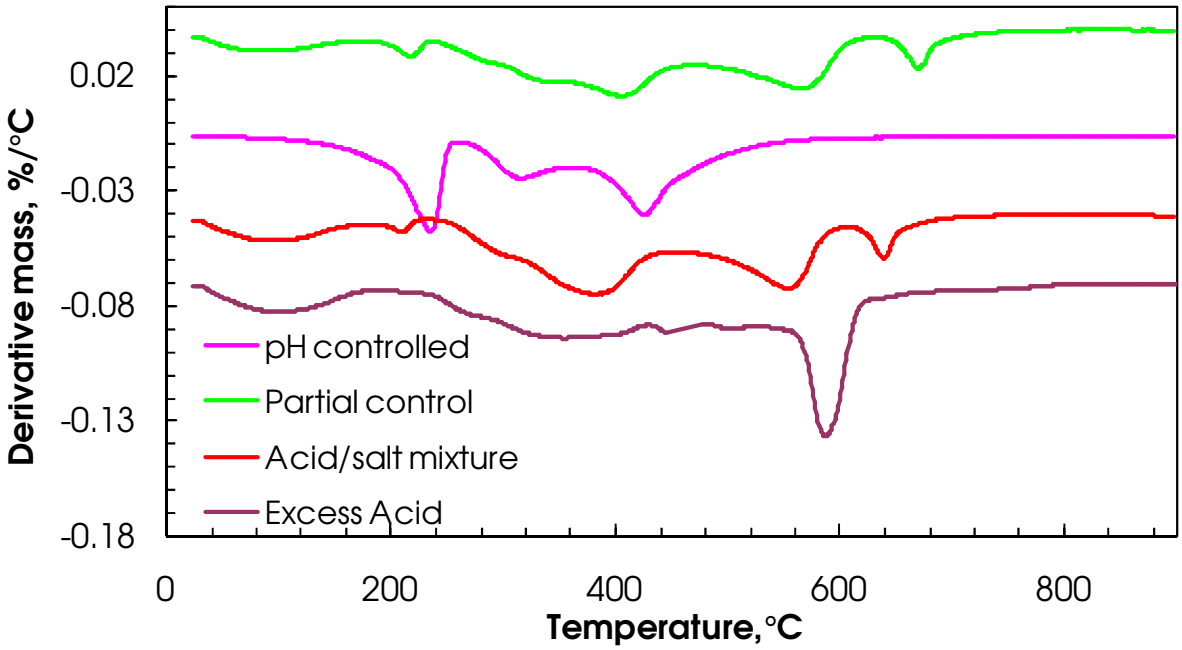

Figure A-6: Comparison of derivative mass loss curves of LDH-DS in varying pH environments for the acid-mediated ion exchange

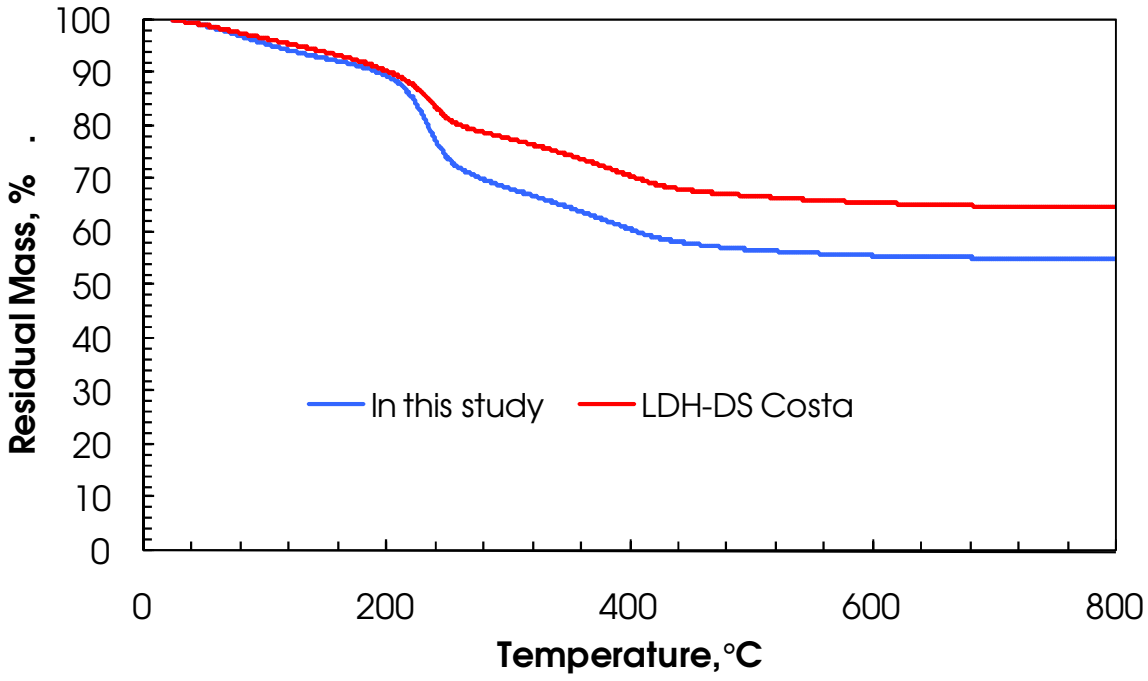

Figure A-7: Comparison of regeneration samples prepared by Costa ***et al.*** (2008) with the LDH-DS prepared in this study

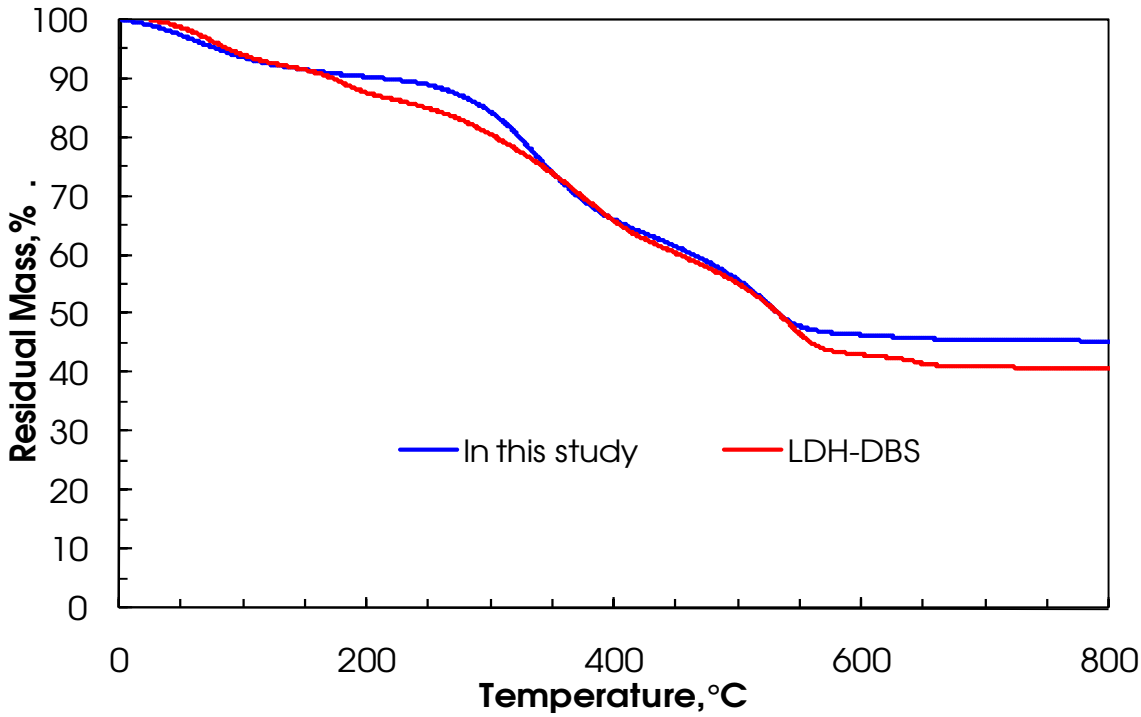

Figure A-8: Comparison of regeneration samples prepared by Costa ***et al.*** (2008) with the LDH-DBS prepared in this study

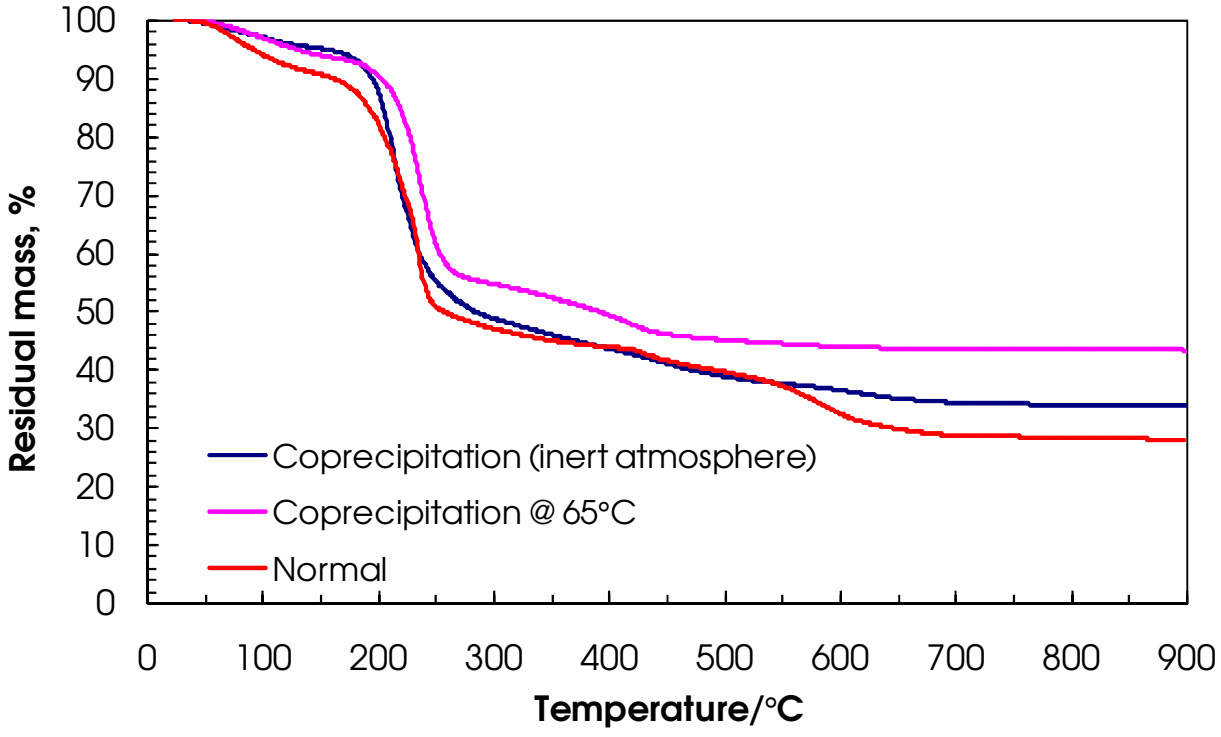

Figure A-9: Co-precipitation LDH-DS prepared by different methods

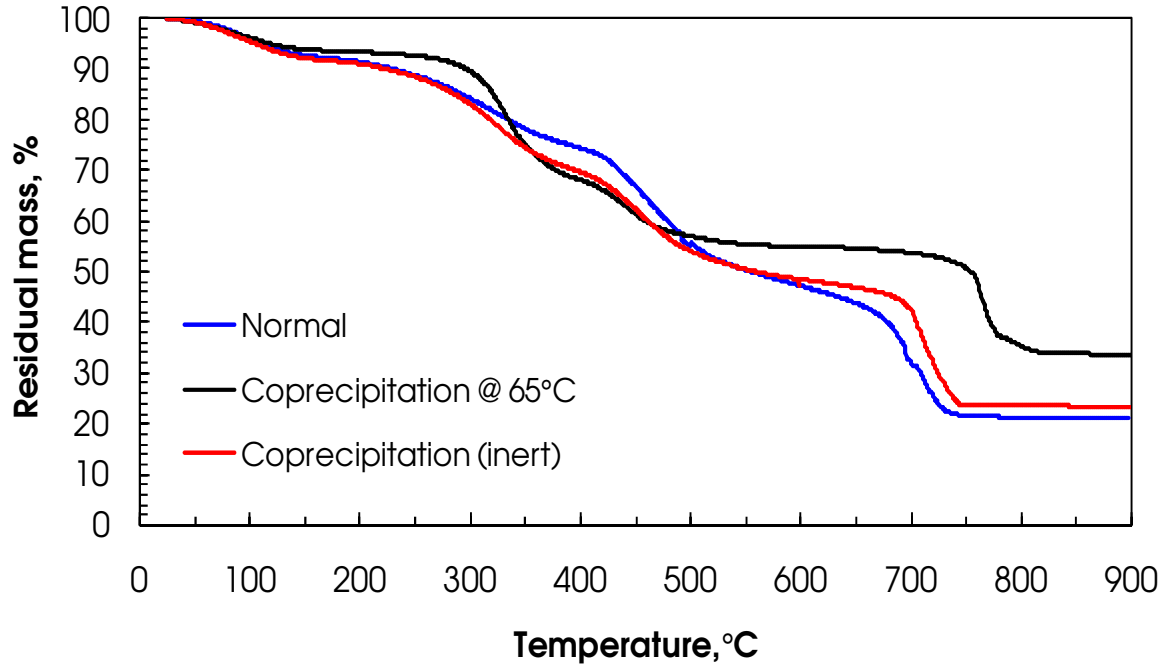

Figure A-10: Co-precipitation LDH-DBS prepared by different methods

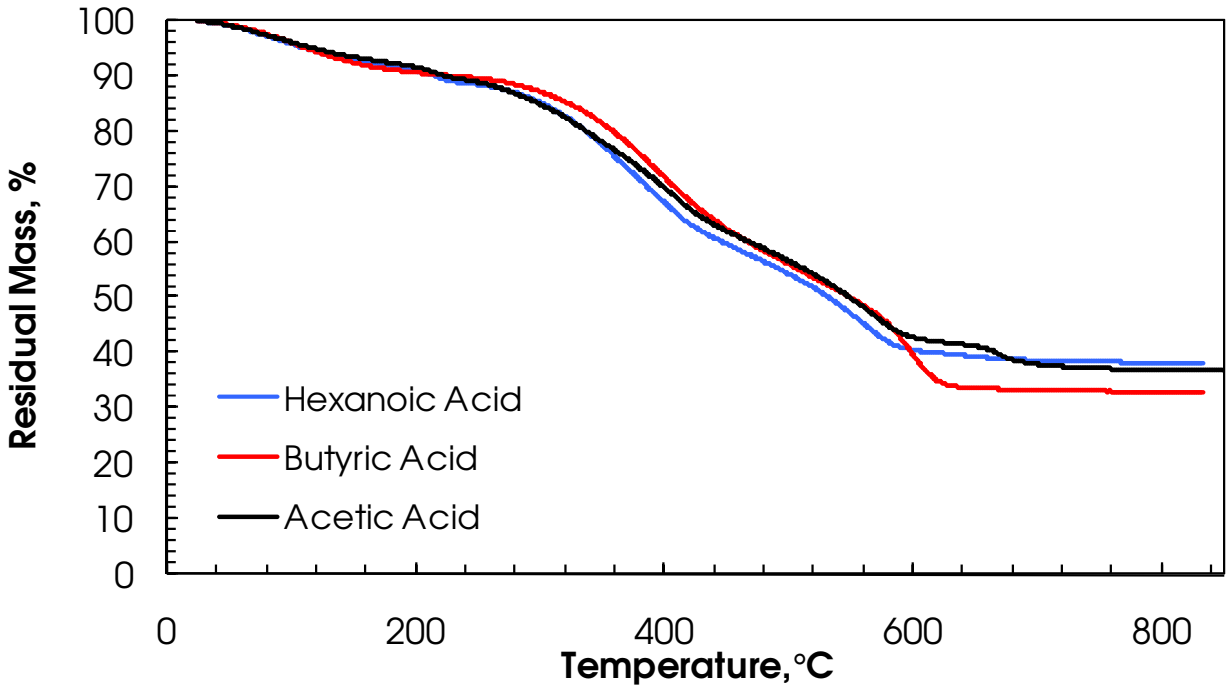

Figure A-11: LDH-DBS mediated with different organic acids

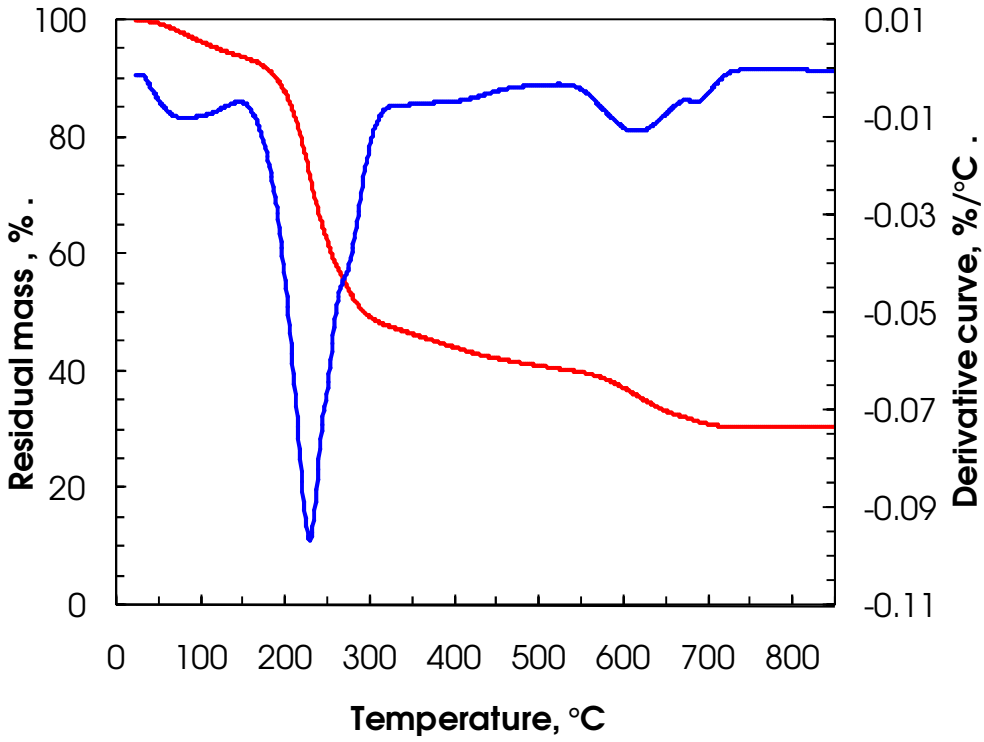

Figure A-12: TG and DTG curves of LDH-DS prepared together with dodecyl alcohol

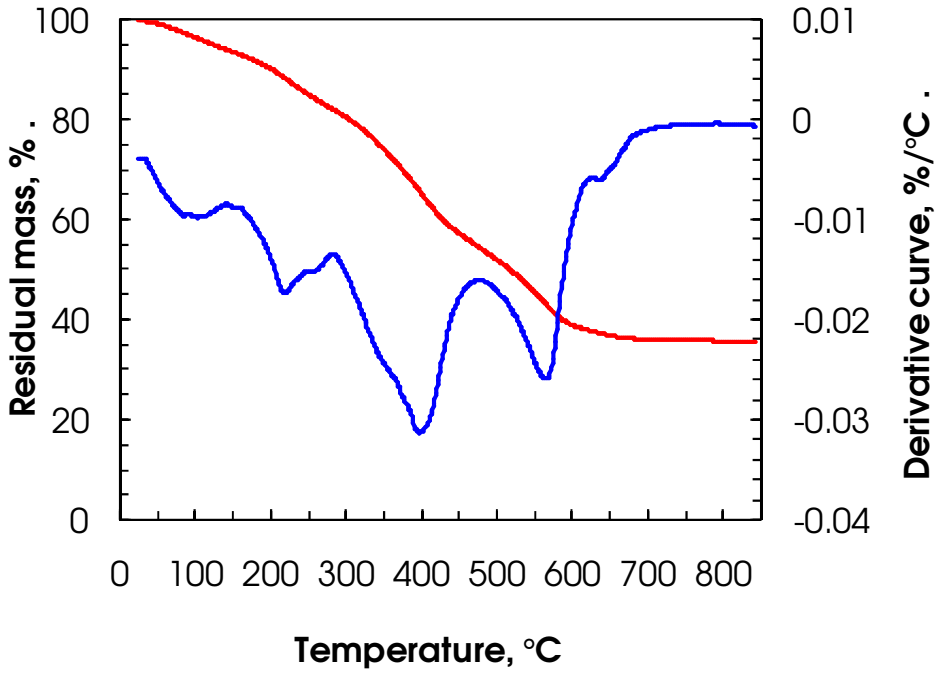

Figure A-13: TG and DTG curves of LDH-DBS prepared together with dodecyl alcohol

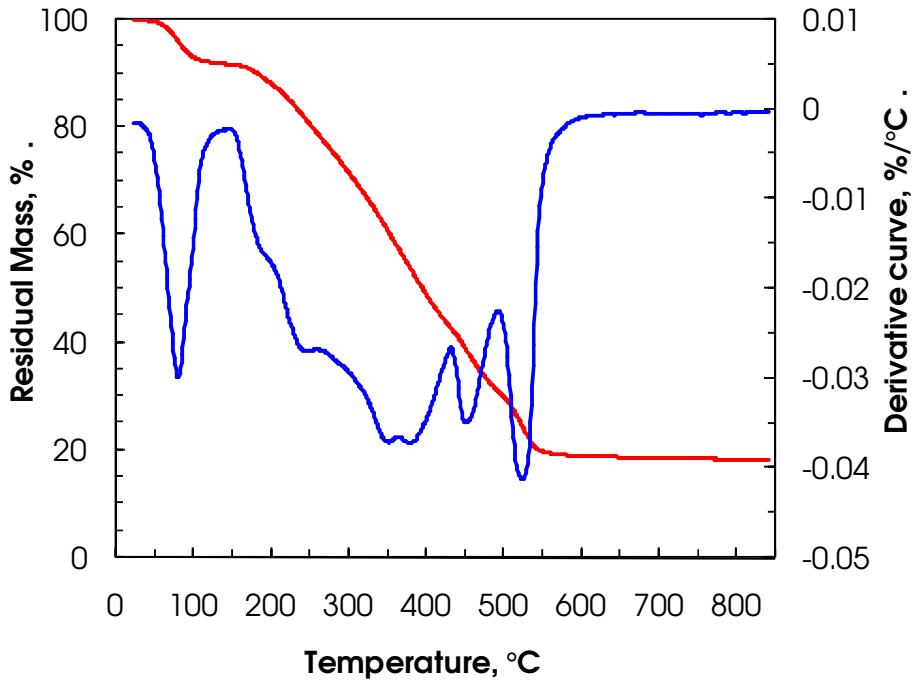

Figure A-14: TG and DTG curves of LDH-DBS prepared together with lauric acid

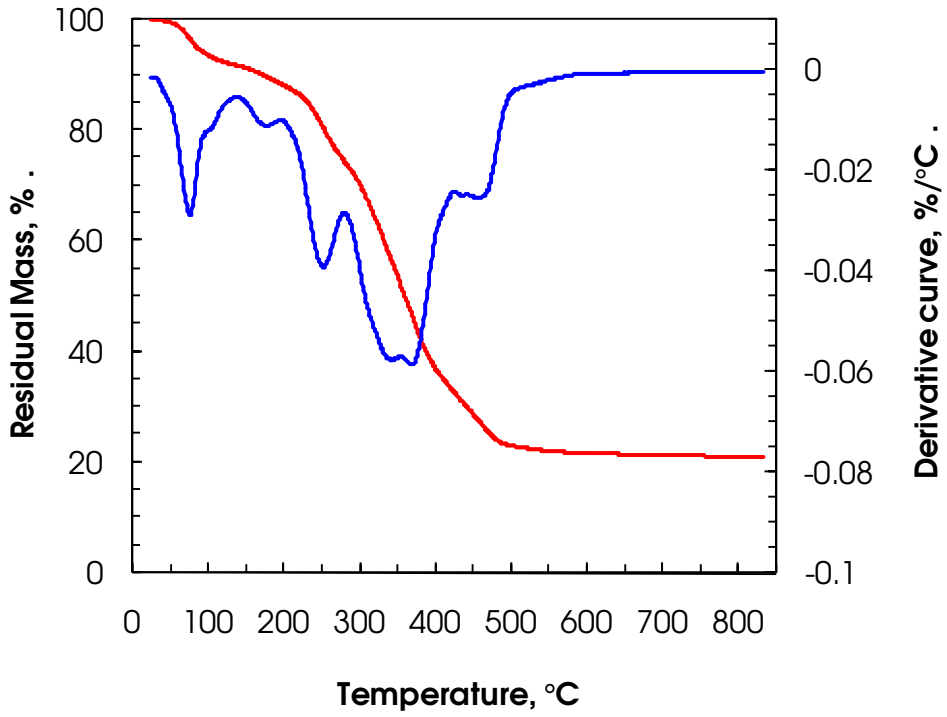

Figure A-15: TG and DTG curves of LDH-DS prepared together with lauric acid

Table A-1: Comparison of preparative methods, their clay content and % organic content

	Residue at 150 °C	Residue at 1 200 °C	Clay content on a dry basis	Actual % clay	Organic content
LDH-CO_3	98.15	57.33	58.41	100	-
LDH-NO_3	96.97	55.09	56.81	100	-
LDH-Cl	80.76	51.64	63.95	100	-
LDH-DBS					
Elimination	92.65	31.91	34.44	58.95	41.05
Ion exchange	93.45	38.43	41.12	64.30	35.70
Regeneration	92.88	46.76	50.34	86.18	13.82
Co-precipitation	91.62	22.19	24.22	42.63	57.37
LDH-DS					
Elimination	93.40	33.50	35.87	61.41	38.59
Ion exchange	94.18	45.38	48.19	75.35	24.65
Regeneration	92.59	45.65	49.31	84.41	15.59
Co-precipitation	94.20	26.41	28.04	49.35	50.65

Formulas used in the calculation of the above clay content on a dry basis; actual clay and % organic content are:

$$\text{Clay content on a dry basis} = \frac{\%\ \text{Residue at 1 200°C}}{\%\ \text{Residue at 150 °C}} \qquad \text{(A-1)}$$

Actual clay content is obtained by multiplication of the ratio of the clay content on a dry basis to that of 100% clay of the LDH precursor. For example, using LDH-CO_3,

Clay content on a dry basis = 57.33/98.51
= 58.19%

Ratio of clay on a dry basis to 100% = 100/58.19

= 1.718

Actual % clay = 1.718 *58.197

= 100%

The ratios obtained were 1.718, 1.76 and 1.56 for LDH-CO_3, -NO_3 and –Cl respectively.

% Organic content = 100 – Actual % clay

APPENDIX III: FT-IR SPECTRA

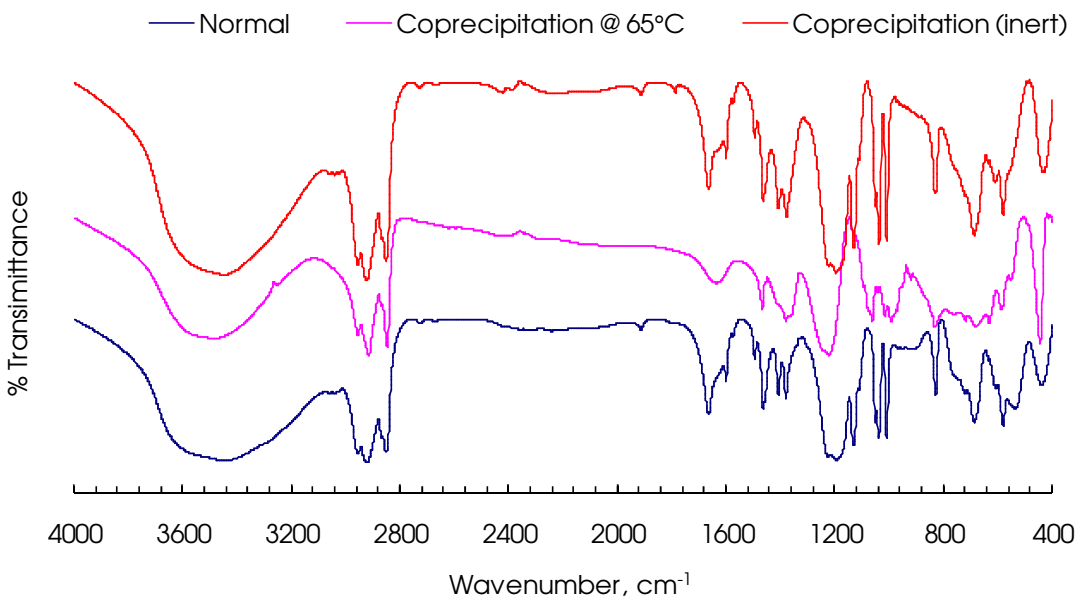

Figure A-16: FT-IR spectra of varying LDH-DBS co-precipitation methods

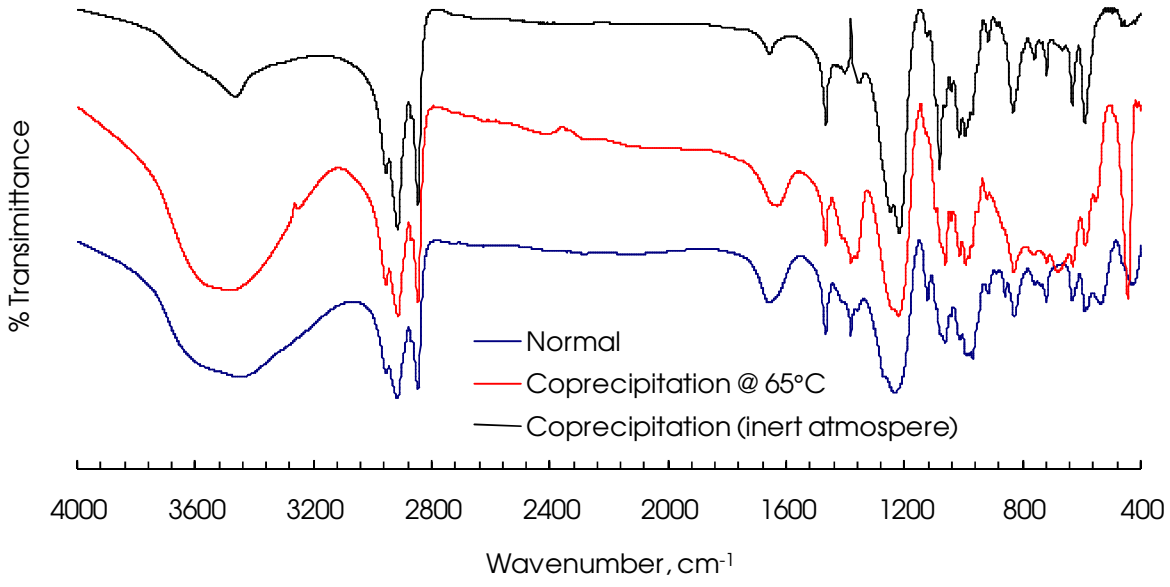

Figure A-17: FT-IR spectra of varying LDH-DS co-precipitation methods

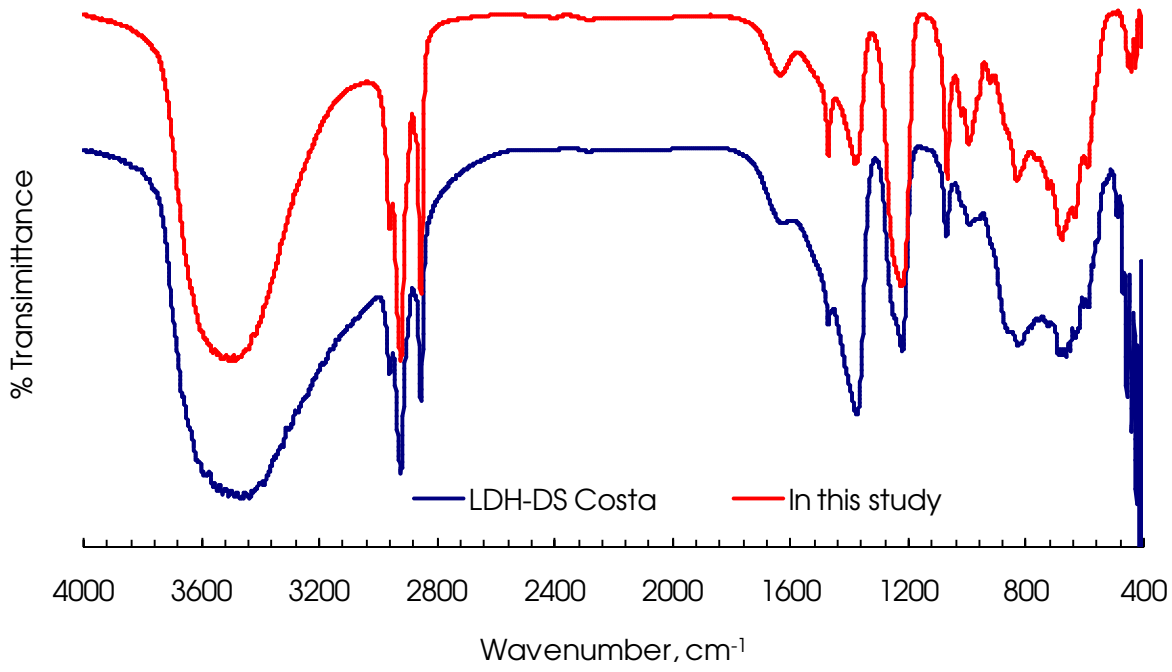

Figure A-18: Comparison of Costa's LDH-DS sample and that prepared in this study

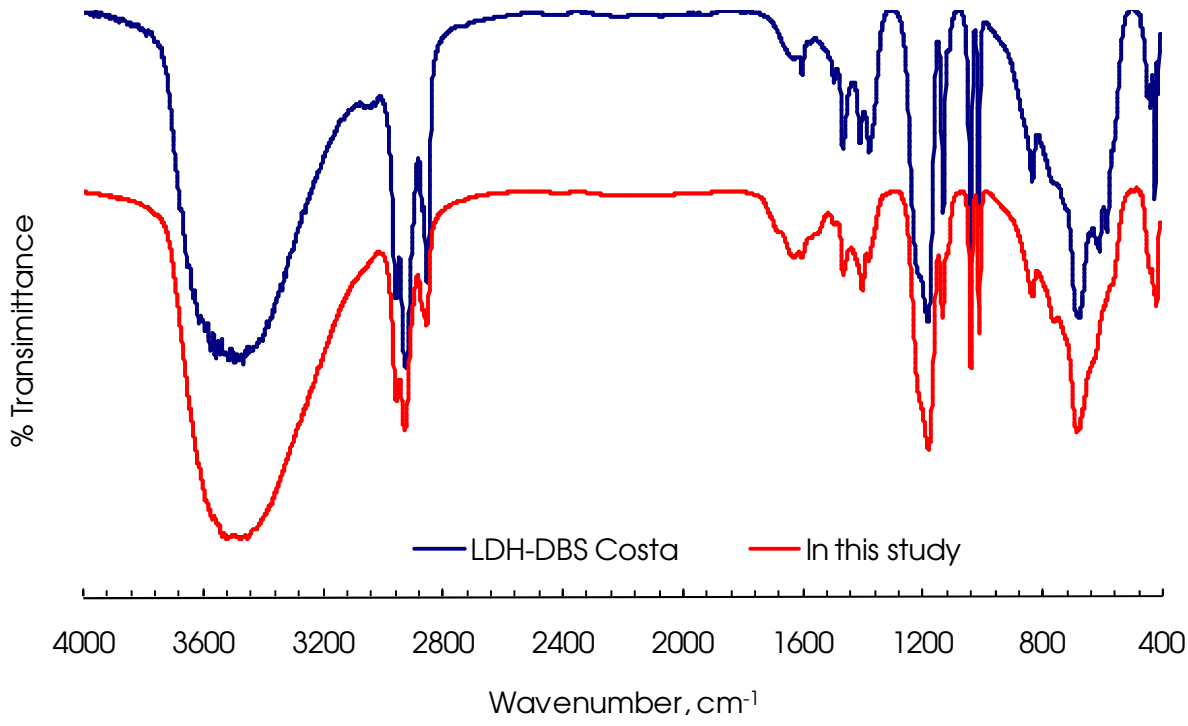

Figure A-19: Comparison of Costa's LDH-DBS sample and that prepared in this study

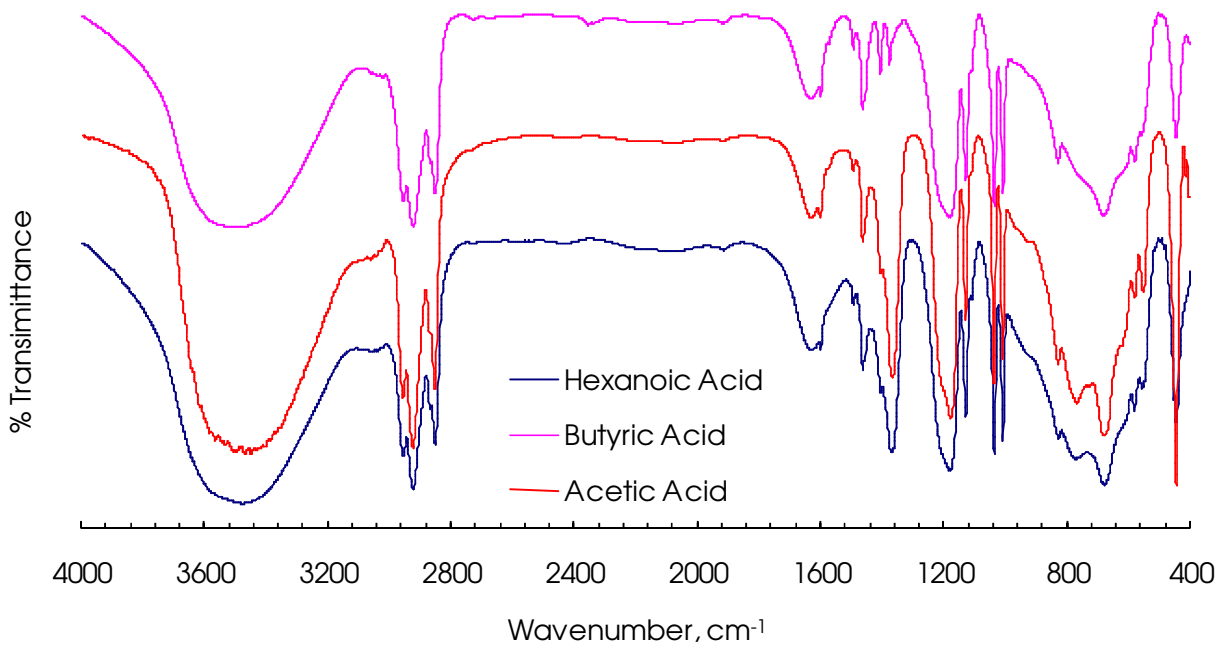

Figure A-20: LDH-DBS acid-mediated ion exchange using acids indicated

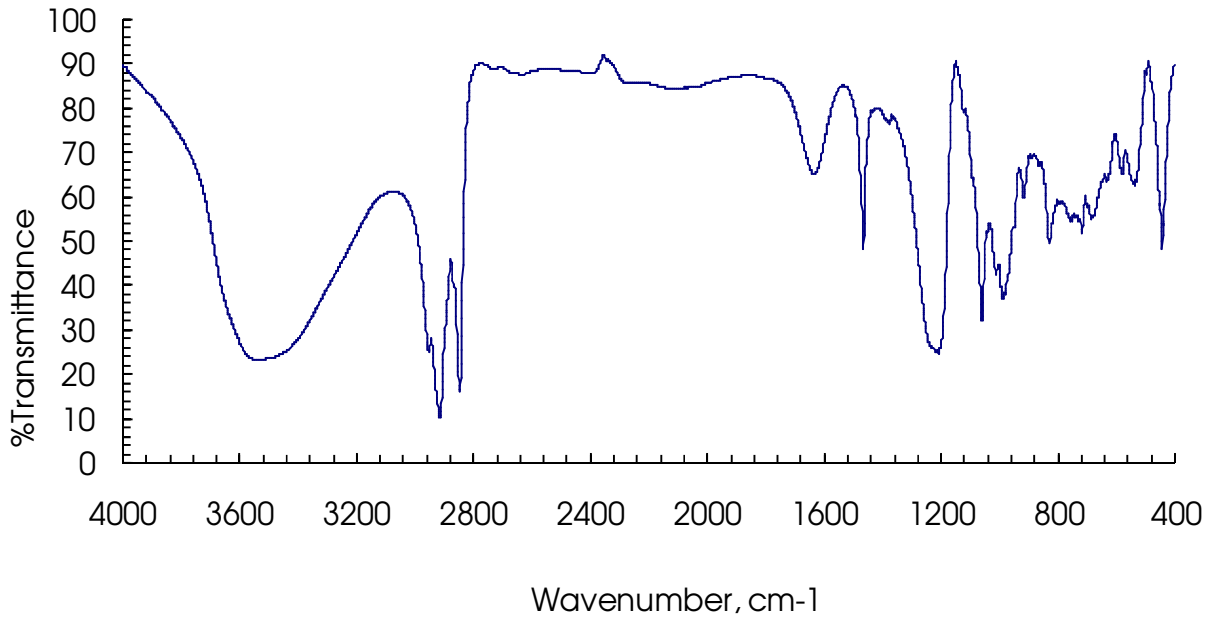

Figure A-21: Spectra of LDH-DS prepared together with dodecyl alcohol

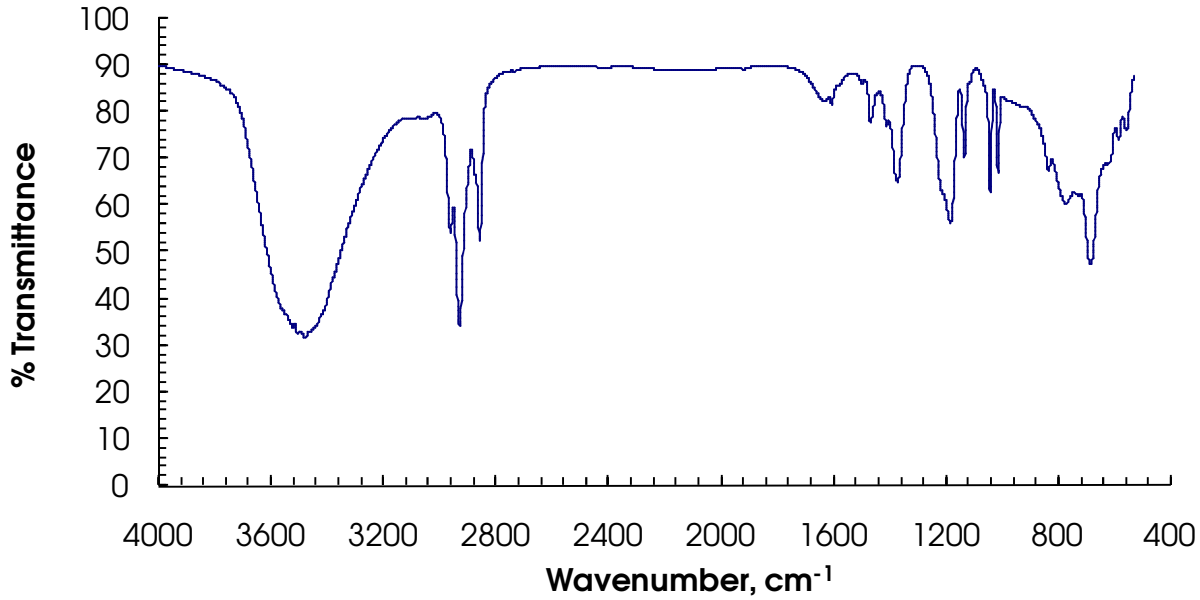

Figure A-22: Spectra of LDH-DBS prepared together with dodecyl alcohol

APPENDIX IV: XRD DIFFRACTOGRAMS

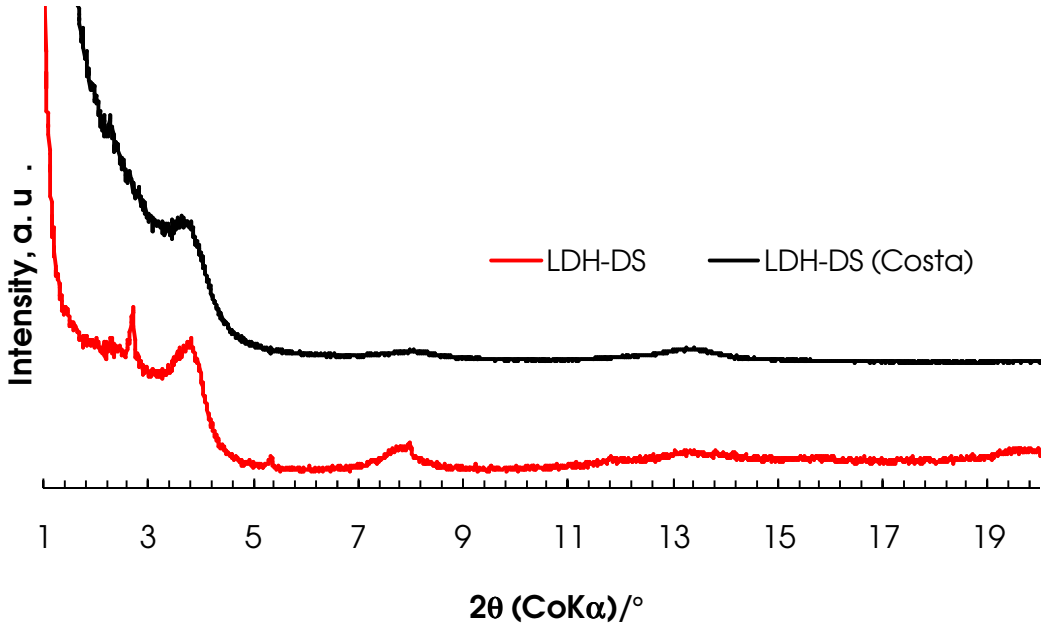

Figure A-23: Comparison of LDH-DS prepared in this study with that received from Costa

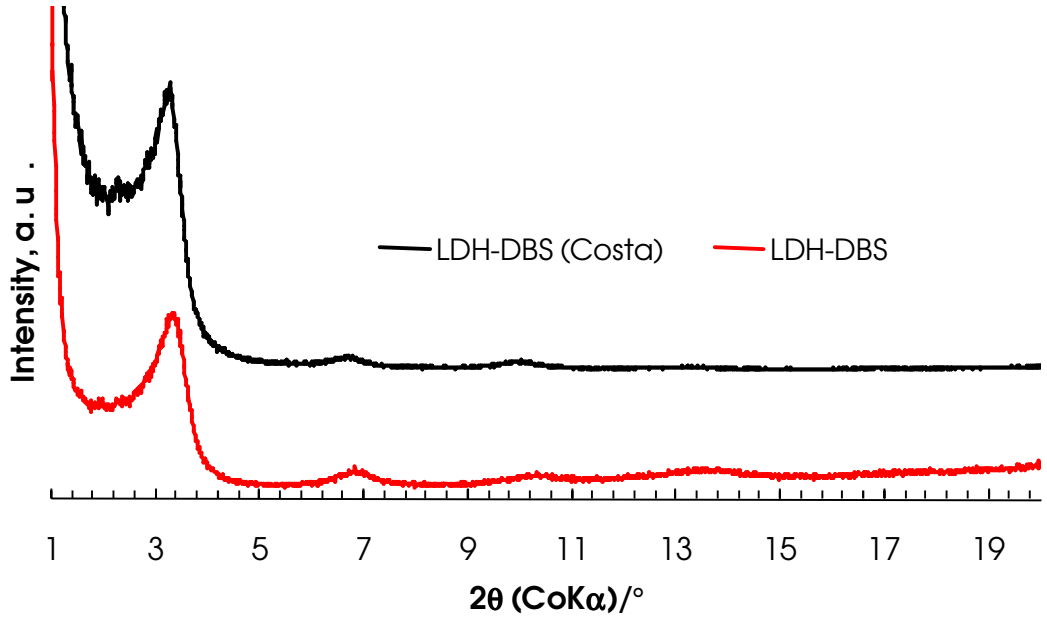

Figure A-24: Comparison of LDH-DBS prepared in this study with that received from Costa

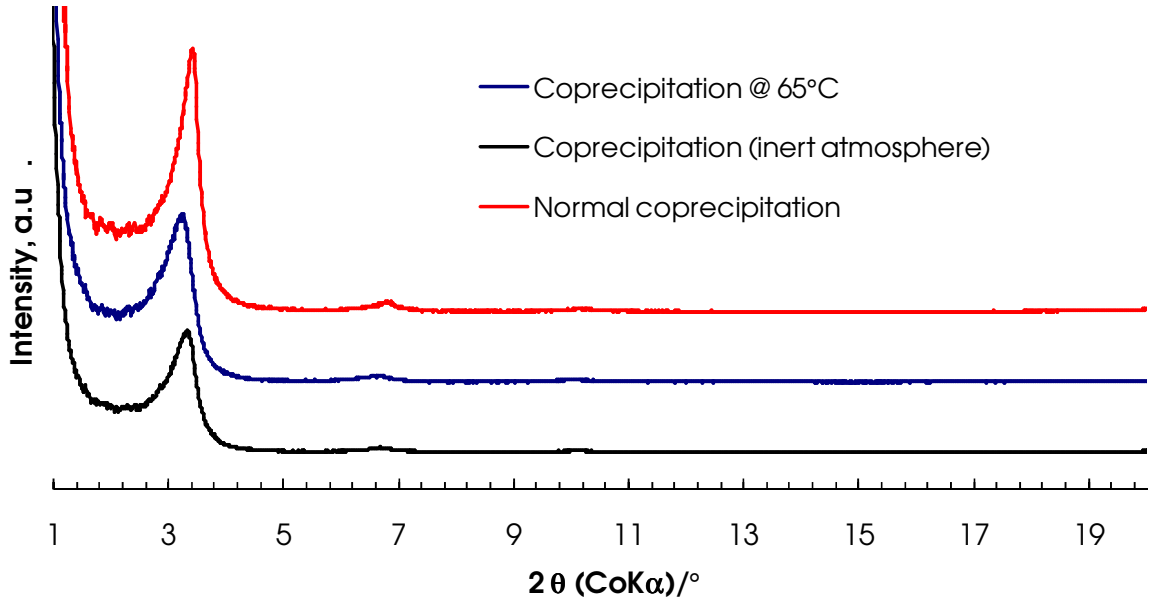

Figure A-25: X-ray diffractograms of LDH-DBS from varying co-precipitation methods

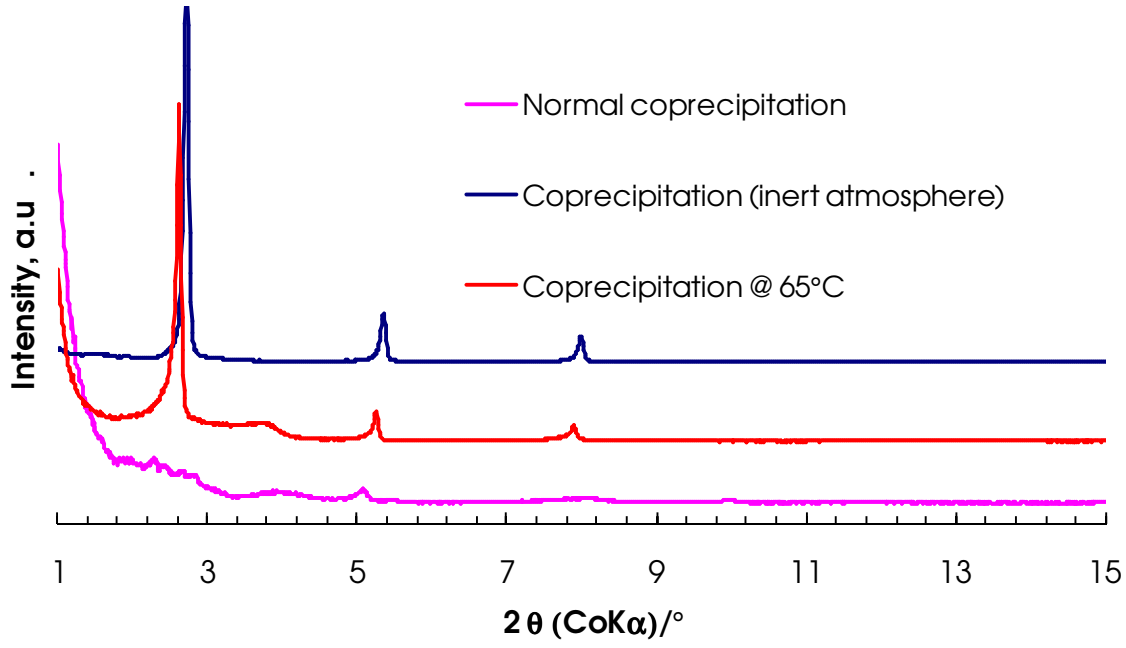

Figure A-26: X-ray diffractograms of LDH-DS from varying co-precipitation methods

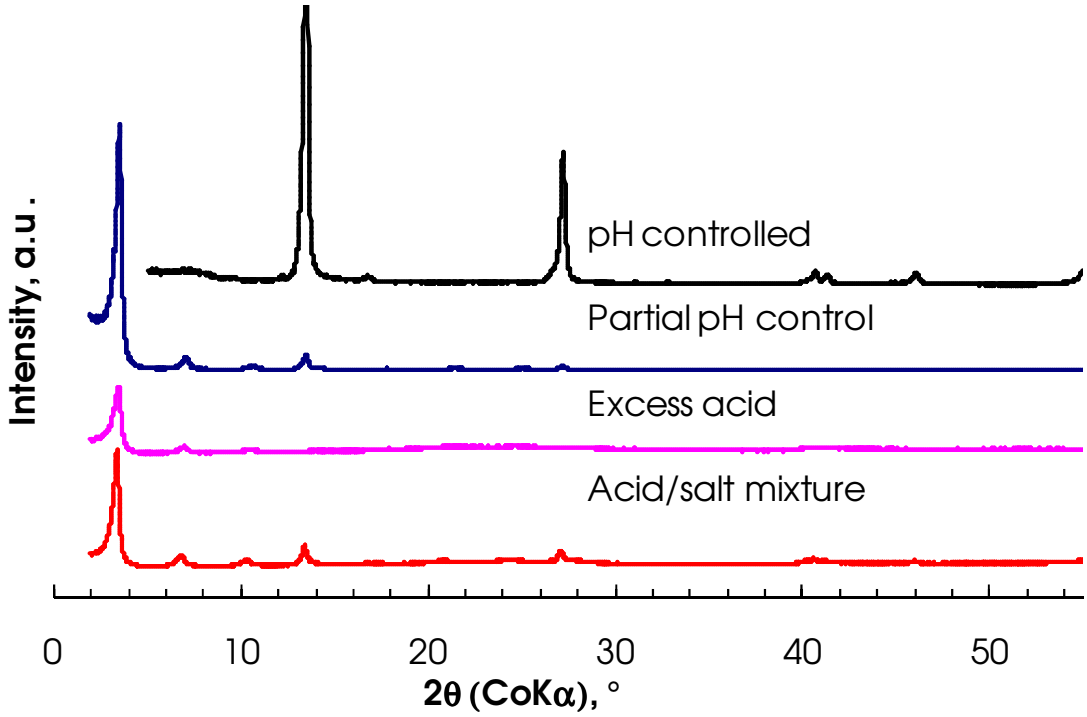

Figure A-27: LDH-DBS diffractograms in different pH environments

From Figure A-27 one can conclude that a substantial amount of acidity is necessary for exchange to occur, at least 1AEC of the acid.

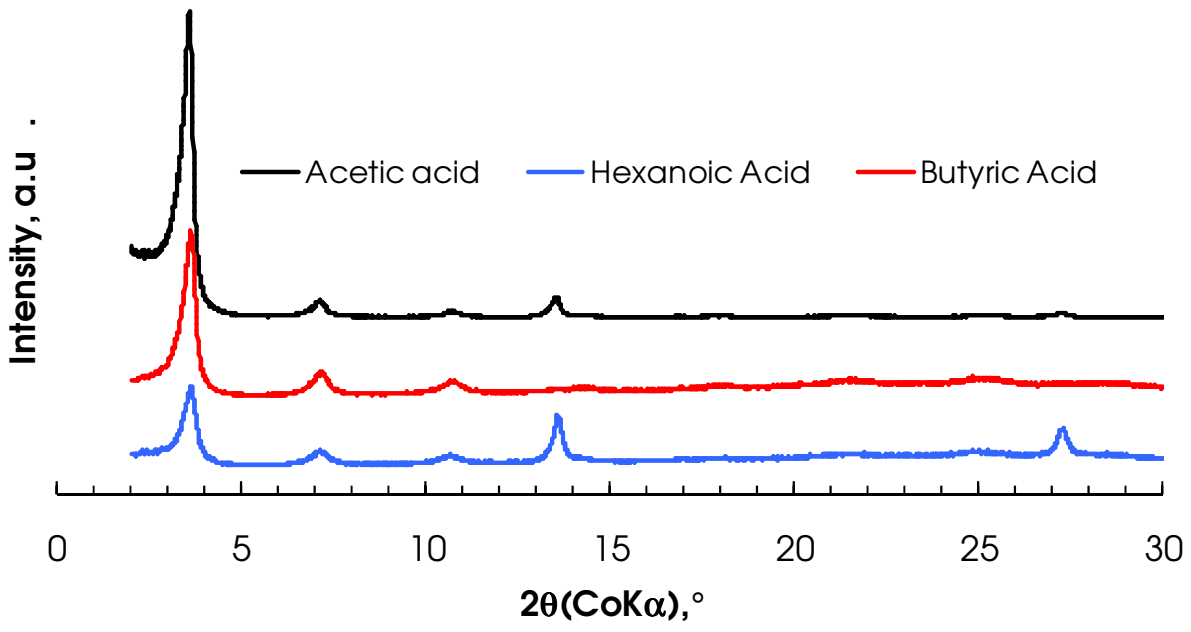

Figure A-28: LDH-DBS diffractograms using different acid mediations

The LDH-surfactants were prepared in the presence of dodecyl alcohol and lauric acid to investigate co-intercalation (see Figures A-22 and A-23). However, no co-intercalation was observed. The surfactant anions were preferentially intercalated in the dodecyl experiment. In contrast, lauric acid intercalated preferentially, hence supporting the claim that long-chain carboxylic acids are incorporated in favour of surfactant anions.

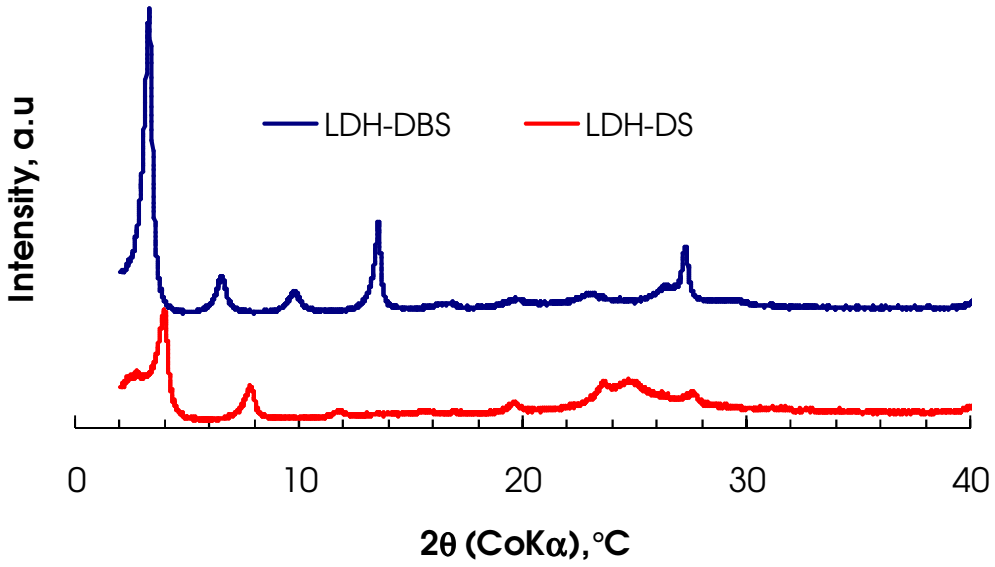

Figure A-29: LDH-surfactant prepared together with dodecyl alcohol

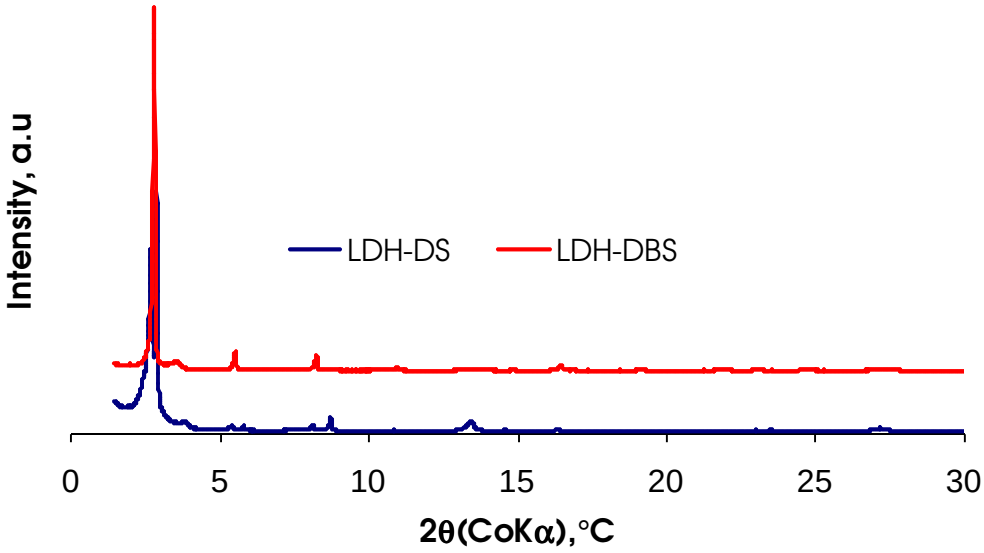

Figure A-30: LDH-surfactant prepared together with lauric acid

APPENDIX V: SCANNING ELECTRON MICROGRAPHS

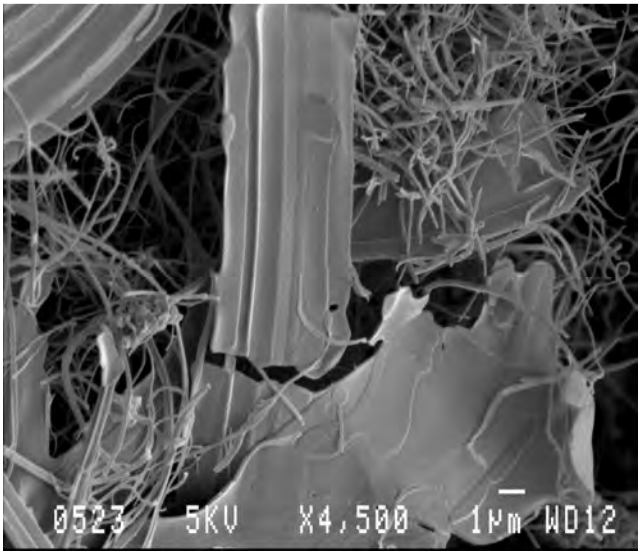

LDH-DS (normal)

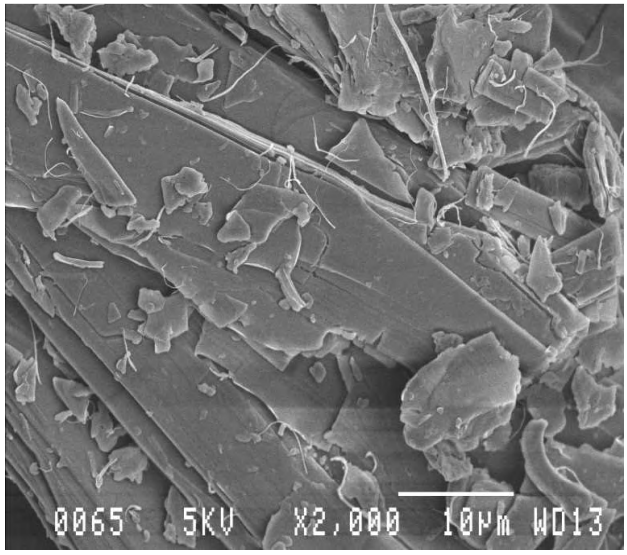

LDH-DS (inert atmosphere)

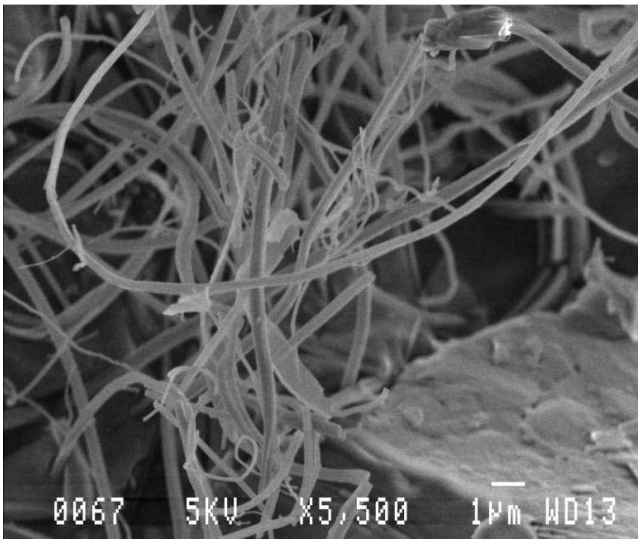

LDH-DS (inert atmosphere)

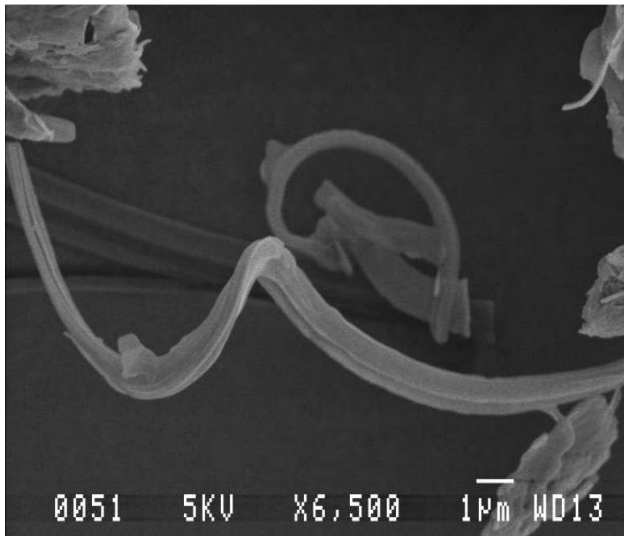

LDH-DS (co-precipitated at 65 °C)

It is evident that the co-precipitation methods yield three crystal growth habits: normal platelets, rods and fibres.

Of equal interest is the morphology of the regeneration method, which appears unusual compared with what is normally obtained.

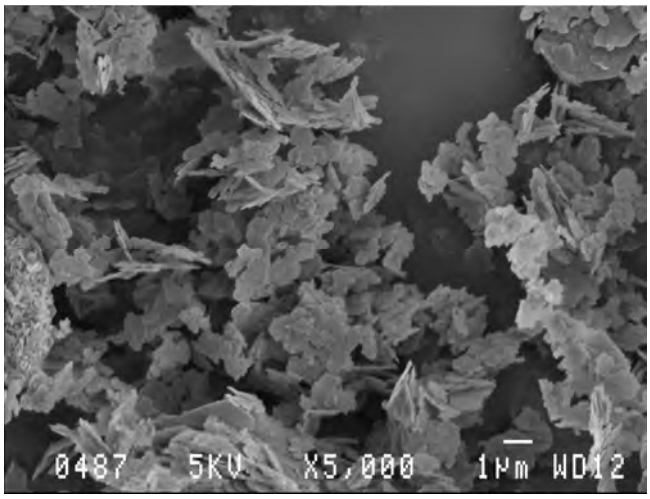

Calcined LDH-CO_3

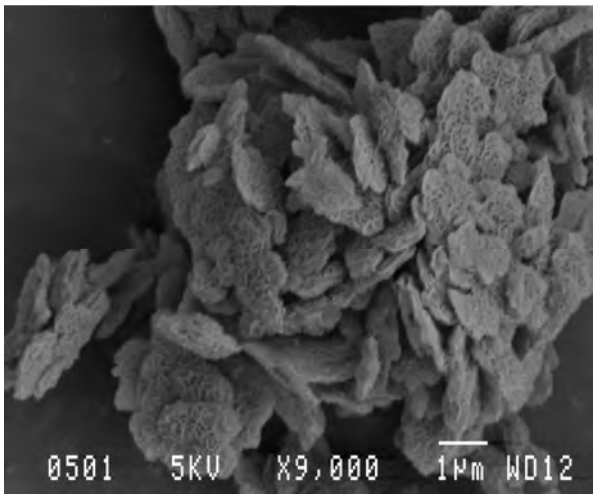

LDH-DS

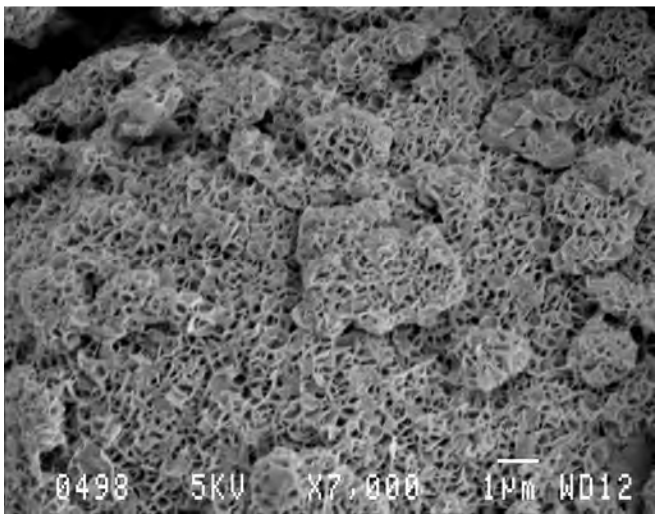

LDH-DBS

APPENDIX VI: PUBLICATIONS ORIGINATING FROM THIS RESEARCH

Published article

Moyo, L, Nhlapo, N. S. and Focke, W. W. 2008. A critical assessment of the methods for intercalating anionic surfactants in layered double hydroxides. ***J. Mater. Sci.,*** 43: 6144-6158.